

# New Families of Beta-Lactamase Inhibitors

By

Janet Gonzalez

A dissertation submitted to the Graduate Faculty in Biochemistry in partial fulfillment of the requirements for the degree of Doctor of Philosophy, The City University of New York

2011

2011

Janet Gonzalez

All Rights Reserved

ii

This manuscript has been read and accepted for the Graduate Faculty in Biochemistry in satisfaction of the dissertation requirement for the degree of Doctor of Philosophy

ii

Dr. Manfred Philipp

---

Date

---

Chair of the Examining Committee

Dr. Edward Kennelly

---

Date

---

Executive Officer

Dr. Miguel Cervantes-Cervantes

Dr. Thomas Haines

Dr. Andrei Jitianu

Supervisory Committee

## Abstract

### New Families of Beta-Lactamase Inhibitors

By Janet Gonzalez

Advisor Dr. Manfred Philipp

A traditional approach to improving the efficacy of  $\beta$ -lactam antibiotics has been to modify natural antibiotics by modifying the nucleus and adding various side chains. It is generally believed that  $\beta$ -lactam based antibiotics have a limited future given increased resistance demonstrated by many strains of bacteria. Therefore the lack of performance among commonly used antibiotics against the rise of resistant bacterial strains has propelled researchers to look for novel types of antimicrobial agents and enzyme inhibitors as tools to combat this serious and growing threat. The focus of this research is to investigate novel small-molecules from different families with antibacterial properties such as peptides, aromatic ketones, biphenyl and stilbene compounds and boronic acids that demonstrate an inhibitory effect on class A  $\beta$ -lactamase. Some of these inhibitors were found by screening natural products other were found by screening libraries of compounds and yet others were found by computational approaches involving molecular docking. Of all the compounds tested as long as the molecule was within hydrogen bonding distance of Ser84, Lys87 Ser142, Asn186, Gly252, Glu182 or Asp142, they demonstrated inhibitory effect which demonstrates that docking for this class of compounds is highly correlated with successful experimental inhibition.

## Table of Contents

List of Figures	Page vii
List of Tables	Page xv
Introduction Chapter 1	Page 1
Historical Perspective of Antibiotics and Infection Control	Page 1
Current Perspectives	Page 5
The Bacterial Cell Wall	Page 6
Beta-Lactam Antibiotics and Their Interactions with Transpeptidases	Page 9
Introduction to Antibiotics	Page 10
Beta-Lactam Antibiotics	Page 10
Beta-Lactamases Chapter 2	Page 15
Enzymatic Inhibition Modes For $\beta$ -Lactam Based Antibiotics	Page 15
Monobactams and Their Derivatives	Page 18
Carbapenems	Page 20
Biphenyls, Ketones and Stilbenes	Page 21
Classification of $\beta$ -Lactamases	Page 22
Class A B-Lactamase	Page 23
The Structure of Class A B-Lactamases	Page 25
The Mechanism of Class A B-Lactamases on B-Lactam Antibiotics	Page 27
Five Forms of Beta-Lactamase Resistance	Page 31
Enzyme Characterization Chapter 3	Page 33
Introduction to Enzyme Kinetics	Page 33
Beta-Lactamase Characterization	Page 35
Kinetic Parameters	Page 36

Materials and Methods	Page 38
Peptides Chapter 4	Page 46
Introduction To Peptide Inhibitors	Page 46
Material and Methods	Page 54
Sculpt	Page 56
Dock	Page 61
Results and Discussion for Peptides	Page 64
Bioinformatics Chapter 5	Page 78
Introduction	Page 78
Identification of Y-49 Recombinant Beta-Lactamase Protein	Page 81
Genomic features of H37Rv and H37Ra	Page 83
Choosing a Molecular Model	Page 84
DNA Sequence Gene ID 888742 H37Rv Strain	Page 85
Amino Acid Sequence for Locus Tag Rv2068c H37Rv Strain	Page 85
Sequence analysis	Page 89
Screened Compounds and Inhibitors Chapter 6	Page 94
Discussion	Page 111
Biphenyls, Aromatic Ketones and Stilbenes	Page 114
Boronic Acids	Page 116
Boronic Acid Thiophenes	Page 119
Boronic Acid Inhibitors	Page 119
Boronic Acids as Carbon Analogs	Page 120
Boron as Serine Protease Inhibitors	Page 121
References	Page 123

## List of Figures

Fig. 1. Mycolic Acid	Page 7
Fig. 2. <i>Mycobacterium tuberculosis</i> Cell Wall	Page 8
Fig. 3. The Transpeptidation Reaction Catalyzed by Bacterial D-D Transpeptidases	Page 9
Fig. 4. Structure of Benzylpenicillin	Page 9
Fig. 5. Core Structures of the $\beta$ -Lactam Family	Page 13
Fig. 6. Branched Pathways for $\beta$ -Lactamase Inhibitors	Page 16
Fig. 7. Structures of Clavulanic Acid, Sulbactam and Tazobactam	Page 17
Fig. 8. Simplified Reaction Mechanism for Class A $\beta$ -Lactamase with Sulbactam	Page 18
Fig. 9. Monobactam and Synthetic Derivatives	Page 19
Fig. 10. Simplified Reaction Mechanism for Class A $\beta$ -Lactamase with Monobactams	Page 19
Fig. 11. Structure of Carbapenems	Page 20
Fig. 12. Overall Fold of Class A $\beta$ -Lactamases	Page 26
Fig. 13. General Scheme for $\beta$ -Lactam Hydrolysis	Page 27
Fig. 14. Proposed Mechanism for $\beta$ -Lactam Hydrolysis	Page 28
Fig. 14. Proposed Mechanism for $\beta$ -Lactam Hydrolysis	Page 28

Fig. 16. Schematic Representation of Residues in the Class A Active Site	Page 30
Fig. 17. Absorbance vs. time for varying substrate concentrations enzyme is constant at 0.05 nM	Page 35
Fig 18. Absorbance vs. Time for Varying Concentrations of Enzyme. Substrate is constant at 24 $\mu\text{M}$	Page 35
Fig. 19. Linearity of Enzyme Velocity with Respect to Enzyme Concentration at Constant Substrate Concentration	Page 36
Fig. 20. Graph of Absorbance vs. Time at Varying Substrate Concentrations. The enzyme is constant at 50 $\mu\text{M}$	Page 37
Fig. 21. Graphical Determination of $K_m$ and $V_{max}$ for Y-49 Recombinant $\beta$ -Lactamase	Page 37
Fig. 22. Lineweaver –Burke Plot	Page 38
Fig. 23. His Trap Column and SDS PAGE Gel	Page 41
Fig. 24. Size Exclusion Chromatogram and SDS PAGE Gel	Page 42
Fig. 25. Western Blot Film	Page 43
Fig. 26. Cefoxitin’s Interaction with Protein Residues	Page 47
Fig. 27. Interactions of RDHY in the Class A Active Site	Page 52
Fig. 28. Interactions of RKHY in the Class A Active Site	Page 53

Fig. 29. Interactions of RSHY in the Class A Active Site	Page 53
Fig. 30. HPLC Chromatogram of Crude RGHY	Page 57
Fig. 31. HPLC Chromatogram of Crude RKHY	Page 58
Fig. 32. HPLC Chromatogram of Crude RRHY	Page 58
Fig. 33. HPLC Chromatogram of Crude RSHY	Page 59
Fig. 34. 1YM1 with Boronic Acid Inhibitor in the Active Site	Page 60
Fig. 35 A. The CPK Representation of the Peptide HNHY in the 1YM1 Active Site	Page 61
Fig. 35 B. A Ball and Stick Representation of the Peptide HNHY in the 1YM1 Active Site	Page 61
Fig. 36. Representation of Clustered Spheres	Page 63
Fig. 37. Representation of Ligands as Spheres in an Active Site	Page 64
Fig. 38. Cefoxitin's Interaction with Protein Residues in 1YM1	Page 66
Fig. 39. Interaction of RDHY in 1YM1 Active Site	Page 67
Fig. 40. Interaction of RKHY in 1YM1 Active Site	Page 67
Fig. 41. Interaction of RSHY in 1YM1 Active Site	Page 68

Fig. 42. Structure Activity Relationship for RXHY Sequence	Page 70
Fig. 43. Structure Activity Relationship for Small Residues	Page 72
Fig. 44. Structure Activity Relationship for Medium Residues	Page 72
Fig. 45. Structure Activity Relationship for Large Residues	Page 73
Fig. 46. Structure Activity Relationship for Hydrophobic Residues	Page 73
Fig. 47. Structure Activity Relationship for Polar Residues	Page 74
Fig. 48. Structure Activity Relationship for Positively Charged Residues	Page 74
Fig. 49. Structure Activity Relationship for negatively Charged Residues	Page 75
Fig. 50. Structure Activity Relationship for charged Aromatic Residues	Page 75
Fig. 51. Structure Activity Relationship for Long Aliphatic Residues	Page 76
Fig. 52. Structure Activity Relationship for OH Group Residues	Page 76
Fig. 53. Structure Activity Relationship for NH <sub>2</sub> Residues	Page 77
Fig. 54. Evolutionary Relationship Between Ambler Class A $\beta$ -Lactamases and DD-Peptidase	Page 78
Fig. 55. Representation of $\beta$ -Lactamase and DD-Peptidase Reactions	Page 80
Fig. 56. DD-Peptidase Reaction	Page 81

Fig. 57. $\beta$ -Lactam, B, D-alanyl-D-alanine Peptide	Page 81
Fig. 58. Global sequence alignment of H37Ra (CP000611) compared to H37Rv (AL123456)	Page 83
Fig. 59. Results FASTA search	Page 86
Fig. 60. Conserved motifs for population of 18 $\beta$ -lactamases	Page 90
Fig. 61. Active site Serine 84 and Lysine 87 Element 1	Page 92
Fig. 62. Serine 142, Aspartic Acid 142 and Glycine 144 Element 2	Page 92
Fig. 63. Glutamic Acid 182 Element 3	Page 93
Fig. 64. Lysine 250, Threonine 251 and Glycine 252 Element 4	Page 93
Fig. 65. Raw Data of Change in absorbance vs. Time for the Inhibitor Benzophenone	Page 95
Fig. 66. Effect of Increasing Concentration of Benzophenone on the Velocity of the Reaction	Page 95
Fig. 67. Velocity vs. the concentration of Benzophenone as Inhibitor. $K_i$ of Benzophenone = $25 \pm 2 \mu\text{M}$	Page 96

Fig. 68. Raw Data of Change in Absorbance vs. Time for the Inhibitor 2-Aminohexanol	Page 96
Fig. 69. Effect of Increasing Concentration of 2-Aminohexanol on the Velocity of the Reaction	Page 97
Fig. 70. Velocity vs. the Concentration of Benzophenone as Inhibitor for the Determination of $K_i$	Page 97
Fig. 71. Benzophenone Imine no Inhibition	Page 98
Fig. 72. Benzophenone Imine Global Docking	Page 98
Fig. 73. Diphenylamine no Inhibition	Page 99
Fig. 74. 2, 2-Dihydroxybenzophenone (Inhibits slightly after 50 $\mu$ M concentration)	Page 99
Fig. 75. Biphenyl $K_i = 123 \pm 18 \mu$ M	Page 100
Fig. 76. Phenanthrene $K_i = 28 \pm 2 \mu$ M	Page 100
Fig. 77. Benzophenone $K_i = 25 \mu$ M	Page 101
Fig. 78. Dibenzylsulfone $K_i = 17 \pm 3 \mu$ M	Page 101
Fig. 79. Resorcinol No Effect	Page 103

Fig. 80. Hydroquinone $K_i = 64 \pm 5 \mu\text{M}$	Page 103
Fig. 81. Benzylamine $K_i = 41 \pm 3 \mu\text{M}$	Page 104
Fig. 82. 2-Aminohexanol $K_i = 19 \pm 4 \mu\text{M}$	Page 104
Fig. 83. <i>p</i> -Hydroxyphenylglycine $K_i = 5 \pm 2 \mu\text{M}$	Page 105
Fig. 84. 4-Amino 4 methoxystilbene Activates	Page 107
Fig. 85. Trans stilbene	Page 107
Fig. 86. 4,4-Dihydroxyethylstilbene $K_i = 191 \pm 11 \mu\text{M}$	Page 108
Fig. 87. 4-Hydroxystilbene $K_i = 141 \pm 12 \mu\text{M}$	Page 108
Fig. 88. 4-Nitrostilbene $K_i = 56 \pm 8 \mu\text{M}$	Page 109
Fig. 89. Epigallocatechin Gallate (EGCG) $K_i = 50 \pm 6 \mu\text{M}$	Page 109
Fig. 90. Diethylstilbestrol $K_i = 32 \pm 5 \mu\text{M}$	Page 110
Fig. 91. 2,4-Diaminoazobenzene $K_i = 30 \pm 6 \mu\text{M}$	Page 110
Fig. 92. Resveratrol $K_i = 14 \pm 4 \mu\text{M}$	Page 111
Fig. 93. General Structure of phosphonate Monoesters	Page 112
Fig. 94. Mechanism of $\beta$ -Lactamase Inhibition by <i>p</i> -nitrophenyl [N-(benzyloxycarbonyl)aminomethyl]phosphonate	Page 112
Fig. 95. General Structure of <i>O</i> -Aryloxycarbonyl Hydroxamates	Page 114

Fig. 96. Characteristic  $\beta$ -lactam Antibiotics and Related  $\beta$ -Lactamase

Inhibitors

Page 118

Fig. 97. 2-Carboxythiophene 5 Boronic Acid Kinetic Data

Page 119

## List of Tables

Table 1. List of $\beta$ -Lactam Antimicrobial Agents, Taken from Reference	Page 13
Table 2. Comparison of Kinetic Parameters	Page 38
Table 3. $\Delta G$ Kcal/mol	Page 47
Table 4. Interactions of Arginine with Protein	Page 48
Table 5. Interactions of N-Terminal Nitrogen with Protein	Page 49
Table 6. Interactions of Tyrosine OH with Protein	Page 49
Table 7. Interactions of Main Chain Carboxylate Group with Protein	Page 50
Table 8. Comparison of $\Delta G$ Values for Substitutions in the P1 and P4 Positions of 4-Mers	Page 51
Table 9 . Gradient HPLC	Page 57
Table 10. Sequence, Charge, $K_i$ and Free Energy. Arranged by the Second Peptide in the Sequence	Page 68
Table 11. Screened Compounds	Page 94
Table 12. Screened Compounds	Page 102
Table 13. Screened Compounds	Page 105

## **Introduction Chapter 1**

### **Historical Perspective of Antibiotics and Infection Control**

The word antibiotic is derived from the Greek  $\alpha\nu\tau\iota$  (against) and  $\beta\iota\omicron\sigma$  (life). Jean Antoine Villemin, a contemporary of Louis Pasteur, coined the term “antibiosis” in 1889 to describe the process by which a chemical substance produced by one organism is destructive to another, essentially a process by which life could be used to destroy life (1).

Although the name Alexander Fleming is synonymous with antibiotics, the antibacterial properties of molds and other substances have been used since ancient times. The earliest physicians and healers were aware the certain compounds stop infection and prevent spoilage. Egyptians used resins and liquid tar to decrease the decomposition of flesh, thus preparing their dead for burial. Ancient Greeks and Romans recognized the antiseptic properties of vinegar, wine and oil, while peasants from all parts of the world would have used warm soil applied to wounds to control infections (2).

The history of modern infection control began in 1847 when Hungarian physician Ignaz Semmelweis, described as the “savior of mothers,” discovered that hand-washing with a chlorinated lime solution (calcium hypochlorite) prior to delivery dramatically reduced puerperal fever otherwise known as childbed fever (3). In the mid nineteenth century puerperal fever claimed the lives of up to 35 % of mothers. Semmelweis published a book of his findings titled Etiology, Concept and Prophylaxis of Childbed Fever (4). The medical establishment disregarded his ideas and declared him a lunatic. In 1865 he was institutionalized and died of blood poisoning ten days after receiving a cut on his finger while being forced into a straightjacket.

Despite the work of Semmelweis, surgeons were not required to wash their hands before seeing patients or before surgery. Joseph Lister, a nineteenth century English surgeon working in Glasgow, Scotland, was aware of Louis Pasteur's germ theory. He reasoned that if airborne microbes could sour milk and rot meat, they might also infect wounds. He decided to experiment by spraying instruments and dressings with phenol. He also began applying phenol to wounds, remarkably reducing the incidence of gangrene. Lister is credited with founding modern antiseptic surgery in the 1860s (5).

German physicians, Rudolf Emmerich and Oscar Löw also conducted infection control experiments in the 1890s. They took tissue from infected bandages, grew cultures and eventually isolated particular bacteria that caused green infections in open wounds. This bacterium *Bacillus pyocyaneus*, (*Pseudomonas aeruginosa*), could lyse other pathogenic bacteria such as those producing cholera, typhoid and diphtheria. Emmerich and Low were the first to make an antibiotic which was called pyocyanase. However, the drug was ineffective and abandoned as a result (1).

In 1928, Scottish scientist Alexander Fleming made the first real breakthrough in antibiotics. Fleming, while on staff at St. Mary's Hospital in London, observed the antibacterial properties of a, "mold broth filtrate" isolated from the fungus *Penicillium notatum* which inhibited the growth of Staphylococcus. He decided to call the filtrate penicillin. Yet, Fleming did not see the practical applications of penicillin. According to one commentator, "*he was obviously aware that such a substance would be highly useful if it could kill pathogenic bacteria in humans, but such a hope seemed much in the future in view of the low broth potencies he was obtaining*" (6). Flemings work remained unnoticed for another nine years.

Not until 1940 was penicillin isolated in pure form for the first time by a research team at Oxford University lead by Howard Florey, Ernst Chain and Edward Abraham. The team envisioned the clinical importance of penicillin in the treatment of bacterial infections in humans. This was the starting point for the development and use of antibiotics to control infections in humans.

Russian-American microbiologist Selman Waksman resurrected the term “antibiotic” in 1941. A new area of soil science opened up in 1939 with the discovery of bacteria-killing agents in soil microorganisms. Waksman, together with his graduate student Albert Schatz, began a search for antibiotics in soil microorganisms and soon discovered streptomycin (7). Waksman isolated and developed many other antibiotics including neomycin. His 1943 discovery of streptomycin, the first specific agent in the treatment of tuberculosis, won him the 1952 Nobel Prize for Physiology or Medicine. He was a professor of microbiology from 1940 to 1958 and director of the Waksman Institute of Microbiology at Rutgers University from 1954 to 1958.

Another important landmark in the story of antibiotics was the X-ray crystallographic determination of the structure of penicillin G (earlier named penicillin) by Dorothy Mary Crowfoot Hodgkin and Barbara Roger-Low in May 1949 (8) who determined the fused bicyclic  $\beta$ -lactam thiazolidine nucleus and the relative stereochemistry of the penicillin molecule.

Originally the term antibiotic only applied to compounds derived from living organisms capable of killing or inhibiting bacterial growth. The term now includes synthetic antimicrobial drugs. Natural antibiotics are recently being seen as secondary metabolites. Secondary metabolites are organic compounds that were assumed not to be directly involved in the normal growth, development, or reproduction of the organisms that produce them. Unlike primary metabolites the absence of secondary metabolites does not result in the immediate death of the producer.

Rather, it is implicated in its long-term survivability. Therefore many secondary metabolites play important roles in bacterial and interspecies defense.

Antibiotics traditionally have always been seen as the chemical weapons of the microbial world where they are used for survival and competitive advantage within a microenvironment (9). A different perspective besides the “war” metaphor, is currently gaining ground, thus in 2007 Davies *et al.* (10) proposed that antibiotics evolved as signaling molecules rather than weapons.

Synthetic antimicrobials such as the fluoroquinolones demonstrate concentration-dependent transcription modulation properties of gene expression at the transcriptional level (11) and their action on specific intracellular targets is similar to that of microbial secondary metabolites.

Naturally-occurring antibiotics (as opposed to synthetic ones) are a subgroup of molecules that affect transcription of genes involved in multiple cellular functions at sub-inhibitory concentrations.

In 2005 Rothstein *et al.* described a  $\beta$ -lactam antibiotic that up-regulated the transcription of a glutamate transporter gene in animals (12). Another example of antibiotic signaling molecules is a family of protein synthesis inhibitors called aminoglycosides that up-regulate virulence functions. At sub-inhibitory concentrations aminoglycosides induce the formation of biofilms (13). A biofilm is an aggregate of microorganisms in which cells adhere to each other and/or to a surface. Biofilms resist antibiotic action and are important contributors to bacterial persistence in chronic infections. When a bacterial population switches to the biofilm mode of growth, it undergoes a phenotypic shift in which large suites of genes are differentially regulated (14). Because these small molecules, produced by well-defined biosynthetic pathways, elicit responses in other micro-organisms they are increasingly being categorized as signaling molecules.

### **Current Perspectives**

Resistance to  $\beta$ -lactam antibiotics is progressing at an alarming rate. Many bacterial species are acquiring the genes encoding for  $\beta$ -lactamases. Much of this expansion is unfortunately because of selective pressure due to the overuse, abuse and misuse of  $\beta$ -lactam antibiotics in animal husbandry and clinical settings. It was estimated that 15 billion dollars was spent worldwide in 2003 on  $\beta$ -lactam antibiotics. This represents 65% of the total world market for antibiotics (15). Resistance is acquired through horizontal gene transfer, via plasmids and integrons, among individuals, species and even between bacterial kingdoms. The efficacy of  $\beta$ -lactam antibiotics decreases as the frequency of microbial resistance increases; therefore, as bacterial resistance continues to grow and threaten current therapies, an urgent need exists to develop new classes of antibiotics and  $\beta$ -lactamase inhibitors.

Beta-lactam antibiotics are the most widely used anti-microbials even though bacterial resistance mechanisms have reduced their effectiveness. Of the five bacterial resistance mechanisms, the most effective involves the production of  $\beta$ -lactamases which hydrolyze  $\beta$ -lactam antibiotics. Today there are over 840 known  $\beta$ -lactamases (16) .

One approach to overcoming the resistance problem is to find substances that can protect the  $\beta$ -lactam antibiotic from hydrolysis by  $\beta$ -lactamases. The first inhibitor to be used clinically was clavulanic acid from *Streptomyces clavuligerus*. Clavulanic acid is a potent inhibitor of  $\beta$ -lactamases and when combined with amoxicillin and ticarcillin, traditional  $\beta$ -lactams, produces broad-spectrum antibiotic combinations effective against  $\beta$ -lactamase-producing bacteria (17). After the discovery of clavulanic acid, various compounds have been found and developed as inhibitors (18). The success of clavulanic acid established  $\beta$ -lactamase inhibitors as one solution to the problem of  $\beta$ -lactam antibiotic-resistant bacteria.

## The Bacterial Cell Wall

The effectiveness of  $\beta$ -lactam antibiotics is in their ability to inhibit a set of transpeptidase enzymes also called penicillin binding proteins that synthesize bacterial cell walls. For prokaryotes the cell wall maintains the shape and rigidity of the cell without which these prokaryotes would lyse in a hypertonic and hostile environment (19). Prokaryotes can be categorized into two groups based on Gram staining. Gram-positive bacteria have a thick cell wall with no outer membrane and readily accept the Gram stain, while Gram-negative bacteria have a thin cell wall and a complex outer membrane that resists staining. In Gram-positive bacteria  $\beta$ -lactamases are excreted into the extracellular matrix while in Gram-negative bacteria  $\beta$ -lactamases are concentrated in the periplasmic space. *Mycobacterium tuberculosis* has no outer membrane and an unusual lipid, mycolic acid, for its cell wall making it resistant to Gram staining techniques. They are therefore classified as acid fast Gram-positive bacteria.

The cell structure of *M. tuberculosis* has three major components: a plasma membrane, a covalently linked mycolic acid, arabinogalactan and the peptidoglycan complex together they are collectively known as MAPc. Beyond the membrane the peptidoglycan base makes four penicillin-binding proteins involved in its biosynthesis which are inhibited by clinically relevant concentrations of  $\beta$ -lactam antibiotics. This bacterial peptidoglycan is a high-molecular-weight polymer that forms a tough, rigid structure made up of three parts; a backbone composed of alternating sugars N-acetylglucosamine (NAG) and N-acetylmuramic acid (NAM), a set of identical tetrapeptide side-chains attached to N-acetylmuramic acid and a set of identical peptide cross-bridges.

The cell wall's carbohydrate backbone is the same in all bacterial species; however, the tetrapeptide side-chains and the peptide cross-bridges vary from species to species. This

peptidoglycan base is covalently attached via a linker to linear galactofuran which is attached to highly branched arabinofuran, which is in turn attached to mycolic acid units.

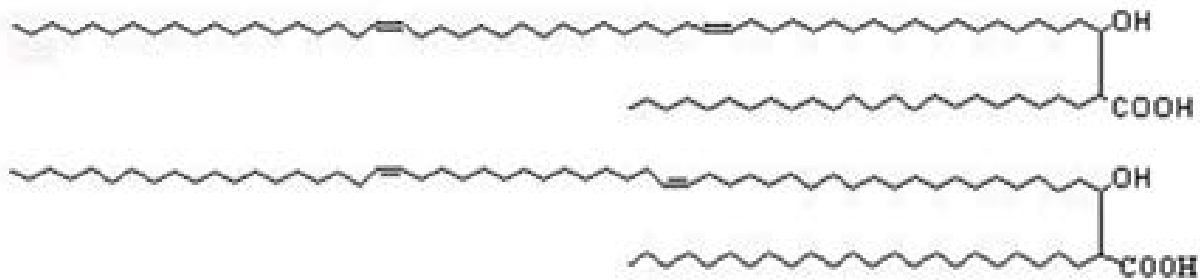


**Fig. 1. Mycolic Acid (20)**

Mycolic acids are composed of a short  $\beta$ -hydroxy chain and a longer  $\alpha$ -alkyl side chain. Each molecule contains between 60 and 80 carbon atoms. The Mycolyl-arabinogalactan-peptidoglycan complex comprises the cell wall core (19). Intercalated in the mycolic lipid environment are cell-wall proteins; phosphatidylinositol mannosides, phthiocerol dimycocerosate, lipomannan, and lipoarabinomannan. The mycolic acids are oriented perpendicular to the plane of the membrane and provide a unique lipid barrier responsible for many of the physiological and disease-inducing aspects of *M. tuberculosis* (21). The cell wall of *M. tuberculosis* is over 60% complex lipids. This high concentration of lipids has been associated with the following properties of the bacterium: impermeability to stains and dyes, resistance to many antibiotics, resistance to killing by acidic and alkaline compounds, resistance to osmotic lysis and resistance to lethal oxidation and survival within macrophages (22).

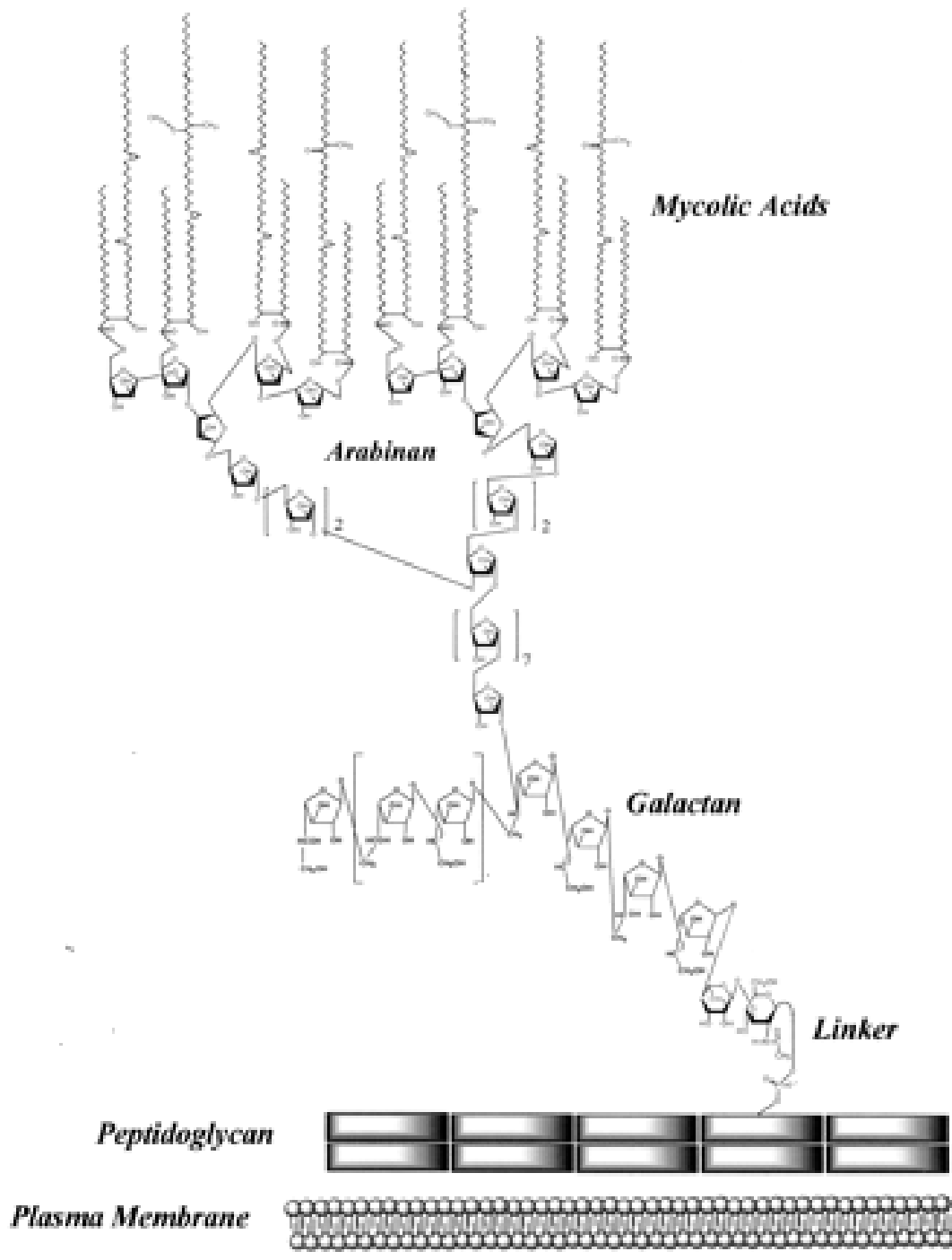
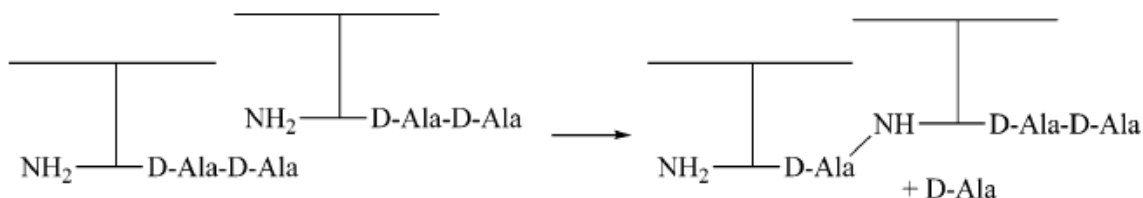


Fig. 2. *Mycobacterium tuberculosis* Cell Wall (23)

### Beta-Lactam Antibiotics and Their Interactions With Transpeptidases

Transpeptidases cleave the bond between the two terminal D-alanine residues on the N-acetylmuramic acid unit of the short peptidoglycan chains enzymatically linking the neighboring chains together via  $\beta$ -1,4 linkages thus forming the rigid support.



**Fig. 3. The Transpeptidation Reaction Catalyzed by Bacterial D-D Transpeptidases (24)**

Penicillins inhibit the D-D transpeptidase enzyme that completes the final steps in the synthesis of the peptidoglycan base. It was postulated that the structure of penicillin acting as a substrate analog of the transpeptidase enzyme must mimic the molecular structure of the peptidyl component (25). Upon closer inspection, penicillins and cephalosporins are really highly constrained tetrapeptides (Figure 4).

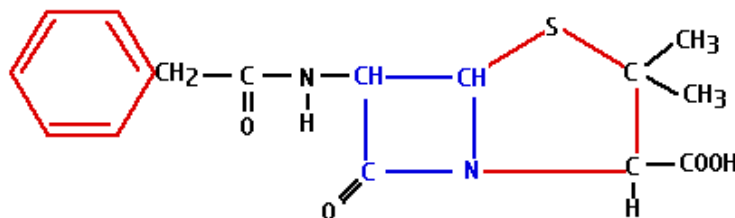


**Fig. 4. Structure of Benzylpenicillin**

In 1979 Yocum *et al.* proved that <sup>14</sup>[C]-benzylpenicillin acylated the active site serine via an ester link of the transpeptidase enzyme isolated from *Streptomyces* in direct competition with

$^{14}\text{C}$ -N,N'-diacetyl-L-lysyl-D-alanyl-D-lactate. The hydrolysis rate of the peptide substrate was fast whereas when the transpeptidase bound the penicillin molecule a long-lived intermediate was formed. The slow deacylation rate ( $t_{1/2} = 2\text{-}3\text{ hr}$  at  $37^\circ\text{C}$ ) of the penicilloyl moiety occupying the enzyme's active site makes these transpeptidases unavailable for catalysis with the normal substrate resulting in the loss of an intact cell wall (26).

## **Introduction To Antibiotics**

Antibiotics are derived from three sources: moulds or fungi such as *Penicillium chrysogenum*; bacterial sources such as *Streptomyces*; or synthetic or semi-synthetic sources. They can either inhibit the growth of pathogens, bacteriostatic, or to kill them, bacteriocidal. Antibiotics can also be divided into broad-spectrum and narrow-spectrum categories. For example, tetracycline, a broad spectrum antibiotic, is active against Gram-positive bacteria, Gram-negative bacteria, and even against mycobacteria. Penicillin, on the other hand, is a narrow spectrum antibiotic used mainly against Gram-positive bacteria. Other antibiotics, such as pyrazinamide, have an even narrower spectrum, and are used against *Mycobacterium tuberculosis*.

Antibiotics inhibit certain vital metabolic processes of bacterial cells and can be categorized into five major classes:

1. Cell wall inhibitors, such as penicillins and cephalosporins and
2. Inhibitors of nucleic acid synthesis, such as fluoroquinolones, which inhibit DNA synthesis, and rifampin, which inhibits RNA synthesis. Rifampin is a semi-synthetic antibiotic derived from the fermentation product of *Streptomyces mediterranei*. It specifically inhibits bacterial DNA-dependent RNA polymerase blocking the RNA primer. Quinolones and fluoroquinolones inhibit bacterial replication by blocking DNA replication. During DNA replication double-stranded DNA needs to unwind to allow for complementary base pairing to occur and synthesis

of new DNA to proceed. DNA gyrase is a topoisomerase II type enzyme that unwinds the DNA by introducing negative supercoils and relaxes positive supercoils allowing the replication fork to proceed around the chromosome. Quinolones and fluoroquinolones inhibit this enzyme by binding to the A-subunit of the enzyme and stabilizing the gyrase-DNA complex effectively blocking the polymerase and causing breaks in DNA synthesis. Quinolones and fluoroquinolones primarily inhibit bacterial topoisomerase IV essential for the separation of inter-linked daughter strands of DNA stopping the binary fission.

3. Protein synthesis inhibitors. An individual bacterial ribosome is a complex ribonucleoprotein molecule. The 70S ribosome is formed by the association of a 30S and a 50S subunit. In prokaryotes the 30S unit is made up of a 16S rRNA and 21 associated proteins. The 50S particle consists of two RNAs, 5S rRNA and the 23S rRNA together with about 31 associated proteins. The primary function of the 30S unit is to monitor base-pairing between the codon on mRNA and the anticodon on tRNA. There are three tRNA binding sites, A (aminoacyl), P (peptidyl) and E (exit) after their tRNA substrates. The anticodon loops of the tRNA for the A and P sites bind the 30S subunit where they base-pair with the codons on the mRNA. The large subunit catalyzes the formation of the peptide bond via a peptidyl transferase. Protein synthesis inhibitors, such as aminoglycosides bind to the 30S subunit and prevent the formation of the initiation complex with mRNA and also induce codon mis-reading.

4. Anti-metabolites, such as the sulfa drugs or sulfonamides. The sulfonamides are synthetic antimicrobial agents acting on most gram-positive and many gram-negative organisms.

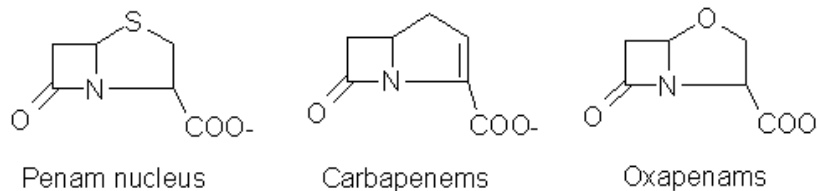
Sulfonamides, as antimetabolites and compete with para-aminobenzoic acid for incorporation into folic acid. All cells require folic acid for growth however in mammals folic acid is a dietary

requirement but bacterial cell need to synthesize folic acid because it cannot cross the cell walls by diffusion or active transport.

5. Peptide antibiotics that change the permeability of the cell membrane, such as Polymyxin B, Gramicidin and Daptomycin. The polymyxins are a group of cyclic polycationic peptide antibiotics with a fatty acid chain attached to the peptide with an amide link. They are product of the fermentation of the strain *Bacillus polymyxins*. These antibiotics contain a seven amino acid ring attached to a three amino acid tail that is finally attached to a fatty acyl group. These compounds are cationic surface-active at physiological pH. The fatty acid part of the molecule penetrates the hydrophobic region of the outer membrane. The ammonium groups of diaminobutyric acid in the ring interact with and displace calcium and magnesium from the negatively charged phospholipid group of the membrane. This displacement disrupts the membrane organization and increases the permeability of the membrane.

### **Beta-Lactam Antibiotics**

Originally limited to the penam and cephem families this group of antibiotics now includes the carbapenems, oxapenams, carbacephems oxacephamycins, as well as the natural and synthetic monocyclic  $\beta$ -lactams (Fig. 1). Until the 1970s, the traditional approach in the development of  $\beta$ -lactam antibiotics had been to modify the classical penam and cephem nuclei by adding various side chain modifications. Today it is generally believed that  $\beta$ -lactam based antibiotics have a limited future given the increased resistance demonstrated by many bacterial strains (27).



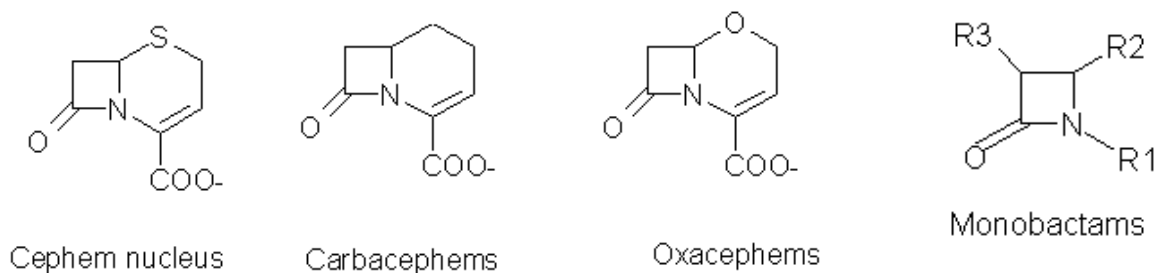


**Fig. 5. Core Structures of the  $\beta$ -Lactam Family**

**Table 1. List of  $\beta$ -Lactam Antimicrobial Agents, Taken from Reference (28)**

$\beta$ lactam groups	Examples of antimicrobial agents
Penicillins	Penicillin G, penicillin
	Penicillinase resistant penicillins: methicillin, nafcillin, oxacillin, cloxacillin
	Aminopenicillins: ampicillin, amoxicillin
	Carboxypenicillins: carbenicillin, ticarcillin
	Ureidopenicillins: mezlocillin, piperacillin
Cephalosporins	First generation: cefazolin, cephalothin, cephalexin
	Second generation: cefuroxime, cefaclor, cefamandole, cefamycins (cefotetan, cefoxitin)
	Third generation: cefotaxime, ceftriaxone, cefpodoxime, ceftizoxime, cefoperazone, ceftazidime
	Fourth generation: cefepime, ceftiprome
Carbapenems	Imipenem, meropenem, ertapenem
Monobactams	Aztreonam

The  $\beta$ -lactam antibiotic resistance process has been expedited and accelerated by a variety of genetic elements that include the bacterial genophore, transferable plasmids, and transposable elements. Interspecies-resistance-transfer can occur during conjugation, (bacterial mating), or transformation which is the incorporation of resistant genes found on plasmids from the environment, or transduction, which is the transfer of genetic material between pathogenic

species via bacteriophage. Gene transfer also occurs between Gram-negative and Gram-positive bacteria (29). The genes transferred include those for  $\beta$ -lactamase enzymes.

There are two questions with respect to combating  $\beta$ -lactamase activity:

Do  $\beta$ -lactams remain the main template for new antibiotic development?

Do we continue to search for mechanism based small molecule inhibitors?

The addition of greater mass and functional complexity to the R groups of existing  $\beta$ -lactams in order to prevent the activity of these  $\beta$ -lactamases led to extended-spectrum antibiotics or later-generation cephalosporins. The use of later-generation cephalosporins has resulted in TEM-type  $\beta$ -lactamase mutants capable of destroying extended spectrum antibiotics. This increasing antibiotic-resistance trend suggests that we are approaching the design limits for the “variations on a theme” strategy.

Small molecule inhibitors such as clavulanic acid and ‘ $\beta$ -lactam-resistant’  $\beta$ -lactams, such as aztreonam, protect  $\beta$ -lactam antibiotics from hydrolysis, thus restoring the potential of the antibiotics, but variant enzymes have also evolved that resist these inhibitors while maintaining the ability to hydrolyze  $\beta$ -lactam antibiotics (30).

We are now left to explore non-  $\beta$ -lactam inhibitors of  $\beta$ -lactamases, such as naturally-occurring peptides, small molecule inhibitors and their synthetic derivatives that may exhibit antibiotic properties. The objective is to find inhibitors of  $\beta$ -lactamases that will not engender bacterial resistance, but rather competitively form reversible or irreversible adducts with the catalytic serine of the enzyme (31).

## Beta-Lactamases Chapter 2

### Enzymatic Inhibition Modes For $\beta$ -Lactam Based Antibiotics

Most  $\beta$ -lactamases are classified as serine hydrolases and form an acyl-enzyme complex that is eventually hydrolyzed to regenerate the free enzyme and an inactive carboxylic acid. The kinetic efficiency of these enzymes differs widely depending on the  $\beta$ -lactam antibiotic involved. Some  $\beta$ -lactamases can achieve catalytic efficiencies ( $k_{\text{cat}}/K_m$ ) close to  $10^8 \text{ M}^{-1} \text{ sec}^{-1}$  indicating that the reaction is diffusion controlled.

Beta-lactamase inhibitors are mostly analogues of known substrates, i.e.  $\beta$ -lactams designed to bind to the active site as mechanism-based inhibitors in four major categories; penicillins, cephalosporins, monobactams, and carbapenems. Two strategies used in the design of  $\beta$ -lactam based, mechanistic inhibitors are the following;

1. Design of a poor substrate that will acylate the enzyme but deacylates slowly creating a reversible or transient inhibition
2. Development of a mechanism-based irreversible inhibitor that is not susceptible to deacylation.

The general scheme for mechanism-based inhibition is to covalently bind the enzyme and the inhibitor to initially form an enzyme-inhibitor complex E:I, then progress through the reaction to form a covalent complex E-I. From this point, two routes exist, the first one being hydrolysis, which produces a normal product turnover, either conventionally or through transient inhibition;

and second an irreversible inhibition that inactivates the enzyme with no product formation.

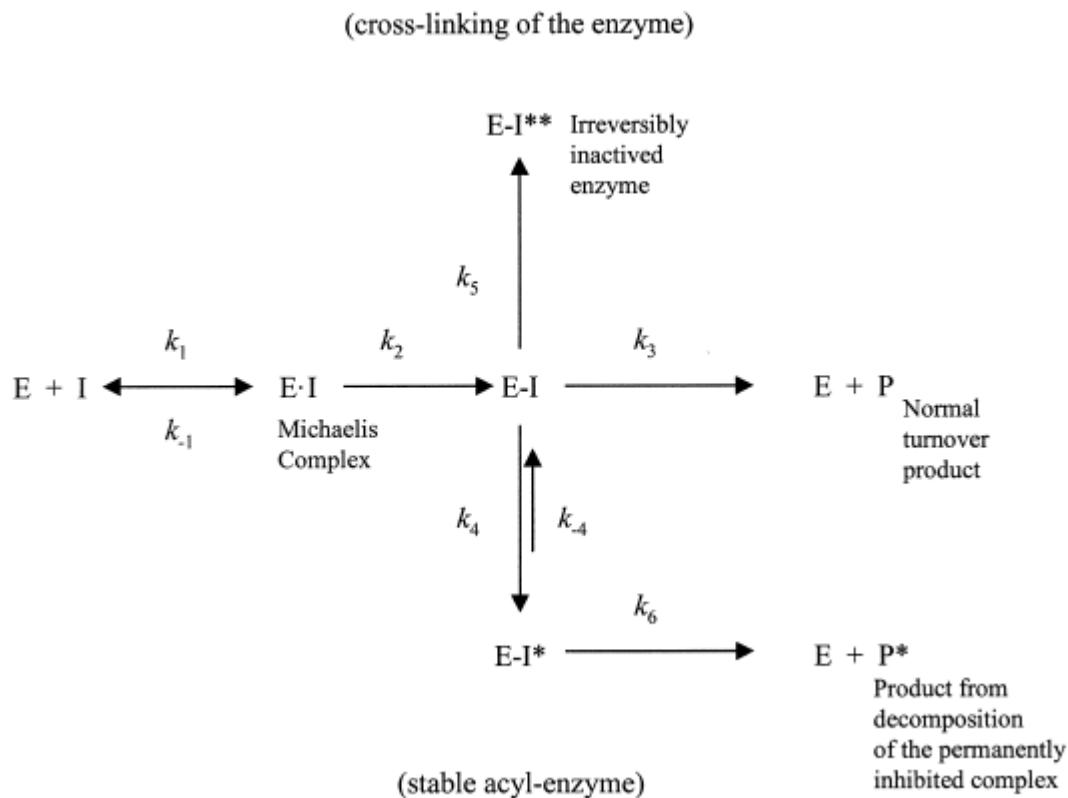


**Fig. 6. Branched Pathways for  $\beta$ -Lactamase Inhibitors (32)**

Examples of the first design strategy are monobactams, carbapenems or extended spectrum cephalosporins all of which form acyl-enzyme complexes that are slowly hydrolyzed.

Irreversible inhibitors permanently inactivate the enzyme through secondary reactions in the active site. Examples of these inhibitors are the naturally occurring penicillin inactivator clavulanic acid and its synthetic derivatives sulbactam and tazobactam.

Clavulanic acid was isolated from *Streptomyces clavuligerus* in the 1970s. Alone it displays almost no antibiotic activity but when combined with penicillin overcame *Staphylococcus*

*aureus*, *Klebsiella pneumoniae*, *Proteus mirabilis*, and *Escherichia coli* antibiotic resistance (33).

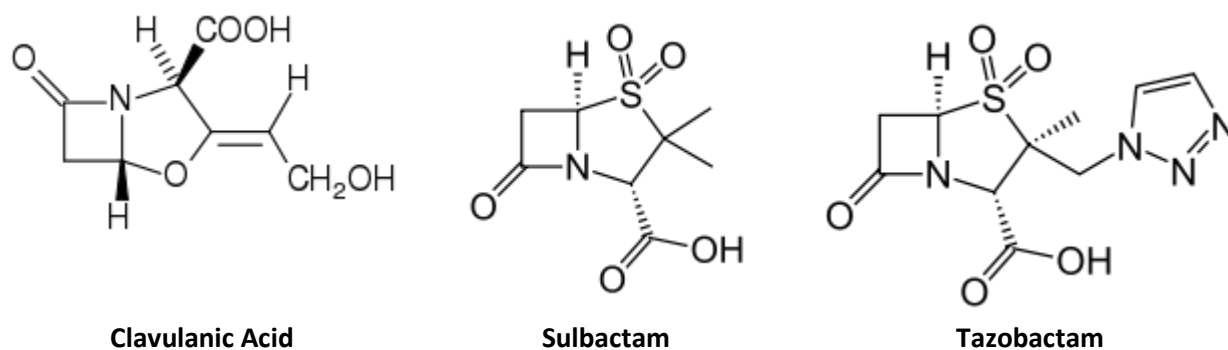


**Fig. 7. Structures of Clavulanic Acid, Sulbactam and Tazobactam**

Sulbactam and tazobactam are synthetic penicillinate sulfones formulated in 1978 and 1980, respectively (34, 35). Along with clavulanic acid they are effective against bacteria expressing class A  $\beta$ -lactamases. These three sulfones differ from  $\beta$ -lactam antibiotics by virtue of a leaving group at position C1 of the 5-membered ring. They acylate the enzyme quickly and have slow deacylation rates therefore they stay in the active site longer reflected by their low  $K_i$  values, (nM to  $\mu$ M range) (36). These compounds form an enzyme-inhibitor complex that locates the lactam's carbonyl group in the enzyme's oxyanion hole causing a larger dipole between the carbonyl carbon and the attached oxygen facilitating the active site serine's nucleophilic attack. Once the acyl-enzyme is formed, the oxazolidinium ring, for clavulanic acid, and the thiazolidinium ring, for tazo and sulbactam, result in an imine structure. If the imine structure predominates (which has no conjugation with the carbonyl of the acyl-enzyme complex making the serine ester more prone to hydrolysis), then hydrolysis reverses the inhibition. Since we know this not the case, the imine therefore must tautomerize to yield the stable *cis* or even more

stable *trans* enamine form. These intermediates were detected by Paul R. Carey *et al.* in 2009 using a deacylation deficient class A SHV (E166A) trapping the intermediates (37).

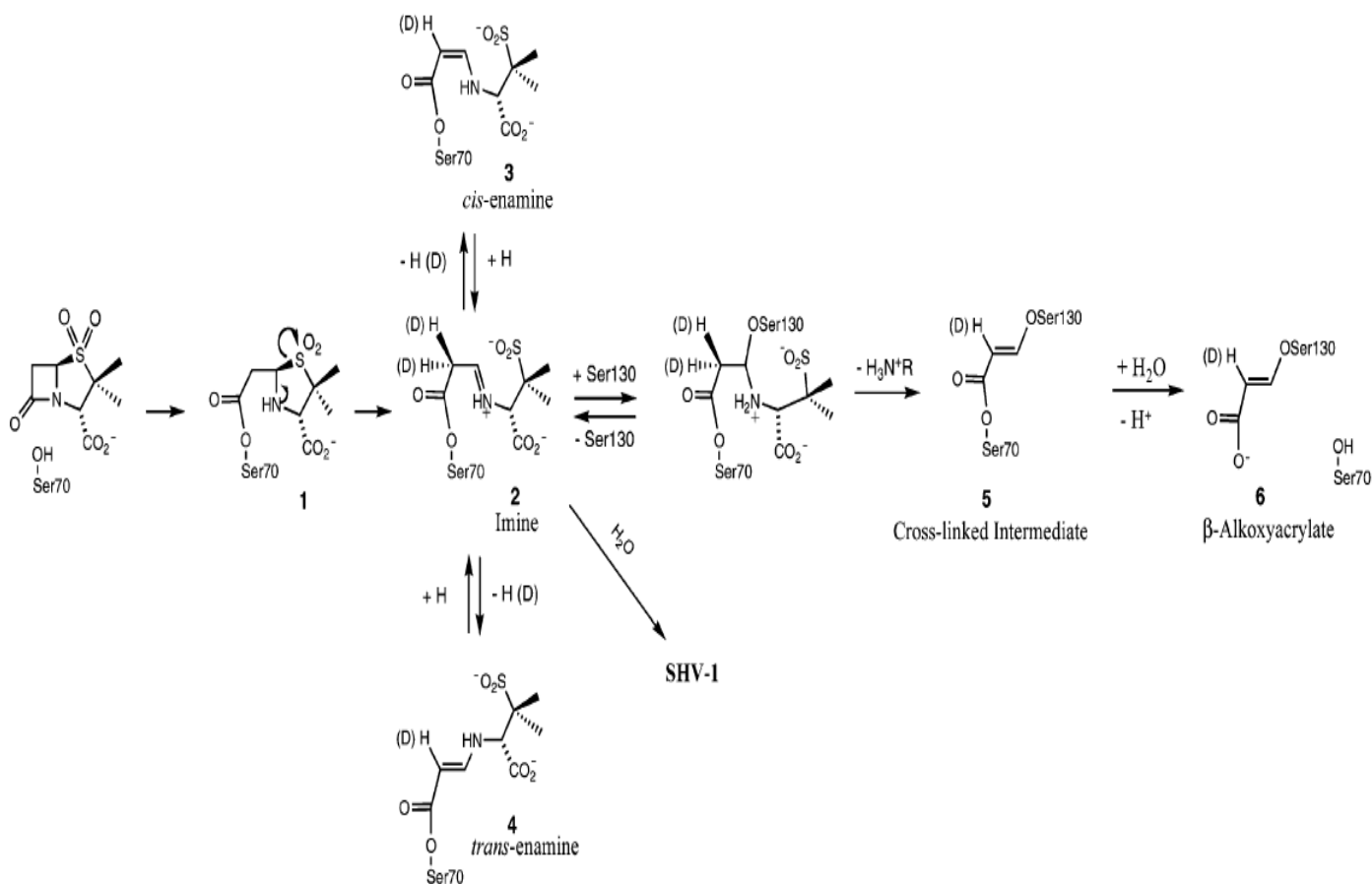


**Fig. 8. Simplified Reaction Mechanism for Class A  $\beta$ -Lactamase with Sulbactam (38)**

### Monobactams and Their Derivatives

Monobactams are a family of monocyclic  $\beta$ -lactams produced by saprophytic bacteria.

Discovered independently in 1979 by both the Sykes and Imada research teams, the characteristic feature of these compounds is the presence of a sulfonic acid moiety on the  $\beta$ -lactam nitrogen (39, 40). Of the naturally occurring monobactams, none really display much antimicrobial activity, but introducing electron-withdrawing substituents on the ring creates biologically active monobactams, such as monophosphams, monosulfactams, and monocarbams.

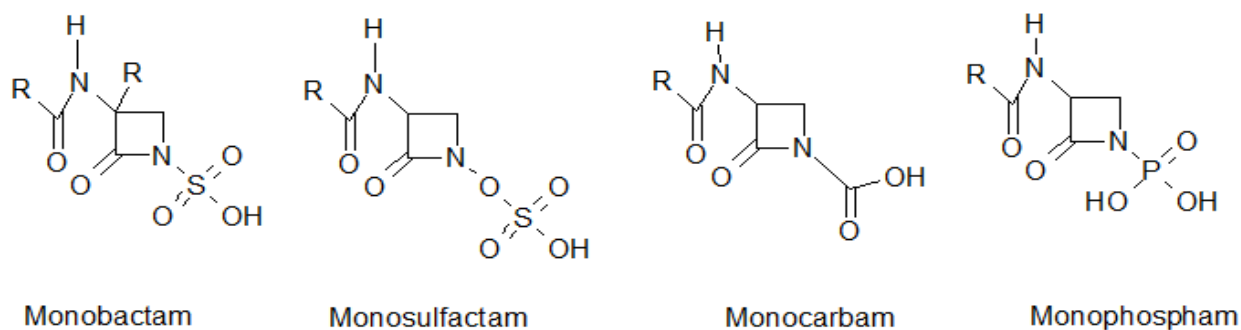


**Fig. 9. Monobactam and Synthetic Derivatives**

A well-known representative of synthetic monobactams is aztreonam (39). These modifications of the  $\beta$ -lactam nitrogen have been successful against  $\beta$ -lactamases, for example, the derivative *N*-sulfonyloxy- $\beta$ -lactam rapidly acylates the active site of TEM-1 enzymes (41). Upon acylation the tosylate is released and three stable intermediates are formed that resist deacylation by moving the ester carbonyl out of the oxyanion hole in the active site. Furthermore bridged monobactams, synthesized by Heinze-Krauss *et al.* in 1998, also proved to inhibit class C  $\beta$ -lactamases (42).

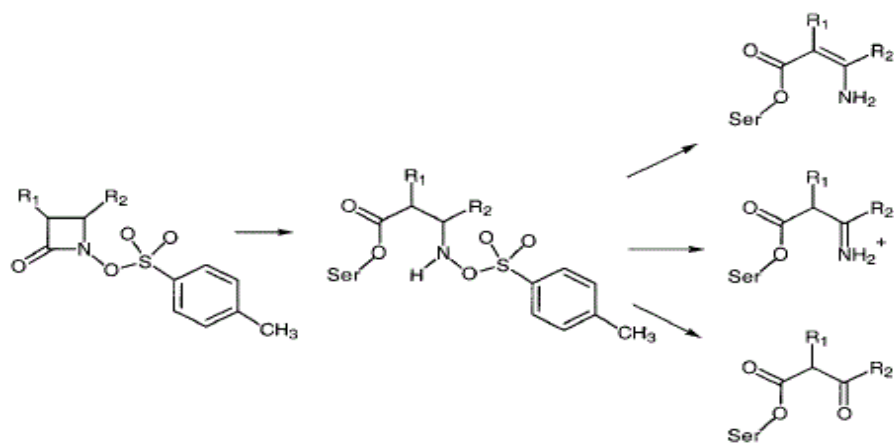


**Fig. 10. A Simplified Reaction Mechanism for Class A  $\beta$ -Lactamase with Monobactams (36)**

## Carbapenems

Originally isolated from soil bacterium *Streptomyces cattleya* these thienamycin derivatives possess broad spectrum activity and are considered the “last resort antibiotics” for treating multi-resistant bacteria. Meropenem, imipenem, ertapenem and doripenem are saved for the most egregious Gram-negative infections. Thienamycins are labile to  $\beta$ -lactamase hydrolysis leading to the development of an *N*-formimidoyl derivative, imipenem (43). These compounds differ from penicillin in that a carbon atom replaces the sulphur atom at position 1 and there is an unsaturated bond between C2 and C3 of the thiazolidine ring. Their resistance to  $\beta$ -lactamase hydrolysis is due to the trans-hydroxyethyl substituent at position 6 which is unique compared to penicillins and cephalosporins (44).

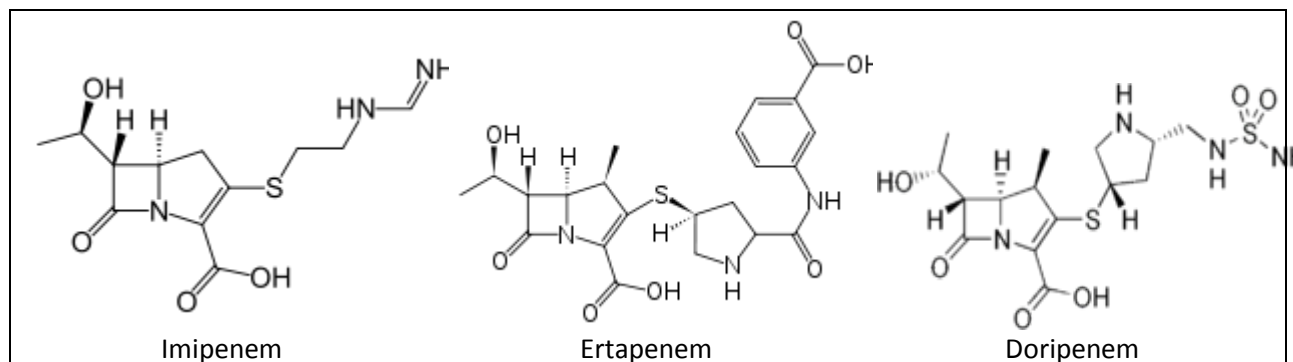


**Fig. 11. Structure of Carbapenems (36)**

Besides the  $\beta$ -lactams, that make-up most of the mechanism-based inhibitors,  $\beta$ -lactamases are also inhibited by transition-state analogues, novel mechanism-based molecules, and non-traditional small molecules that block the entrance of the active site. Class A and C  $\beta$ -lactamases are strongly inhibited by boronic acid derivatives. Steven Ness *et al.* synthesized two inhibitors that mimic the interactions of penicillin substrates with TEM-1 enzymes namely 1-phenylacetamido-2-(3-carboxyphenyl) ethylboronic acid and 1-acetamido-2-(3-carboxy-2-

hydroxyphenyl) ethylboronic acid with inhibition constants of 5.9 and 12 nM respectively by hydrogen bond formation, water displacement and rearrangement of the side chains (45).

### **Biphenyls, Ketones and Stilbenes**

In 1944 Faulkner discovered the bactericidal properties of some stilbenes and diphenyl derivatives. The common feature for all compounds that he tested and displayed bactericidal properties was the presence of one or more phenolic-type hydroxyl groups attached to the ring and ethyl groups between the rings (46).

Stilbenes are small molecules with molecular weights in the range of 200 to 300 g/mol.

They are naturally-occurring plant secondary metabolites and are derived from the phenylpropanoid pathway. Stilbenes are structurally similar to estrogen and are produced in many unrelated plant species (47). When a plant is subjected to abiotic stress, which is the negative impact of non-living factors on a living organism, such as drought, temperature, heavy metals, and salinity, the phenylpropanoid pathway is activated and stilbenes are produced and secreted. Stilbenes are protective molecules; they are able to defend the plant from viral and bacterial attack, as well as ultraviolet exposure. The most widely studied stilbene is resveratrol which has been shown to slow the progress of cancer. It has been known for more than sixty years that resveratrol inhibits viral, bacterial and fungal growth *in vitro* (48, 49).

In 2005 Xue & Seto designed a combinatorial library to probe the serine protease plasmin. This library was designed to react the ketone functional group of the cyclohexanone ring with the active site serine to form a hemiketal link. Four of their compounds had  $IC_{50}$  values between 2.7-3.6  $\mu$ M and hence were good inhibitors of plasmin (50).

### **Classification of $\beta$ -Lactamases**

Hailed as the “wonder drug” penicillin was introduced into therapeutic use in the early 1940s by the end of that same decade Abraham & Chain (51) had described the first  $\beta$ -lactamase with the ability to hydrolyze penicillin. Clearly antibiotic use was encouraging the growth of resistant strains. With each introduction of new  $\beta$ -lactams into clinical use, unfamiliar or previously unknown  $\beta$ -lactamases appeared.

Rapid classification and identification of these new enzymes becomes essential given the fact that  $\beta$ -lactams still account for about half of the antibiotics in use, and the appearance of new  $\beta$ -lactamases pose a serious problem that complicates medical treatment of bacterial infections worldwide.

In 1968 Sawai *et al.* (52) classified  $\beta$ -lactamases based on hydrolysis of cephalosporin versus penicillin as substrates. Jack & Richmond (53) in 1970 also classified  $\beta$ -lactamases according to substrate profile and added other parameters such as  $V_{max}$ , (hydrolysis rate), and  $K_m$ , (binding affinity) their individual susceptibility to inhibitors, and whether they were encoded by the chromosome or by plasmids.

This classification scheme was expanded in 1973 by Richmond & Sykes (54), and further reorganized and updated by Bush in 1995 (28). Recently a new classification scheme was developed to integrate functional and molecular characteristics, the Bush-Jacoby-Medeiros scheme. This four-group system classifies  $\beta$ -lactamases from naturally occurring bacterial isolates by substrate and inhibitor profiles, with substrate preferences among penicillin, oxacillin, carbenicillin, cephloridine, extended-spectrum cephalosporins, and imipenem, and inhibition by clavulanic acid.

There are four groups, 1, 2, 3, and 4 with multiple sub-groupings.

1. Cephalosporinases, not inhibited by clavulanic acid
2. Penicillinases, inhibited by clavulanic acid
3. Metallo- $\beta$ -lactamases
4. Penicillinases, not inhibited by clavulanic acid

Group two includes a vast array of enzymes including the common TEM  $\beta$ -lactamases (Group 2b), and the extended spectrum  $\beta$ -lactamases (Group 2be) that are inhibited by clavulanic acid but show resistance to expanded spectrum cephalosporins and aztreonam. These classification parameters face the problem that any point mutation can alter the substrate specificity and inhibition susceptibility changing the group to which the enzyme is assigned. Therefore, the older Ambler (1980) classification scheme based on amino acyl residue sequence is the most stable and widely used for  $\beta$ -lactamases that have been characterized so far (55). The Ambler classification scheme recognizes 4 classes of  $\beta$ -lactamases namely A, C, and D which are evolutionarily distinct groups of serine enzymes, and class B the zinc-dependent metallo- $\beta$ -lactamases (EDTA-inhibited) enzymes. There are four families of class A  $\beta$ -lactamases according to primary sequence alignments, *Escherichia coli* TEM-1, *Serratia marcescens* SME-1, *Klebsiella pneumoniae* SHV-1, *Bacillus anthracis* Bla1; they all share 30% sequence identity (56).

#### **Class A B-Lactamases**

The major classes within Ambler Group A are the TEM and SHV (sulfhydryl variant) types (56). They belong to the so-called clavulanic acid-inhibitory extended-spectrum  $\beta$ -lactamases

(ESBLs) and they also confer resistance to at least several expanded-spectrum cephalosporins (57).

TEM-1 is the most commonly-encountered beta-lactamase in Gram-negative bacteria. It was named after Temoniera (full name unknown), a patient from Athens, Greece, who was the first person from whom a  $\beta$ -lactamase in *E. coli* was isolated in 1963. Up to 90% of ampicillin resistance in *E. coli* is due to the production of TEM-1, and it is also responsible for ampicillin and penicillin resistance seen in *Haemophilus influenzae*. Single amino acid substitutions at positions 104, 164, 238, and 240 are responsible for the ESBL phenotype. These substitutions change the configuration at the active site allowing access to oxyimino-beta-lactam substrates. Opening the active site also enhances the susceptibility of the enzyme to clavulanic acid, a  $\beta$ -lactamase inhibitor. ESBLs displaying the broadest spectrum usually have more than a single amino acid substitution. Currently there are 140 TEM-type enzymes described based on combinations of amino acid substitutions. TEM-10, TEM-12, and TEM-26 are among the most common in the United States (58-60).

SHV-1 (sulfhydryl variant) shares 68% of its amino acid sequence with TEM-1 and has a similar overall structure. The name SHV was given by M. Mathew and colleagues in reference to the enzymes interaction with *p*-chloromercuribenzoate (PCMB) an agent that binds to sulfhydryl groups. (61) This is unique to SHV-1 since that other  $\beta$ -lactamases are unaffected by PCMB.

SHV-1 beta-lactamase is most commonly found in *Klebsiella pneumoniae* and is responsible for up to 20% of cases of plasmid-mediated ampicillin resistance in this species. ESBLs in this family also have amino acid changes around the active site, most commonly at positions 238 or 238 and 240. At present time more than 60 SHV varieties are known. These enzymes are the

predominant ESBL type found in Europe and the United States. SHV-5 and SHV-12 are among the most common (58).

The CTX-M  $\beta$ -lactamases were named for their greater activity against cefotaxime than against other oxyimino-beta-lactam substrates (e.g., ceftazidime, ceftriaxone, or cefepime). Rather than arising by mutation, they represent examples of plasmid acquisition of  $\beta$ -lactamase genes normally found on the genophore of *Kluyvera*, a new genus constituted by organisms formerly known as Enteric Group 8. *Kluyvera* strains share the properties of most members of the family Enterobacteriaceae (62).

CTX enzymes are not very closely related to TEM or SHV  $\beta$ -lactamases and they only show approximately 40% identity with the latter. More than 80 CTX-M enzymes are currently known and they are mainly found in strains of *Salmonella enterica* and *E. coli*. CTX-M-14, CTX-M-3, and CTX-M-2 are the most widespread (63).

### **The Structure of Class A $\beta$ -Lactamases**

The numbers of distinct protein folds are limited compared to the actual number of proteins found in nature. As of 2009, there are 1195 folds described of which one fifth represent the most common folds. (64) The DD-peptidase/ $\beta$ -lactamase superfamily is an example of a functionally diverse fold. (65) Class A  $\beta$ -lactamases are monomeric medium-sized proteins with  $M_r$  values of about 29 000 and they have 2 major structural domains, one entirely  $\alpha$ -helical and a second  $\alpha/\beta$  domain. The entirely  $\alpha$ -helical domain consists of eight helices where the central helix (A2) is surrounded by five other helices namely A4, A6, A8, A9. The second  $\alpha/\beta$  domain contains 5 anti-parallel  $\beta$ -strands, B2, B1, B5, B4, and B3, surrounded by 3  $\alpha$ -helices (Fig. 8).

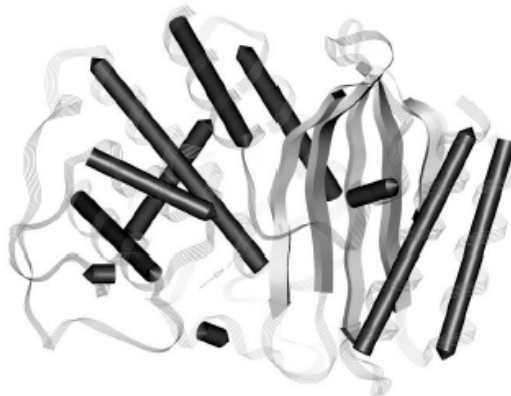


**Fig. 12. Overall Fold of Class A  $\beta$ -Lactamases** (66)

Nine residues in class A  $\beta$ -lactamases are strictly conserved; Ser70, Lys 73, Ser130 and Glu166 and are essential for catalysis the other five are responsible for maintaining important structural characteristics. It has been shown that aminoacyl residues at position 132(usually Asn) 234 (Lys or Arg) and 235 (Thr or Ser) and Gly236 are important for enzyme activity (67).

Four features have been identified in class A  $\beta$ -lactamases that appear to be involved in substrate recognition and catalysis. The first feature contains an active site serine residue located at the N-terminus of the long hydrophobic first helix of the all  $\alpha$ -domain. One helix-turn downstream, there is a lysine residue that its side chain points into the active site. The serine and lysine side chains are hydrogen bonded, suggesting that the lysine side chain amino group is involved in the catalytic process (68).

The second feature consists of a Ser-Asp-Asn motif (called the SDN loop) located in a short loop in the all  $\alpha$ -domain. The serine and asparagine residues point into the active site cleft. The third feature is a Lys-Thr-Gly (KTG) sequence that is situated on the innermost strand of the  $\beta$ -sheet, in the  $\alpha$  / $\beta$ -domain, and forms the opposite wall of the catalytic cavity.

The fourth and last feature is a negatively charged residue, usually Glu, located in the so-called  $\Omega$ -loop. In most cases this loop contains the sequence Glu-X-Glu-Leu-Asn. The Glu residue

seems essential in positioning a conserved water molecule close to the active-site serine. It has been hypothesized that this glutamate acts as a proton shuttle activating Ser70 for nucleophilic addition to the  $\beta$ -lactam ring (69).

### The Mechanism of Class A $\beta$ -Lactamases on $\beta$ -Lactam Antibiotics

Beta-lactamases hydrolyze  $\beta$ -lactam antibiotics in a two-step reaction and the mechanism involves acylation of the active site serine followed by the deacylation of the acyl-enzyme species. The catalytic pathway starts with a non-covalent encounter complex (Michaelis-Menten complex) that proceeds through a high energy intermediate to form an enzyme-acylated ground state. The acylated complex is attacked by water and proceeds through to the rate-determining step through a second high-energy intermediate that collapses into enzyme and product (Fig. 9).

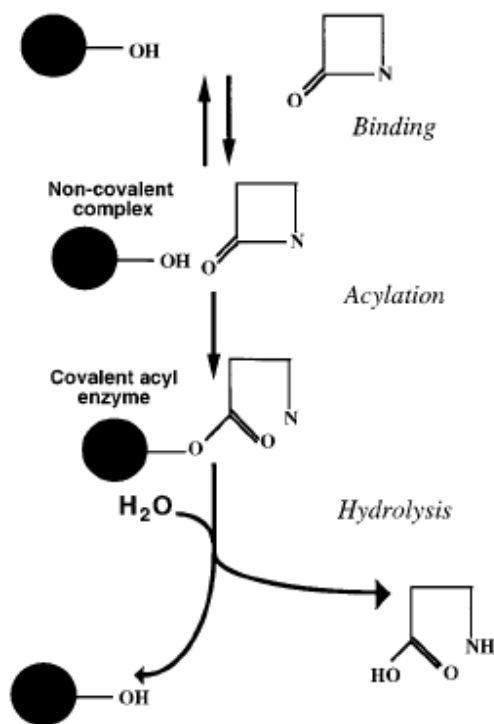
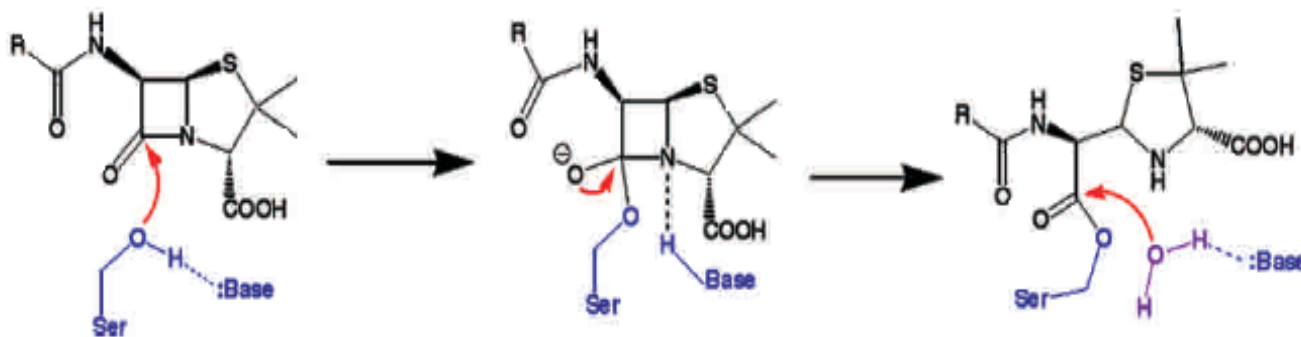


Fig. 13. General Scheme for  $\beta$ -Lactam Hydrolysis (70)

The reaction starts when the general base accepts a proton from the nucleophilic serine increasing the nucleophilicity of its  $\gamma$ O atom, which then attacks the carbonyl carbon of the  $\beta$ -lactam ring forming the acyl-enzyme tetrahedral intermediate.



**Fig. 14. Proposed Mechanism for  $\beta$ -Lactam Hydrolysis (71)**

The general acid then back donates the proton to the departing nitrogen breaking the scissile C4-N7 bond. In the second half of the reaction a general base abstracts a proton from water activating the water oxygen to attack the carbonyl carbon of the acyl-enzyme again forming a tetrahedral intermediate. The general acid back donates the proton to the  $\gamma$ -oxygen of serine and the serine is regenerated with the concomitant release of the inactive  $\beta$ -lactam antibiotic.

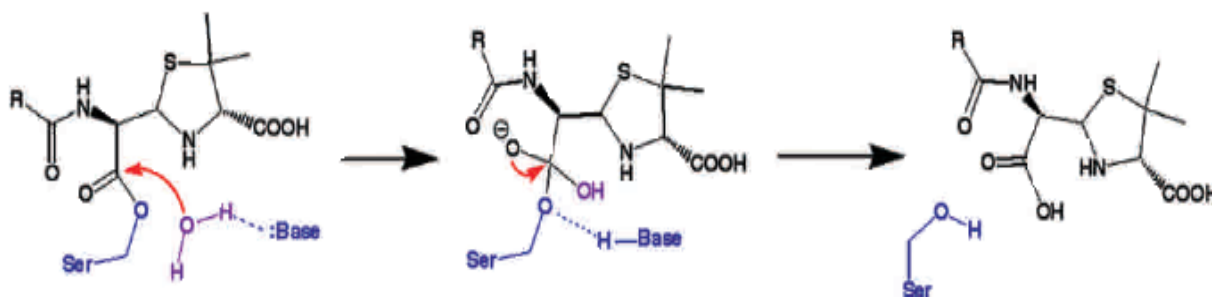


**Fig. 14. Proposed Mechanism for  $\beta$ -Lactam Hydrolysis (71)**

Class A  $\beta$ -lactamases sequester the  $\beta$ -lactam carbonyl in the oxyanion hole which contributes two hydrogen bonds from the main chain nitrogen atoms of Ser70 and Ala237 to the  $\beta$ -lactam carbonyl, thus causing a polarization that facilitates the acylation of the active-site serine. The nucleophilicity of the side chain hydroxyl group of Ser70 is augmented by a hydrogen bond to an active site water molecule (71). Formation of the acyl-enzyme intermediate requires at least two proton transfers: proton removal from the attacking serine and proton donation to the departing  $\beta$ -lactam amine. The general base that accepts the proton from nucleophilic serine is a conserved water molecule activated by Glu166. This results in two ion pair:

1. The  $\epsilon$ N group of Lys73 with the  $\gamma$ O of Ser70
2. The  $\epsilon$ O1 of Glu166 with the  $\text{H}_3\text{O}^+$ .

These ion pairs are balanced out by two hydrogen bonds between the  $\gamma$ O of Ser130, activated by the  $\epsilon$ N of Lys234. The first hydrogen bond is with the lone pair of nitrogen electrons on the  $\beta$ -lactam ring, and the second hydrogen bond is formed with the oxygen of the carboxyl group of the thiazolidine ring (Figure 16).

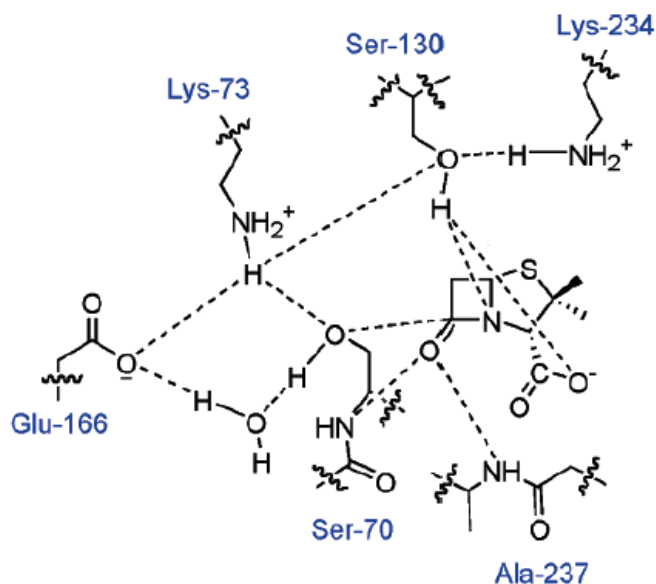


**Fig. 16. Schematic Representation of Residues in the Class A Active Site (72)**

Following the formation of the enzyme-substrate complex, the  $\gamma$ O of Ser70 attacks the C7 carbonyl carbon of the  $\beta$ -lactam ring, cleaving the scissile amide N4-C7 bond leading to covalent bond formation between the serine oxygen and the carbonyl carbon of the  $\beta$ -lactam ring. This creates a covalent transition state species containing an oxyanionic tetrahedral carbon center whose charge is stabilized by hydrogen bonding with two main chain nitrogen atoms of Ala237 and Ser70 (73).

Hydrolysis of the serine-ester linked penicillinoyl-enzyme occurs when Glu166 activates water to attack the carbonyl carbon C7 of the acyl-enzyme and back deliver the abstracted proton to the  $\gamma$ O of serine 70 leading to hydrolysis of the acyl- intermediate and regeneration of the enzyme.

### **Five Forms of Beta-Lactamase Resistance**

The extensive and often inappropriate use of  $\beta$ -lactam antibiotics for over sixty years has created an enormous selective pressure on bacteria which have in turn produced resistant strains of new  $\beta$ -lactamases or variants on the classical plasmid-mediated  $\beta$ -lactamases of the parent class A enzymes, TEM and SHV. In the last twenty years there has been an alarming acceleration in the number of  $\beta$ -lactamases produced by clinical isolates. For example, in 1984 only 19 plasmid-mediated  $\beta$ -lactamases (74) were reported, while today the number of known  $\beta$ -lactamases stands at 840. (75) When the carbapenem, imipenem, was first introduced in the 1970s, it was resistant to hydrolysis by most  $\beta$ -lactamases, now, there are a variety of bacteria producing carbapenamases (76).

There are five principal mechanisms that confer resistance with respect to  $\beta$ -lactams:

1. Changes in the target specificity. This resistance mechanism is seen in both Gram-positive and negative bacteria and is independent of  $\beta$ -lactamase production. PBPs interact with  $\beta$ -lactams forming a covalent complex via the active-site serine.  $\beta$ -lactams have varying affinities for different PBPs, and conversely, PBPs have distinct affinities for different  $\beta$ -lactams. Exposure of bacteria to  $\beta$ -lactam antibiotics causes changes in the composition and nature of PBPs through point mutations, so that either resistance to a particular antibiotic is acquired or the efficiency of the antibiotic is greatly reduced (77).

2. Loss or modification of outer membrane porins. after exposure to  $\beta$ -lactams over a period of time, some Gram-negative species either lose or modify outer membrane porins (78). For example, it has been observed that *Klebsiella pneumoniae* produces a new porin that is highly homologous to two major nonspecific porins that permit the general diffusion of molecules

across the outer membrane: a modified gene produces a porin that is narrower and therefore does not allow  $\beta$ -lactams to penetrate (79).

3. Efflux pumps. Found in both Gram-negative and Gram-positive bacteria, these energy-dependent transport proteins use the proton and sodium motive forces (pmf and smf, respectively) or hydrolysis of ATP to remove toxic substrates from either the periplasm or the cytoplasm of the bacteria to the outer environment. These pumps may be specific for one substrate or may transport a range of structurally dissimilar compounds such as antibiotics of different classes, and increased expression of efflux pump genes contribute to antibiotic resistance in a number of clinically important bacteria such as *Escherichia coli*, *Pseudomonas aeruginosa*, *Streptococcus pneumoniae*, and *Staphylococcus aureus*. All of these bacteria export fluoroquinolones. Some of them export multiple antibiotics (80).

4. Beta-lactamase inhibitor protein. The soil bacterium *Streptomyces clavuligerus* not only produces clavulanic acid but also a 165 amino acyl residue protein called  $\beta$ -lactamase inhibitor protein (BLIP), which inhibits  $\beta$ -lactamases from both Gram-positive and Gram-negative bacteria to varying degree. BLIP also inhibits some cell wall transpsptidases.

5. Beta-lactamase enzymes. The production of  $\beta$ -lactamases in both Gram-negative and Gram-positive bacteria is one of the most efficient and prevalent mechanisms of resistance to  $\beta$ -lactam antibiotics hydrolyzing the drugs before they can reach their target and exert the desired effect. All of these resistance mechanisms are important and each bacterium can create a combination of defenses depending on the selective pressures placed on it.

## Enzyme Characterization Chapter 3

### Introduction to Enzyme Kinetics

In order to use an enzyme for kinetic work, the kinetic parameters,  $K_m$ ,  $V_{max}$  and  $k_{cat}/K_m$  must be determined. There are two approaches to analyze these parameters. The first is to use a reaction progress curve, otherwise known as the integral method. This approach extracts information about the kinetic properties of an enzyme from the full time course of the reaction. The second method uses only the initial rates. This consists of measuring the initial velocity of the reaction at various substrate concentrations. In 1913 Leonor Michaelis and Maude Menten introduced the use of initial velocities and published the famous kinetic equation that bears their name (81). This treatment avoids the problem of changing conditions and time dependent inactivation of the enzyme during the course of an assay. It remains one of the most powerful and widely used assumptions for the kinetic characterization of an enzyme. To simplify kinetic treatment of enzyme-catalyzed reactions, Michaelis and Menten made the following assumptions;

1. The initial-rate  $v_0$  is measured during the initial-rate phase where less than 5-10% of the substrate has been depleted and little or no product has accumulated (no possibility of product inhibition).
2. The total concentration of active enzyme remains constant and equals the sum of the concentrations of the free and combined forms ( $[E_{total}] = [E_{free}] + [ES]$ )
3. The enzyme obeys saturation kinetics (steady-state assumption) such that the catalyzed rate depends on the concentration of  $[ES]$ , ( $v_0 = k_3 [ES]$ ) The rate-limiting step is the conversion of  $[ES]$  to product
4. The total enzyme concentration is small relative to substrate concentration and is kept constant ( $[S] \gg [Et]$ )

At low substrate concentrations the initial velocity is the linear portion of the graph where less than 10% of the substrate has been converted to product. It is the section of the reaction curve that exhibits the full effect of the initial substrate concentration while the effect of product formation is minimal. Within this region product formation has no effect on the rate of the reaction. As the reaction proceeds, the initial velocity begins to slow down as more substrate is depleted from the reaction mixture. Also the reverse reaction begins to influence the rate of the reaction as the concentration of product increases over time. At initial velocity conditions these factors do not have a chance to influence the reaction. The initial reaction rate  $V_{\text{initial}}$  is determined as the slope ( $\Delta[P]/\Delta t$ ) of a tangent line drawn from time zero. Under steady-state conditions where the concentration of substrate far exceeds the concentration of enzyme, the substrate concentration does not significantly change and the reverse reaction does not contribute to the rate. Under initial-rate conditions product formation is linear with respect to time and  $V_{\text{initial}}$  remains constant. Doubling the reaction time results in doubling the product formed, and the relationship between enzyme velocity and enzyme concentration is linear. When the reaction progress curve shows significant curvature, the relationship between product vs. time is no longer linear due to depletion of the substrate, accumulation of inhibitory products or accumulation of product. At this point the initial velocity is inexact. At non-linear portions of the curve there is an unknown concentration of substrate and steady state kinetic treatment is invalid.

## Beta-Lactamase Characterization

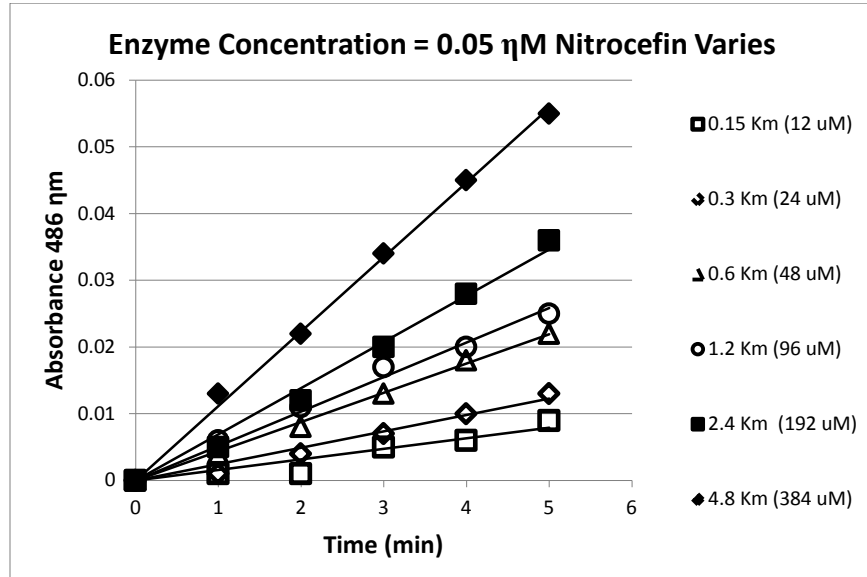


Fig. 17. Absorbance vs. time for varying substrate concentrations enzyme is constant at 0.05 nM

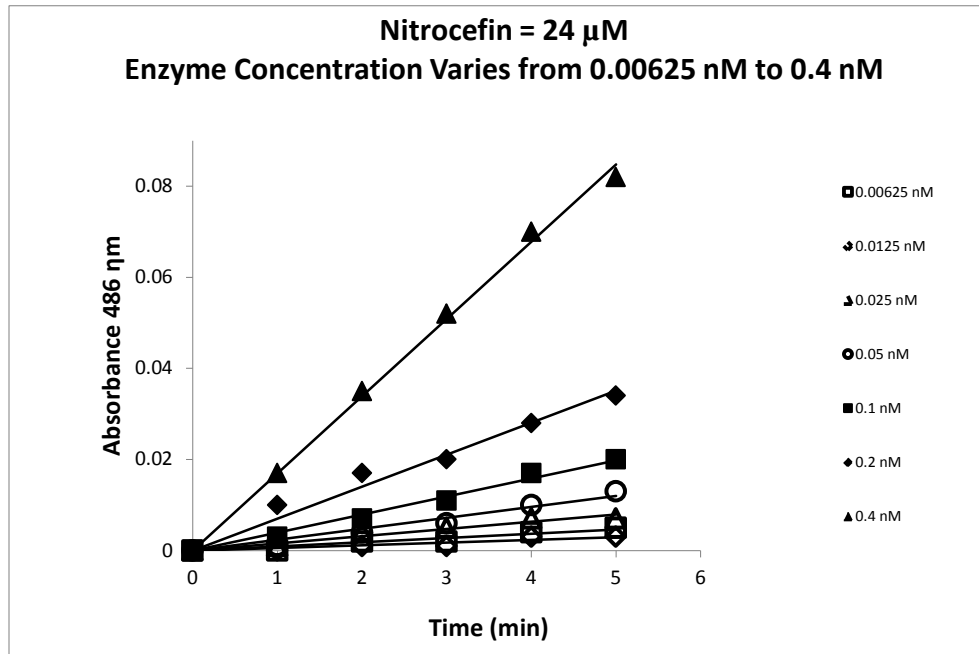
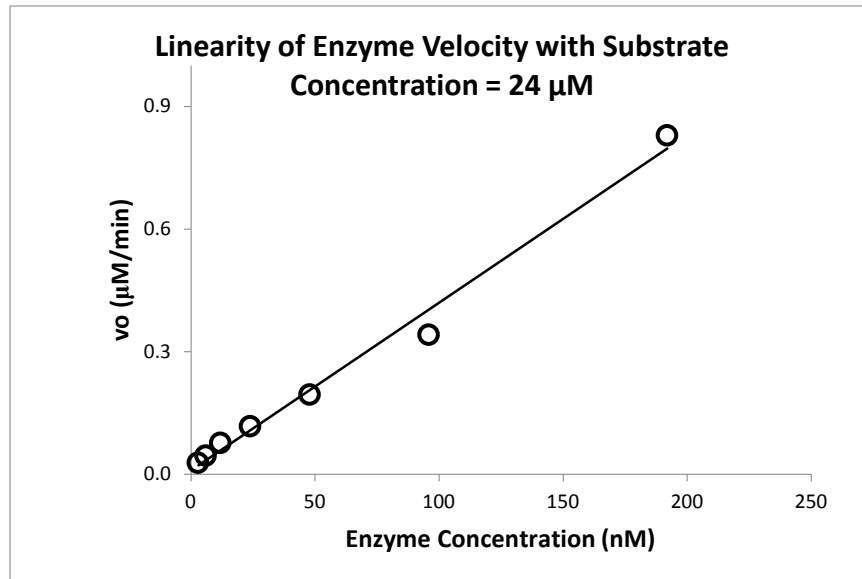


Fig 18. Absorbance vs. Time for Varying Concentrations of Enzyme. Substrate is constant at 24 uM



**Fig. 19. Linearity of Enzyme Velocity with Respect to Enzyme Concentration at Constant Substrate Concentration**

### **Kinetic Parameters**

Kinetic parameters ( $V_{\max}$ ,  $K_m$ ,  $k_{\text{cat}}$ ) for recombinant Y-49  $\beta$ -lactamase were determined from initial steady state velocities using a Biotek Synergy HT Multi-detection Microplate reader. The kinetic determinations were performed at 30 °C, 25 mM HEPES, pH 7.3. Data from duplicates were averaged, and the  $V_{\max}$  and  $K_m$  were obtained with nonlinear least squares fit of the data (Michaelis-Menten equation) using GraphPad Prism Software version 5.03 for Windows, (GraphPad Software, San Diego, California, USA).

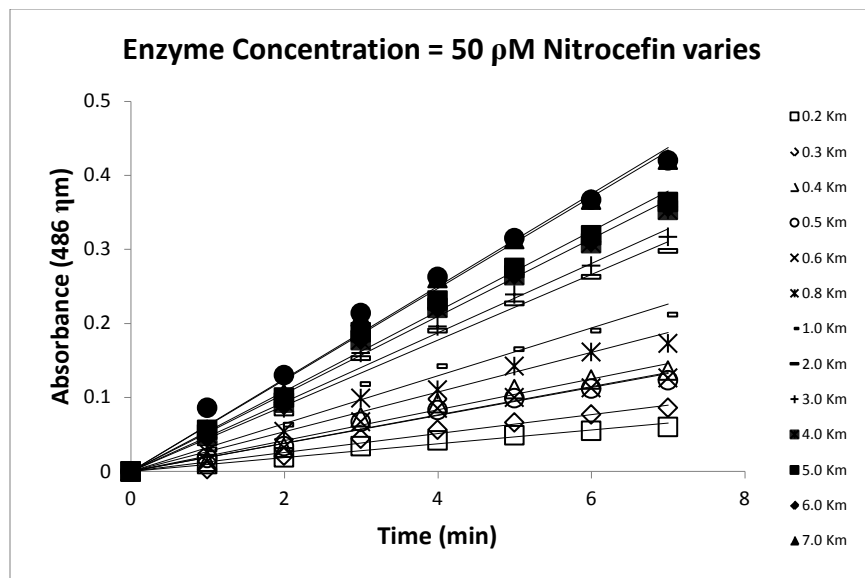


**Fig. 20. Graph of Absorbance vs. Time at Varying Substrate Concentrations. The enzyme is constant at 50  $\mu$ M**

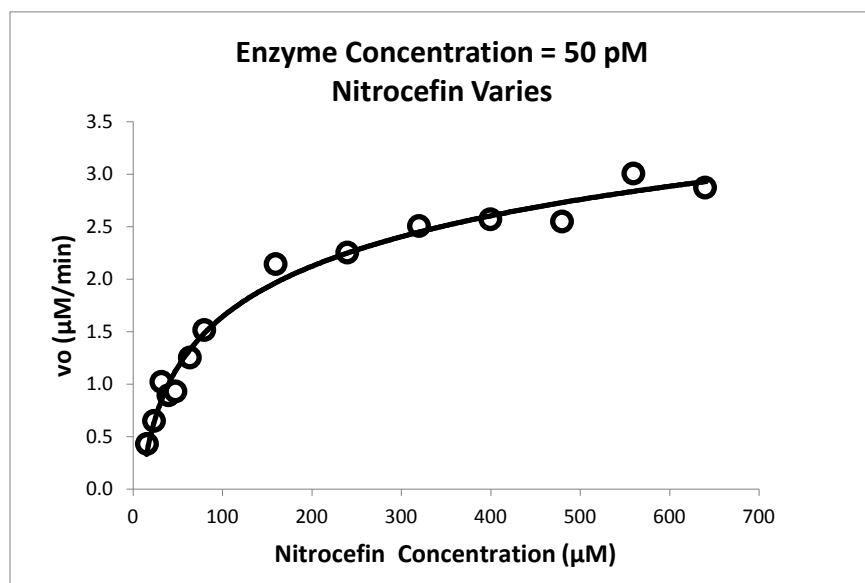


**Fig. 21. Graphical Determination of  $K_m$  and  $V_{max}$  for Y-49 Recombinant  $\beta$ -Lactamase**

**Table 2. Comparison of Kinetic Parameters**

Kinetic Parameters	Literature Values	Experimental Values
$k_{cat}$ ( $s^{-1}$ )	31	$15.34 \pm 0.5$
$K_m$ ( $\mu M$ )	81	$95.71 \pm 10.1$
$k_{cat} / K_m$ ( $\mu M^{-1} s^{-1}$ )	0.21	$0.16 \pm 0.05$

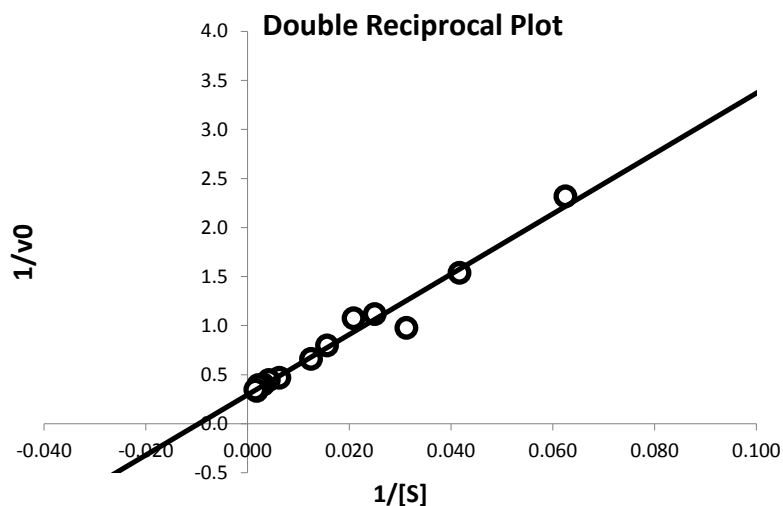


**Fig. 22. Lineweaver –Burke Plot**

## Materials and Methods

### Expression, and Purification of B-Lactamase

The host for the recombinant protein expression was *E. Coli* Top10 (Invitrogen), containing the pTrcHis B plasmid (Invitrogen), expressing Y-49, a Class A  $\beta$ -lactamase from *Mycobacterium tuberculosis*, a gift from Douglas S. Kernodle, M. D., Vanderbilt University School of Medicine, Division of Infectious Diseases, Nashville, TN (43).

### **Vector Ptrchish in *E. Coli* Top 10**

*Trc* promoter is a hybrid of *trp* and *lac* promoters for high level expression of fusion proteins.

*Lac* operator permits binding of the *Lac* repressor that represses transcription. The polyhistidine region allows for purification of recombinant fusion protein on metal chelating resins. Multiple cloning sites allow insertion or extraction of genes. The ampicillin resistance gene allows for the selection of the plasmid, and pBR322 is a low copy origin of replication.

### **Plasmid Isolation**

The  $\beta$ -lactamase gene insert is 900bp and is located between the XhoI and EcoRI restriction enzyme sites. Plasmid isolation was done using a Qiaprep Spin Miniprep Kit Protocol (catalog # 27106). The insert was verified via a 0.8% agarose gel in TAE buffer against a molecular weight marker using 5 lanes with uncut plasmid, XhoI, and EcoRI, separate digest, and a double digest. The empty plasmid molar mass is 4.4 Kb and the molar mass of the plasmid with insert is 5.3 Kb

### **Verification Blac Sequence**

Forward and reverse primers were synthesized by MWG Biotech, Inc., Atlanta GA. The insert was excised by digestion with EcoRI and XhoI restriction enzymes. The 900-bp insert was polymerase chain reaction (PCR) amplified and sequenced by Biotechnology Resource Center of Cornell University, Ithaca N.Y. The sequence was verified via GenBank accession no. Z73966.

```
MRNRGFGRRELLVAMAMLVSVTGCARHASGARPASTTLPAGADL
ADRFAELERRYDARLGVYVPATGTTAAIEYRADERFAFCSTFKAPLVAAVLHQNPLTH
LDKLITYTSDDIRISIPVAQQHVQTGMTIGQLCDAAIRYSDGTAANLLLADLGGPGGG
TAAFTGYLRS LGDTVSR L DAEPELNRDPPGDERDTTTPHAIALVLQQLVLGNALPPD
KRALLTDWMARNTTGAKRIRAGFPADWKVIDKTGTGDYGRANDIAVVWSPTGVYVVA
VMSDRAGGGYDAEPREALLAEAATCVAGVLA"
```

### **Expression of B-Lactamase**

One colony was used to prepare the starting culture in 15 mL of Luria-Bertani (LB) media at 37 °C containing 50  $\mu$ g/mL ampicillin. The next day the overnight was used to inoculate five 1L

bottles of LB media each containing 50  $\mu\text{g}/\text{mL}$  ampicillin at 37°C until an  $\text{OD}_{600}$  reached 0.8 absorbance. Expression of the recombinant six-histidine tagged-Y49  $\beta$ -lactamase fusion protein was induced with 0.4  $\mu\text{M}$  isopropyl- $\beta$ -D-thiogalactopyranoside (IPTG). After the addition of IPTG the temperature was decreased to 23°C and left in the LEX48 fermenter overnight. The following morning the cells were harvested via centrifugation at 4000 g for 15 min in a Sorvall RC BP+ with the HBB6 rotor. The cell pellets were resuspended in 100 mL of 20 mM HEPES at pH = 7.4 with 500 mM NaCl with 0.5 mM TCEP (Tris (2-Carboxyethyl) phosphine hydrochloride, an antioxidant), and 100 mM PMSF (phenylmethanesulfonylfluoride a protease inhibitor).

The cells were broken using a microfluidizer at 1500 lbs per square inch at 4 °C. In order to eliminate the cell debris, the broken cells were centrifuged at 23000 g in a Sorvall RC5C+ for 20 min using a SS34 rotor. The pellet was discarded and the supernatant was again centrifuged to eliminate cell membranes, at 200000 g in a Beckman 45ti rotor for 40 min. The supernatant was saved the pellet was discarded.

### **Purification of B-Lactamase**

One hundred mL of supernatant was injected into a 5 mL HisTrap column (APBiotech) in an FPLC AKTA purifier at 0.5mL /min at 4°C. The protein was eluted with imidazole in a step gradient as follows 10 column volumes of buffer containing 20 mM imidazole, followed 3 column volumes of buffer with 50 mM imidazole, then 3 column volumes of buffer with 100 mM imidazole and finally 10 column volumes of buffer with 250 mM imidazole. The fractions were analyzed by SDS PAGE gel and the first 3 fractions of the 250 mM imidazole elution were pooled and later concentrated to 0.5 mL volume for size exclusion chromatography.

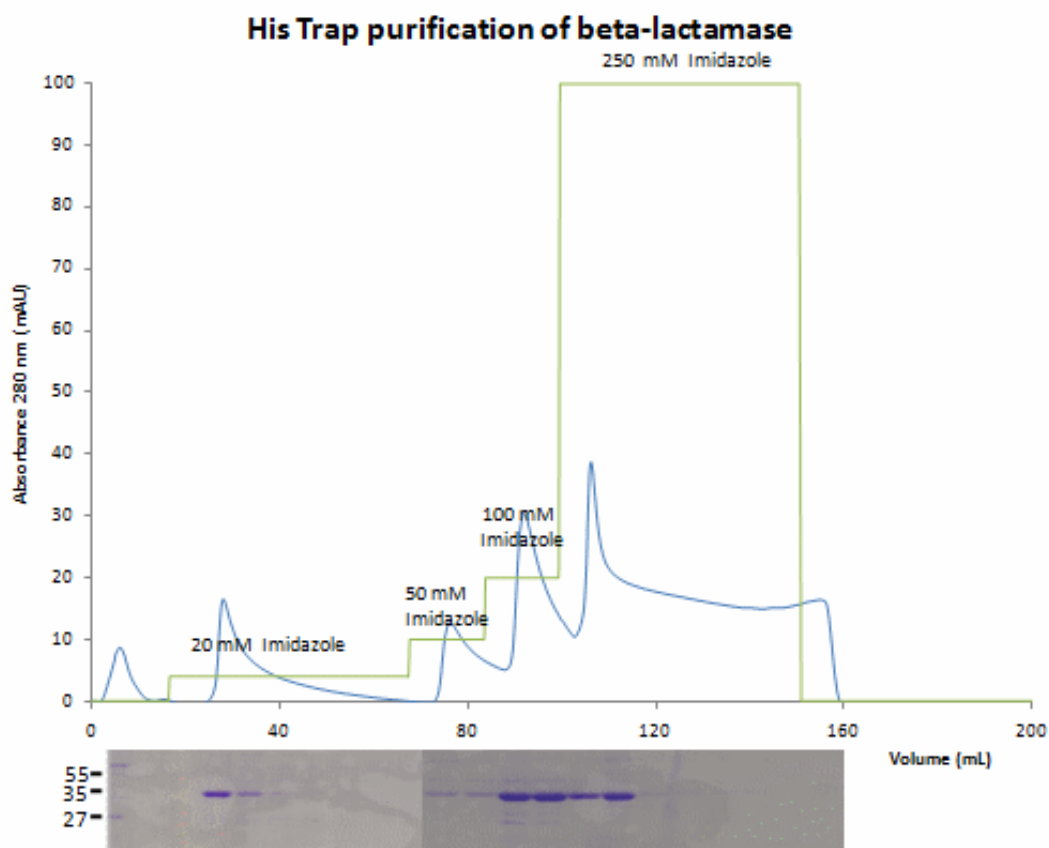


**Fig. 23. His Trap Column and SDS PAGE Gel**

The first 3 fractions were collected and pooled and concentrated to a final volume of 0.5 mL. The 0.5 mL was injected into a Superdex 200 10/300 size exclusion column. The chromatography was run at 0.5 mL/min at 4 °C. The 1 mL fractions were analyzed by SDS PAGE and the largest peak fractions were pooled giving a final volume of 2 mL.

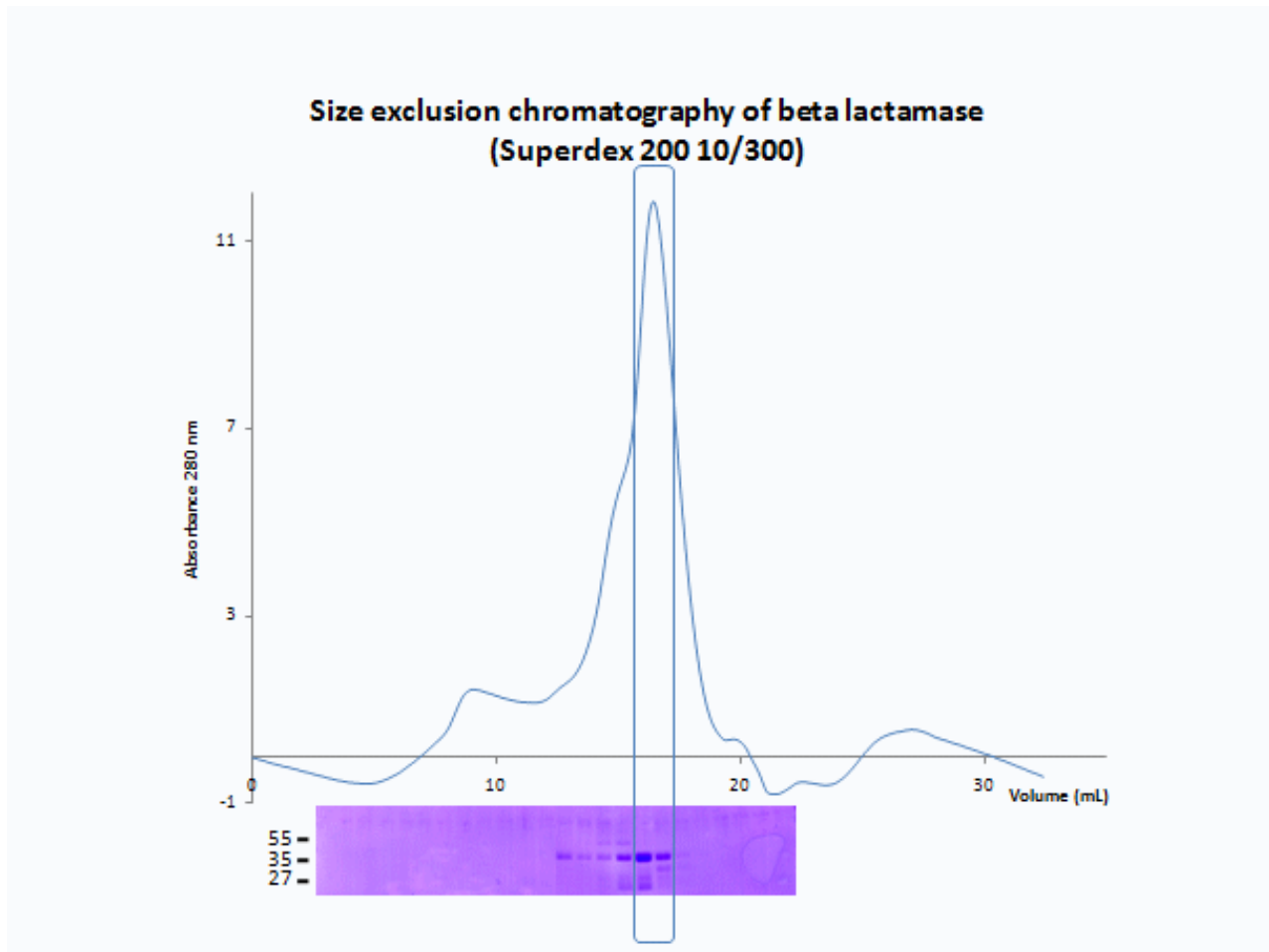


**Fig. 24. Size Exclusion Chromatogram and SDS PAGE Gel**

The protein was injected into a 10/300 Superdex 200 HR column for further purification. Protein concentration was determined by BCA assay, 0.84 mg/mL. The total protein = 1.68 mg. (0.84 mg/mL x 2 mL = 1.68 mg)

### **Western Blot**

The samples were run in a 10 to 20 % SDS PAGE gradient gel. The gel was blotted to a nitrocellulose membrane for 1 hour at 80 milliamps using a Fischer Biotechnology western blot apparatus in a western blot buffer (25 mM Tris, 192 mM glycine, 10% methanol).

The membrane was blocked with 5% milk powder in TTBS (Tween-Tris Buffered Saline: 0.1% Tween-20 in 100 mM Tris-CL (pH 7.5), 0.9% NaCl) on a rocker for 1 h at room temperature.

The blot was rinsed 3 times in TTBS then incubated in 20 mL of TTBS plus 2.5% milk powder with 4  $\mu$ L (1/5000) of the primary anti His Tag antibody (Sigma H1029). After 1 h the blot was washed three times in TTBS for 5 min each wash. The blot was then probed with the enzyme-linked secondary antibody in 20 mL of TTBS plus 2.5% milk powder with 4  $\mu$ L (1/5000) of anti Mouse IgG conjugated with HRP (Bethyl) for 1h at room temperature. Excess secondary antibody was rinsed from the membrane with 3 rinses in 20-25 mL TTBS for 5 min each wash. Finally the membrane was ready to expose using ECL, chemoluminescent detection reagent (Pierce 3210G).

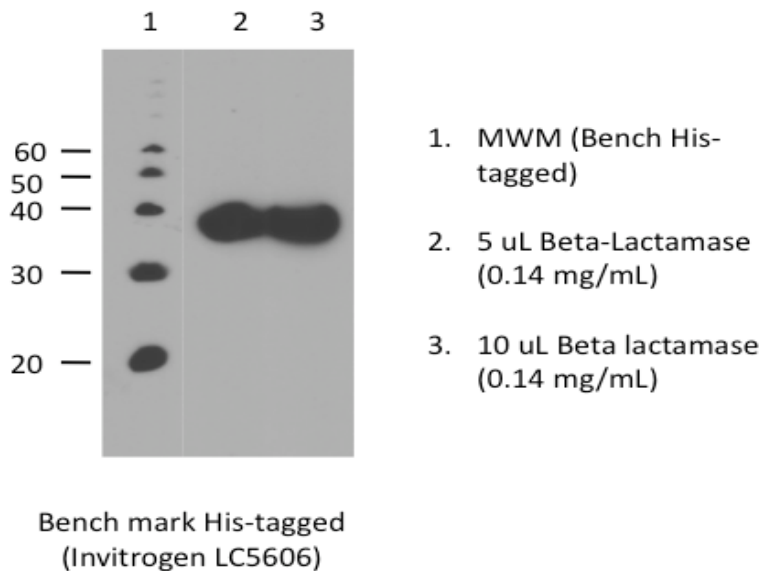


**Fig. 25. Western Blot Film**

### **Determination of Protein Concentration**

The bicinchoninic acid (BCA) assay is for the colorimetric detection and quantitation of total protein. This method combines the well-known reduction of  $\text{Cu}^{2+}$  to  $\text{Cu}^{1+}$  by protein in an alkaline medium with the sensitive and selective colorimetric detection of the cuprous cation ( $\text{Cu}^{+1}$ ) using a reagent containing bicinchoninic acid. The purple-colored reaction product of this

assay is formed by the chelation of 2 molecules of BCA with one cuprous ion. This water-soluble complex strongly absorbs at 562 nm over a working range of 20-2,000 µg/ml.

### Assay Protocol for Kinetic Inhibition

We measured the ability of a series of compounds to inhibit our recombinant Y-49 β-lactamase.

After determining the kinetic parameters for our enzyme substrate pair, we then performed direct competition assays using 24 µM (0.3  $K_m$ ) Nitrocefin (Calbiochem, CA.) as the indicator substrate ( $\epsilon_{486} = 20\,500\text{ M}^{-1}\text{ cm}^{-1}$ ), and 0.05 nM for the enzyme concentration.

The reaction was initiated with the addition of enzyme to the wells. The initial velocity readings were limited to the first 720 seconds (12 min) so that the only inhibition observed would be from the formation of the Michaelis-Menten complex. Duplicate experimental determinations were made for each unique nitrocefin/inhibitor concentration, and the data were analyzed by nonlinear regression using a competitive inhibition model. Each initial velocity was plotted *versus* concentration of inhibitor and fit to determine  $K_i$ .

According to Williams & Morrison (82), the binding inhibition constant  $K_i$  (shown as  $K$  in equation (1) (82) can be determined by nonlinear least-squares fit (83) of reaction velocities to equation (1), where  $v$  is the initial reaction velocity at inhibitor concentration  $[I]$ ,  $v_0$  is the initial reaction velocity in the absence of inhibitor, and  $[E]$  is the active enzyme concentration. The total enzyme concentration is treated as a constant under steady state conditions.

$$v = v_0 \frac{[E] - [I] - K + \sqrt{([E] - [I] - K)^2 + 4[E]K}}{2[E]} \quad (1)$$

Formula for the inhibition constant is rearranged to find  $K_i$  (K) (82).

$$K = \frac{[I] - [E] (1 - v/v_0)}{v_0/v - 1} \quad (2)$$

Because no experiment is without errors, it would be fine to perform only two velocity experiments to determine  $v$  and  $v_0$  then calculate the inhibition constant  $K_i$ . Each measurement of  $v$  and  $v_0$  is affected by random experimental error therefore one must perform experiments at different concentrations of inhibitor  $[I]_j$  ( $j = 1, 2, \dots, n$ ), and finally approach the true value of  $K$  as an average according to equation (3) (82).

$$K = \frac{1}{n} \sum_{j=1}^n K_j \quad (3)$$

## Peptides Chapter 4

### Introduction To Peptide Inhibitors

Predicting enzymatic reactions is one of the important and essential areas of biochemistry. The new paradigm in drug design is information analysis using developments in the areas of molecular structure description, combinatorial chemistry, and computer simulations. Within this broader outlook there has evolved the following approach towards drug design: probing a biological system with a series of molecules with known structure to discover a correlation between these structures and some measurable parameter, activity, inhibition or a physical property of the biological system, and turn the relationship into a mathematical model to interpret experimental data. This approach is known as structure-activity relationship, (SAR), and traditionally SAR uses three types of properties hydrophobic, steric, and electronic.

The challenge is to find some code that is information-rich for the molecule or a fragment of the molecule and use it to predict and design compounds. However, this approach has been quite successful, for example, in the development of inhibitors targeting malaria proteases (84, 85), influenza inhibitors (86), dopamine antagonists (87), and thrombin inhibitors. (88)

The key features for the binding of cefoxitin are the interactions between the carbonyl carbon of the  $\beta$ -lactam ring with the main chain nitrogens of Ser237 and Ser70 so that the tetrahedral intermediate is stabilized within the oxyanion hole of the enzyme. The second feature necessary for electrostatic and hydrogen binding interactions are between with the carboxylate group oxygens of dihydrothiazine ring and conserved residues Lys234, Ser130, and Thr235/237. The third feature that forms energetically favorable hydrogen bonds between oxygen 21 of cefoxitin that binds with Asn103 and 132 (Fig. 22). The idea is to mimic as much of these interactions as possible in the design of the tetrapeptide.

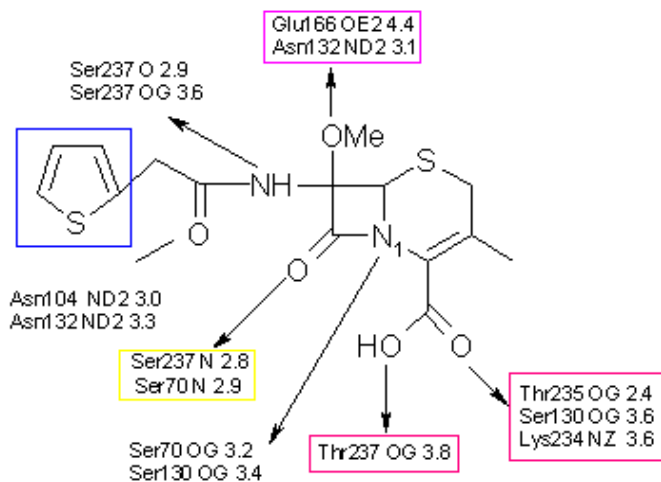


**Fig. 26. Cefoxitin's Interaction with Protein Residues**

Based on the work of Wanzi Huang *et al.*, using phage display, a 6-mer linear peptide with the sequence RRGHYY was found to inhibit class A *Bacillus anthracis* Bla1, ( $K_i = 42 \mu\text{M}$ ) and class A TEM-1  $\beta$ -lactamase, ( $K_i = 136 \mu\text{M}$ ). (89) Table 3 illustrates the differences in  $\Delta G$  Kcal/Mol between the original Huang 6-mer and shorter variations approaching from the N-terminal and the C-terminal sides.

**Table 3.  $\Delta G$  Kcal/mol**

Peptide	Class A enzyme PDB number	$\Delta G$ Kcal/Mol
RRGHYY	1YM1	6800.0
	1YMX	282.0
RRGHY	1YM1	750.0
	1YMX	1759.0
RRGH	1YM1	987.0

	1YMX	-147.1
RGHY	1YM1	-145.6
	1YMX	-172.1
GHYY	1YM1	307.8
	1YMX	-171.1

We inspected eight structures from an initial library in which the N-terminal group is arginine (13) and the C-terminal group is tyrosine (Tyr). The guanidino group is ideal for binding negatively charged amino acid residues and because of this arginines are often found in protein binding sites.

The guanidine group of Arg in all eight cases interacts with either Asn between distances of 2.6 to 3.9 Å, or with Asp from 2.9 to 4.7. The bond distances between the guanidino group of Arg and Asp are within salt-bridge distances (Table 4). Furthermore the N-terminal Arg residue positions the N-terminal main chain nitrogen to within donating hydrogen-binding distance of Ser237 or Asn104 in the active site (Table 5).

**Table 4. Interactions of Arginine with Protein**

Tetrapeptide Guanidino	Protein Residue	Distance in Å
RDHY	Asn104 ND	2.6
RRGY	Ser237 OG	3.6
RSHY	Asp240 OD1	2.9
	Asp240 OD2	3.8
RPHY	Asp240 OD1	4.7
	Asn104 ND	2.6

RGMY	Asn104 ND	2.6
RGSY	Asn104 O	3.0
	Asn104 O	3.9
RDYY	Asn104 ND	2.6
RKHY	Asp240 OD1	3.6
	Asn104 ND	3.8

**Table 5. Interactions of N-Terminal Nitrogen with Protein**

Tetrapeptide N-Term N	Protein Residue	Distance in Å
RDHY	Ser237 O	2.5
	Ser237 OG	3.3
RRGY	Ser237 O	2.3
RSHY	Ser237 O	2.7
RPHY	Ser237 O	2.5
	Ser237 OG	3.3
RGMY	Ser237 O	2.5
RGSY	Asn 104 ND	2.4
	Asn104 O	3.3
RDYY	Ser237 O	2.5
RKHY	Ser237 OG	4.1

**Table 6. Interactions of Tyrosine OH with Protein**

Tetrapeptide OH Tyr	Protein Residue	Distance in Å
RDHY	Met68 O	2.0

	Asn245 ND	3.2
RRGY	Asn132 ND	2.5
RSHY	Thr216 O	3.6
RPHY	Met68 O	2.0
	Asn245 ND	3.2
RGMY	Met68 O	2.0
	Asn245 ND	3.2
RGSY	Thr216 O	3.6
RDYY	Met68 O	2.1
	Asn245 ND	3.2
RKHY	Ser220 OG	2.4
	Thr216 O	2.8

Another binding feature seen in these eight structures is the interaction of the Tyr hydroxyl group with Met, Asn, and/or Thr and Ser (Table 6).

**Table 7. Interactions of Main Chain Carboxylate Group with Protein**

Tetrapeptide main chain COO- group	Protein Residue	Distance in Å
RDHY	Ser237 N	3.3
	Thr235 OG	3.4
RRGY	Asn132 ND	2.5
	Asn104 ND	3.0
RSHY	Thr216 O	3.6
RPHY	Asn245 ND	3.2

RGMY	Ser237 N	3.3
	Thr235 OG	3.4
RGSY	Arg276 NHZ	3.1
	Arg276 NE	3.7
RDYY	Ser237 N	3.3
	Thr235 OG	3.4
RKHY	Ser220 OG	2.4
	Thr216 O	2.8

The main chain carboxylate group of the tetrapeptides is within binding distance of Ser/Thr, Arg, and Asn adding to the binding affinity of these 4-mers (Table 7).

When we substituted Ala for Arg in this position the binding free energies all became much more positive, Table 8. These interactions are important for stabilizing the binding of the substrate in the active site.

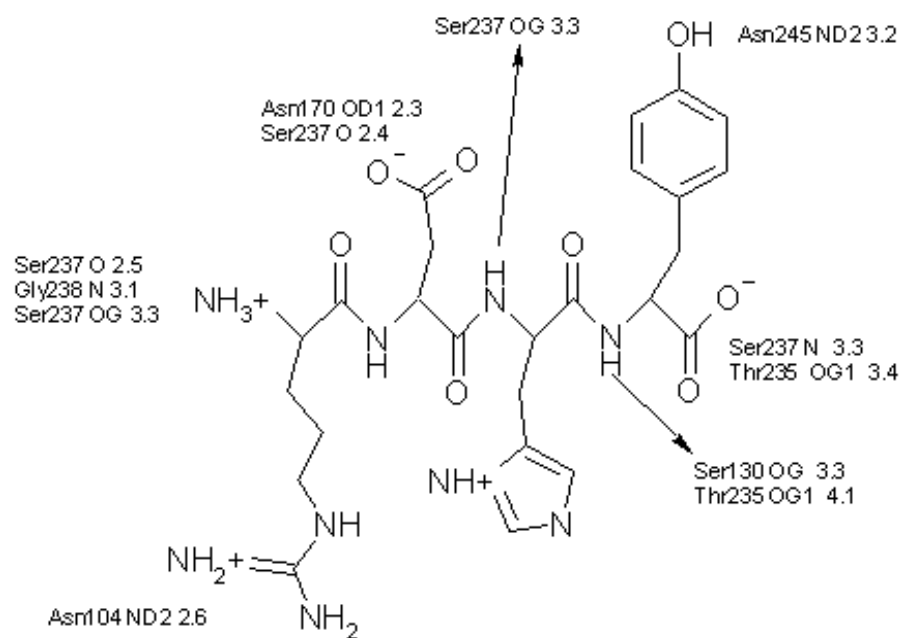
The hydroxyl group of Tyr at the C-terminal end, not unlike the Huang 6-mer, binds either Asn, or Thr only 1 structure binds Ser. We substituted Phe for Tyr and the  $\Delta G$  values were more positive see Table 8.

**Table 8. Comparison of  $\Delta G$  Values for Substitutions in the P1 and P4 Positions of 4-Mers**

Ala 4-mer	$\Delta G$ Kcal/Mol	Phe 4-mers	$\Delta G$ Kcal/Mol	RXXY 4- Mers	$\Delta G$ Kcal/Mol
ADHY	3057.0	RDHF	-57.7	RDHY	-151.6
ARGY	668.0	RRGF	-42.3	RRGY	-154.6
ASHY	-27.0	RSHF	-40.0	RSHY	-183.0

APHY	142.3	RPHF	-59.6	RPHY	-207.5
AGMY	1196.4	RGMF	-59.3	RGMY	-163.5
AGSY	-46.5	RGSF	-56.9	RGSY	-171.7
ADYY	118.0	RDYF	235.0	RDYY	-85.1
AKHY	-176.9	RKHF	507.2	RKHY	-206.1

With these four features in mind I constructed a tetrapeptide library (RXHY) with arginine in position 1, histidine in position 3 and ending with tyrosine in position 4 to find correlations that relate the binding pattern in question to molecular descriptors and develop this relationship into lead peptides. The ligand-protein contacts were derived with LPC software. (90)



**RDHY-17 -151.6 Kcal/Mol**

**Fig. 27. Interactions of RDHY in the Class A Active Site**

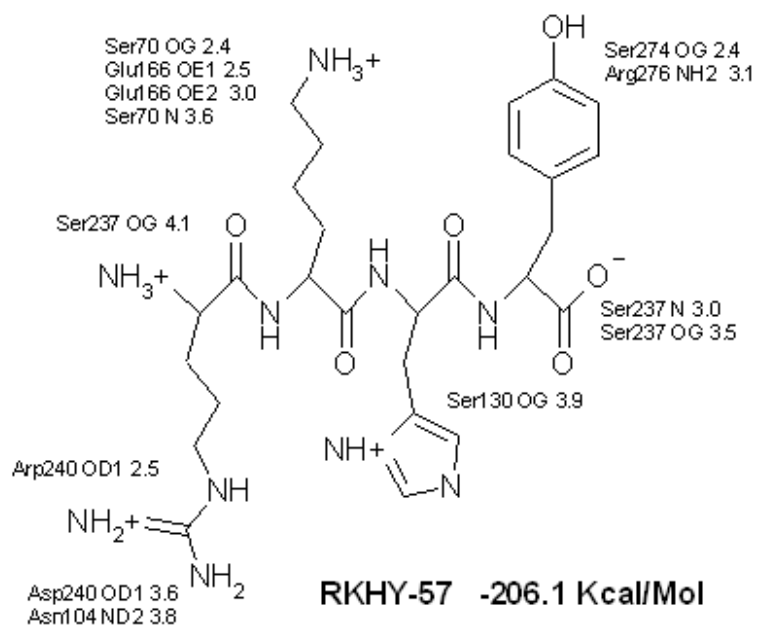


**Fig. 28. Interactions of RKHY in the Class A Active Site**

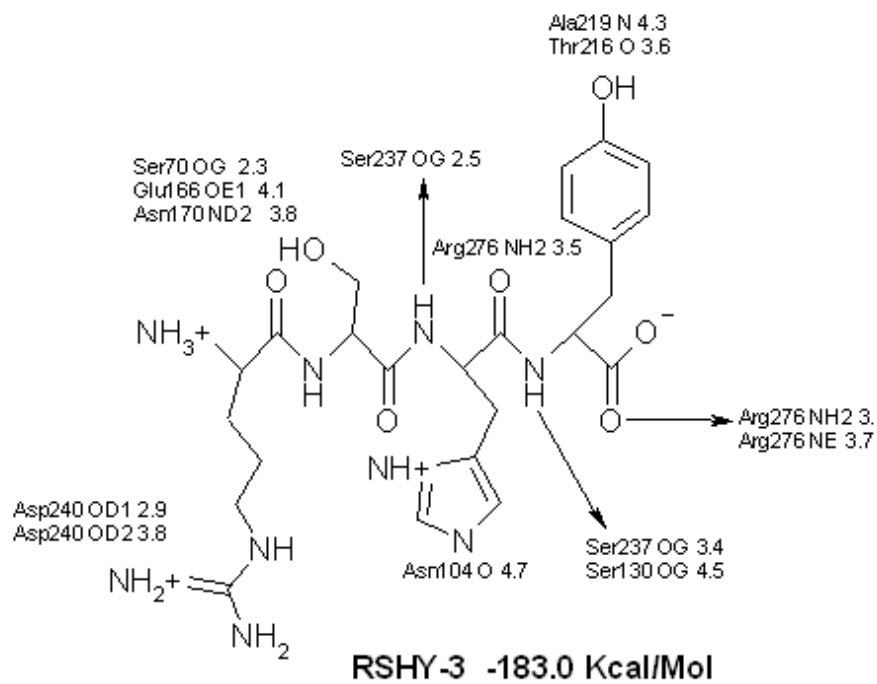


**Fig. 29. Interactions of RSHY in the Class A Active Site**

We propose to generate molecular data including geometries, distances, energies, hydrogen bonding, electronic, steric, and hydrophilic/phobic interactions to create a paradigm for manipulating these data in the attempt to find consistent relationships between the molecular properties of each putative inhibitor activity with respect to  $\beta$ -lactamase stability.

These rules may predict correlations between structural and functional interactions such that potential compounds may be modeled and estimated to fit the target by computing scoring functions or energy functions. These functions will then be used to compare variables with one another in the initial design phase. The best scoring compounds will be synthesized. Empirical data, protein binding assays will be collected and the tetrapeptides further refined. Therefore, using peptides as initial leads and scaffolds we can increase the probability of developing a viable family of inhibitors to aid in the quest for new  $\beta$ -lactamase stable non- $\beta$ -lactam inhibitors.

## **Material and Methods**

### **Solid Phase Synthesis of Peptides**

#### **Deprotection and Swelling of The Resin**

Fmoc-Rink-Amid-MBHA Resin 4'-(R,S)-alpha- [1-Fmoc-amino]-2,4-dimethoxybenzyl-phenoxyacetyl-amido- (4-methylphenyl)methyl polystyrene resin (Anaspec, 100-200 mesh, 0.64 mmol/g) was swollen in 20 ml of dimethyl formamide (DMF) in a continuous N<sub>2</sub> stream for 30 min followed by 30 min in vacuo. The swollen resin was 9-Fluorenylmethoxycarbonyl, (Fmoc), deprotected for 20 min by adding 20 ml of a 40% piperidine solution prepared in DMF. All traces of piperidine were removed by filtering and washing 3 times each with DMF (~15 ml), followed by methanol (MeOH) (~15ml). The washes were repeated until pH paper changed from

basic to neutral. The resin was vacuum dried and the Kaiser Test performed on a small amount of the resin in an ignition tube.

#### **Kaiser Test**

The following solutions were prepared:

- 1) 5g ninhydrin in 100 mL ethanol
- 2) 80g of liquefied phenol in 20 mL of ethanol
- 3) 2 mL of 0.001 M aqueous solution of potassium cyanide in 98 mL of pyridine .

Three drops of solution 1 is added to the ignition tube holding the resin followed by 3 drops each of the other two solutions. This is mixed well with a Pasteur pipette and placed in an oven at 110 °C for ~5minutes. A positive test, indicated by blue resin beads, suggests the presence of free primary amino groups. The Kaiser Test is indirect proof of free primary amino groups.

#### **Attachment of Amino Acids to Resin**

A 4 fold excess (0.170 mmol) was used for each amino acid in the P<sub>1</sub>' position. The carboxylic group of each amino acid was activated by dissolving equimolar amounts of P<sub>1</sub>' amino acid, HBTU in HOBt (0.5 M), 2-(1H-Benzotriazole-1-yl)-1,1,3,3-tetramethyluronium hexafluorophosphate in 0.5 M 1-Hydroxybenzotriazole solution in DMF. The swollen deprotected resin is divided among the activated P<sub>1</sub>' position amino acids and an equimolar amount of DIEA (N, N-Diisopropylethylamine) is added. All reaction mixtures are left to couple at room temperature for 1.5 h. The coupling mixture is quantitatively transferred to a sintered Buckner funnel, filtered and washed 3 times with DMF (~15 ml), followed by 3 washes with MeOH (~15 ml), and dried in vacuo. A new Kaiser test is performed to indicate the absence of any free primary amino groups. Transparent beads indicate coupling.

### **Elongation of the Peptide Chain**

The resin was washed as usual with DMF followed by methanol. The resin with the P<sub>1</sub>' amino acids in position is cycled through another Fmoc deprotection while the P<sub>1</sub> amino acid is activated. The cycle is repeated. The last amino acid is Fmoc deprotected after the last cycle in 2 ml of 40% piperidine solution prepared in DMF, and the resin dried in vacuo.

### **Cleavage from Resin and Deprotection of Side Chains**

The peptide is cleaved from the resin and the acid labile protecting groups using 95% TFA, 2.5% EDTA, and 2.5% thioanisole. The cocktail is shaken for 3 h at RT then washed exhaustively in DMF. Peptides are precipitated by adding cold methyl tert-butyl ether (MTBE) and left at -20°C overnight. The solution, which should have a white precipitate and colored yellow resin, is filtered and 4 times with MTBE (~15 ml) the filtrate is discarded. The resin is washed with 50% acetonitrile in distilled water 4 times (~10ml). The aqueous phase is retained, rotor-evaporated to dryness and resuspended in 200 µL of distilled water. The crude peptide libraries were analyzed via HPLC and ESI-MS mass spectrometry.

### **Chromatographic Analysis**

All peptide synthesis should include an amino acid composition and an analytical chromatographic analysis. Amino acid analysis will show gross amino acid deletions. Analytical chromatographic analysis will indicate the overall homogeneity of the product.

Both a Waters 2695 HPLC instrument and a Shimadzu (LCMS-2010EV) were used to purify the crude peptides with a reversed phase C-18 Varian column, 100 Å pore size, 5-10 micron packing. Separation was achieved using the following buffers: buffer A = 0.1% TFA in 100% de-ionized water, the aqueous phase and, buffer B = 0.05% TFA in 100% acetonitrile, the organic phase. The total run time per sample is 45 min at a flow rate of 1 ml/min, monitored at

UV 215 nm. The % A in the gradient described below in table 3 is implied. The column was equilibrated for 20 minutes between each run to the high aqueous phase.

**Table 9 . Gradient HPLC**

Time (min)	% Buffer B
0	5
65	55
35	95
43	5
45	Stop

The following chromatographs show the purification of several peptide sequences from the initial library achieved using the gradient in Table 3.

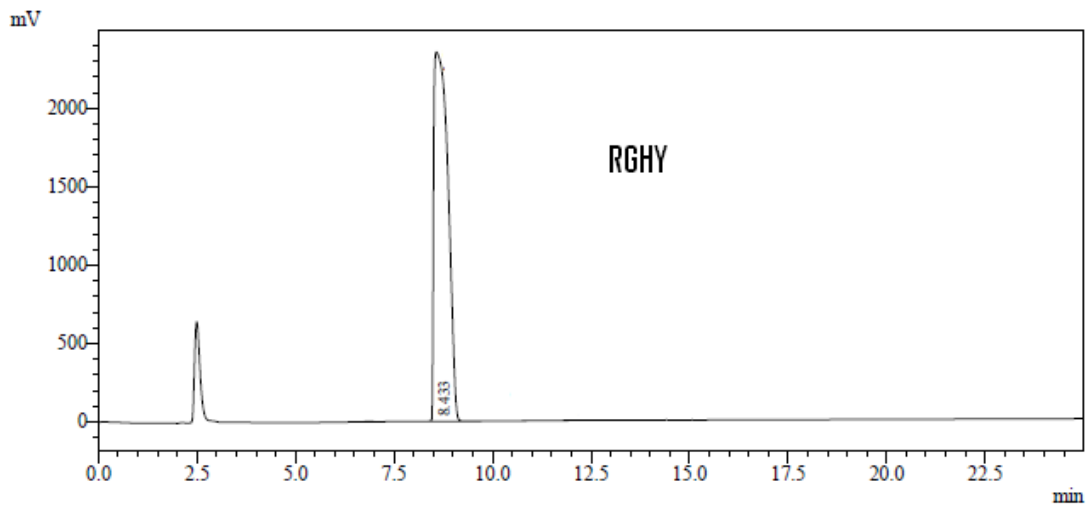


**Fig. 30. HPLC Chromatogram of Crude RGHY**

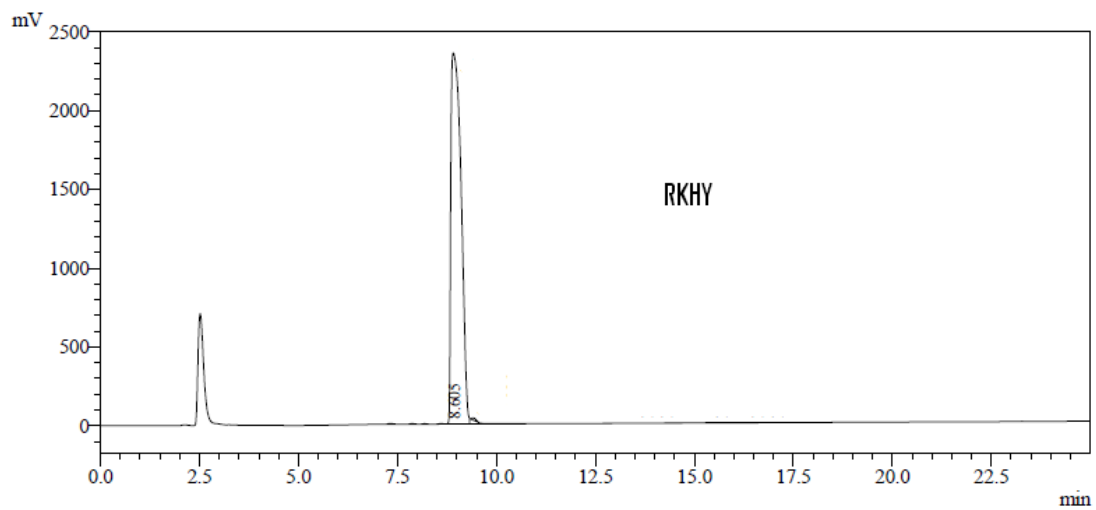


**Fig. 31. HPLC Chromatogram of Crude RKHY**

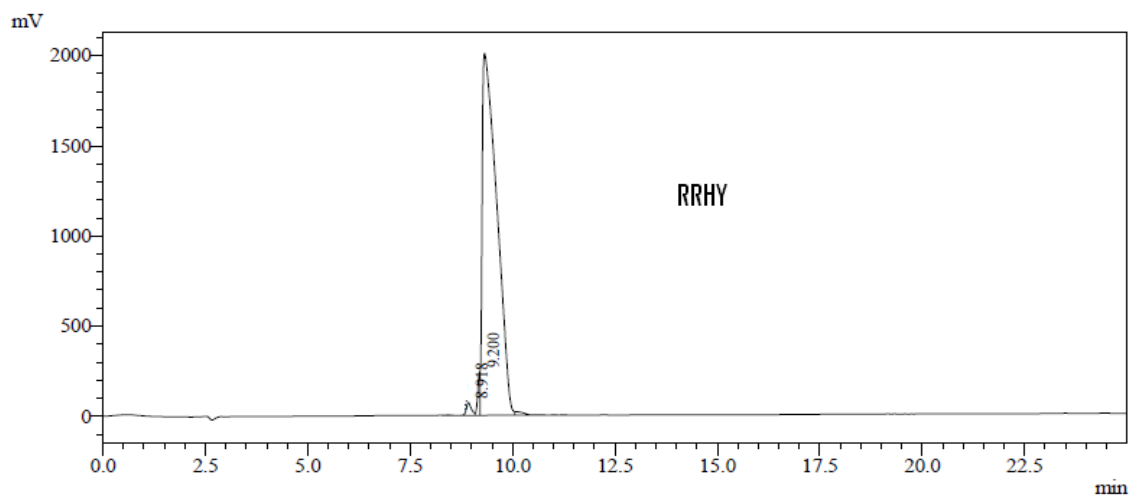


**Fig. 32. HPLC Chromatogram of Crude RRHY**

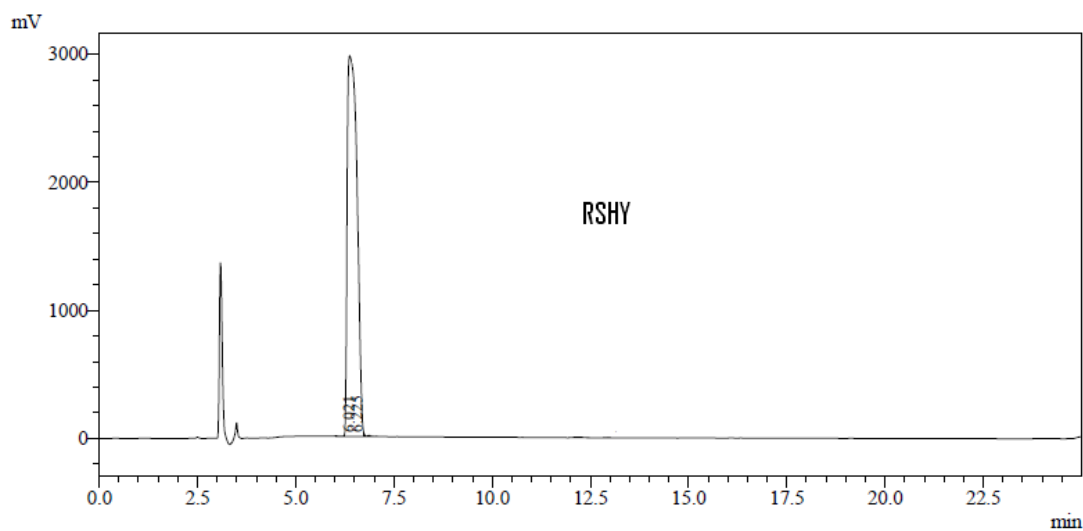


**Fig. 33. HPLC Chromatogram of Crude RSHY**

### **Sculpt**

SCULPT software facilitates the visualization, interpretation, and manipulation of structural and molecular information present in PDB files. It seamlessly combines an intuitive, point-and-click interface with interactive and real-time simulation technology. SCULPT allows a user to interact with molecular structures directly. Its applications include: exploration of conformational flexibility, superposition of multiple molecules to discover similarities, visualization and interactive minimization of MDL ISIS/Draw sketches, interactive ligand docking into flexible receptors and active sites, 3D visualization of molecules, 2D to 3D conversion of small molecules.

Initial docking experiments characterized each tetrapeptide by predicting  $\Delta G$ s. The peptide HNHY was docked in to the active site of 3M6B as follows: the PDB file was downloaded and opened using Sculpt (Fig. 30).

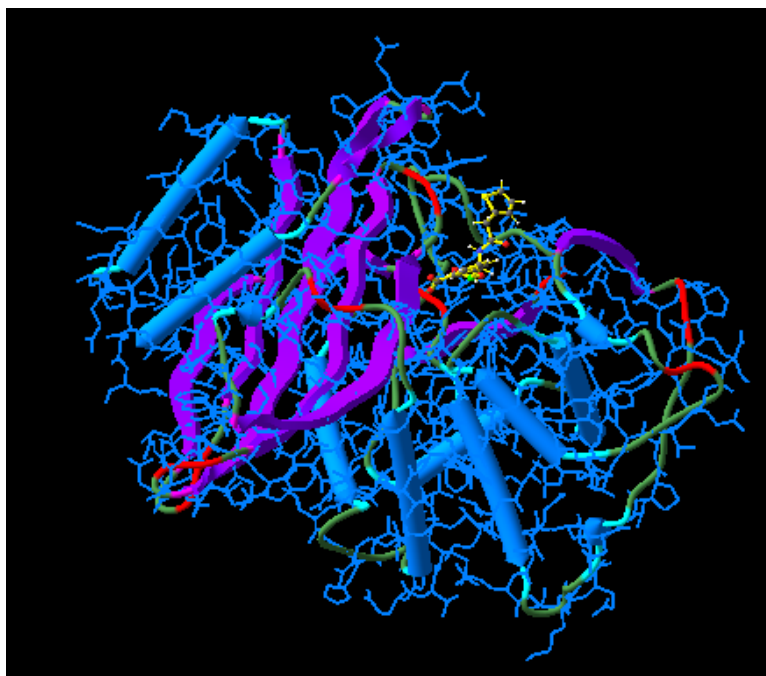


**Fig. 34. 1YM1 with Boronic Acid Inhibitor in the Active Site**

A tetrapeptide, drawn with Isis Draw, was imported, and using the paste align function, was superimposed on the original ligand within the active site. The atoms of each tetrapeptide were adjusted until its structure was maximally superimposed on that of the original inhibitor co-crystallized with the  $\beta$ -lactamase. Then the original substrate was deleted. To compute the best conformation we froze the binding site and treated it as a fixed collection of atoms, and thawed the docked peptide to allow it to adjust its conformation until an energetically favorable orientation was achieved. The energy of the new substrate was minimized using the general-purpose molecular mechanical (4) force field algorithm that considers molecules to be a collection of spheres of different masses (atoms) joined by springs (bonds). The degree of complementarity between the substrate and the binding site was calculated based on contributions of van der Waals, and electrostatic interactions. Fig. 31 A is the CPK

representation and Fig. 21 B is a ball and stick representation of the peptide HNHY in the active site with a predicted  $\Delta G$  of -212.6.

Once a minimum potential energy was obtained the active site was isolated and labeled to include the primary residues interacting with the tetrapeptide. This process can be repeated many times until the most stable conformation is obtained. Molecular modeling also reveals favorable and unfavorable interactions between the binding site and the substrate that can be modified to optimize the final structures.

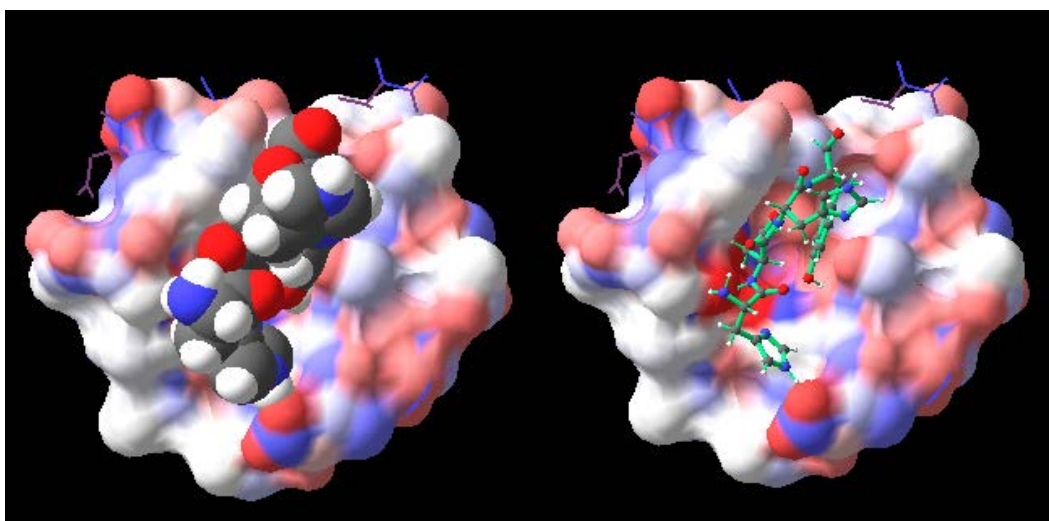


**Fig. 35 A. The CPK Representation of the Peptide HNHY in the 1YM1 Active Site**  
**Fig. 35 B. A Ball and Stick Representation of the Peptide HNHY in the 1YM1 Active Site**

### **Dock**

The basic goal of protein docking is to empirically determine the mode of interaction between ligands and their target proteins. Before undertaking expensive and time consuming bench work there is an emerging area of in-silico methods that can be used to investigate these interactions. In-silico studies of protein-ligand pairs involve binding energy, geometry of ligands, reference substrates, and protein environment to consider possible interaction candidates for drug development.

The major types of docking are protein-protein and protein-ligand docking. Since two 3 dimensional structures are considered each with six degrees of freedom (translations and rotations in the x, y, and z axes) predicting whether these molecules bind is a complex problem. Adding to this complexity is the fact that the pairs of molecules are not rigid resulting in thousands of degrees of freedom and a VAST number of conformations. The task is to minimize the intra- and intermolecular energies between the two molecules of interest. To this end different algorithms are used to explore the space of hypothetical conformations.

Molecular docking calculations consist of the following steps;

1. Optimize the geometry of the ligand, pH, charges and identify rotational bonds
2. Calculate electrostatic properties of the protein ligand binding region
3. Score the ligand-protein binding with a scoring function that describes the molecular energies. The result is a visual representation of the binding complex and the corresponding binding energy.

DockingServer integrates a number of computational chemistry software aimed at ligand geometry optimization, energy minimization, charge calculation, docking calculation and protein-ligand complex representation. AutoGrid/AutoDock 4.0 allows the docking of flexible ligands to proteins. Chemaxon and MOPAC2007 programs allow for calculations with pH protonation and partial charges on the ligand. Geometry optimization and refinement of the ligand are achieved with PM6.

Most docking programs use surface representation known as clustered spheres. This representation generates a sphere for every pair of points  $i$  and  $j$  that lie on the surface (Fig. 32). The generated sphere is centered at point  $i$ . Schematic representation of a small binding site

formed by five atoms (purple). The spheres (blue) are generated using points from the molecular surface (green) with their centers lying along the surface normals (thin line). Regions where these spheres overlap define possible cavities on the protein and protrusions on the ligand.

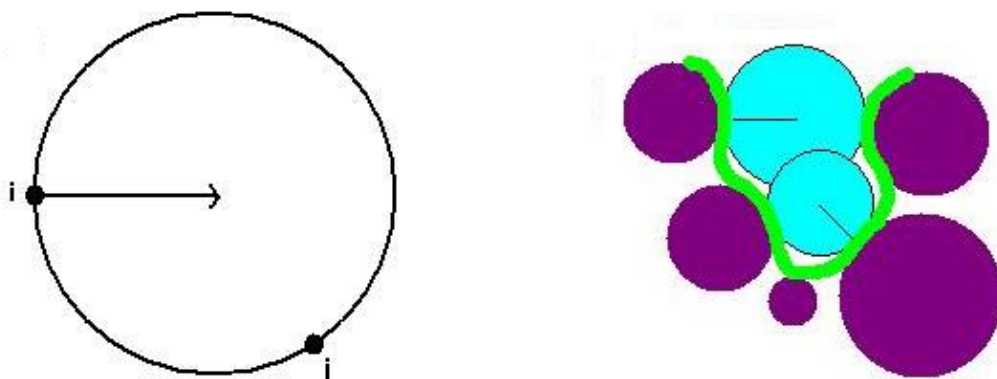


**Fig. 36. Representation of Clustered Spheres (91)**

Docking programs require the coordinates of the target protein and the location of the active site. It then generates a molecular surface for the active site of the protein. The program generates spheres to fill the active site of the protein. These spheres represent the volume (Fig. 33 a.) that could be occupied by the ligand and estimates the ligand volume (Fig. 33 b.) which is matched against an input ligand to determine possible orientations for the input ligand. The distances between the spheres are used for scoring, there are three scoring schemes: shape scoring, electrostatic scoring and force-field scoring. The top scoring ligand configuration is used as the predicted docking conformation.

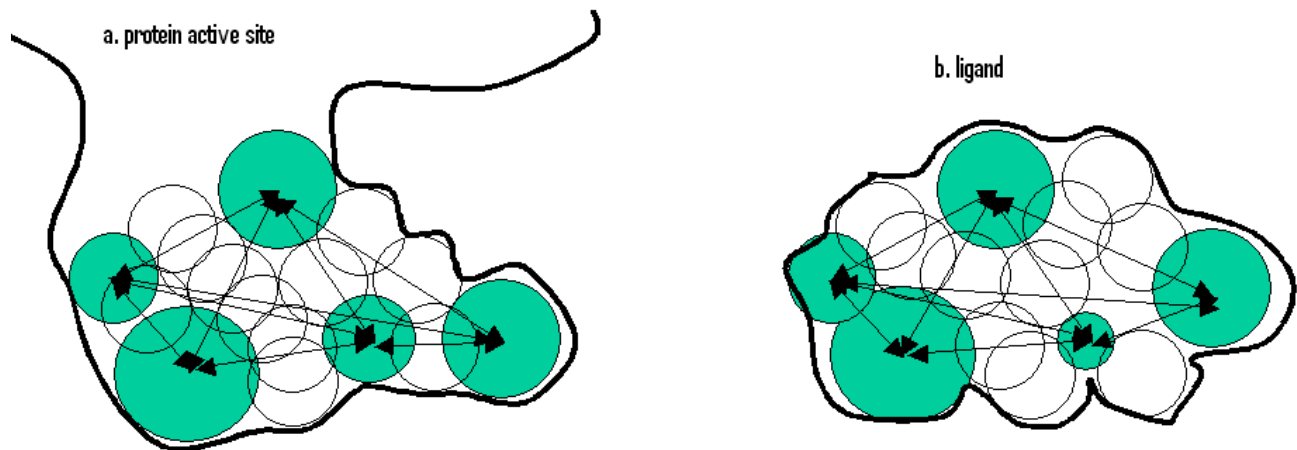


**Fig. 37. Representation of Ligands as Spheres in an Active Site (91)**

The basic five steps are;

1. Start with the crystal coordinates of a target protein
2. Generates a molecular surface for the target protein
3. Generates spheres to fill the active site of the target protein. The spheres become potential locations for ligand molecules
4. The spheres are matched to the ligand to determine possible orientations for the ligand
5. The ligands are scored finding the top scoring ligand

### **Results and Discussion for Peptides**

One of the traditional approaches to improving the efficacy of  $\beta$ -lactam antibiotics has been to modify natural antibiotics by modifying the nucleus and adding various side chains. It is generally believed that  $\beta$ -lactam based antibiotics have a limited future given increased resistance demonstrated by many strains of bacteria. Therefore the lack of performance among commonly used antibiotics against the rise of resistant bacterial strains has propelled researchers

to look for novel types of antimicrobial agents and enzyme inhibitors as tools to combat this serious and growing threat.

An alternative is to develop and investigate novel small-molecules with antibacterial properties such as naturally occurring peptides and the truncation of proteins to mini-peptides that retain protein-binding functions (92). These peptide antibiotics do not act like enzyme inhibitors, and therefore, hopefully will not engender bacterial resistance. Several instances of this strategy where protein inhibitors have been converted into small-molecule inhibitors that bind their target substrates with high affinities (93) are; the binding of fibrinogen to glycoprotein IIb/IIIa (GPIIb/IIIa). A cyclic peptide was synthesized with analogous amino acids residues and shown to binds GPIIb/IIIa and inhibit platelet aggregation (94).

Another example on a different enzyme system involves the molecular design of peptides that reversibly bind to the active site of thrombin (95, 96). These peptides mimics have the advantage that they are soluble in water and readily pass different physiological barriers, in contrast with small organic molecules that are less soluble thereby limiting their usefulness (97).

The  $\beta$ -lactamase inhibitor protein (BLIP) is a 165-amino-acid protein produced by the gram-positive soil bacterium *Streptomyces clavuligerus* (98). It is a naturally occurring antibiotic. *S. clavuligerus* also produces  $\beta$ -lactam antibiotics such as cephamycins as well as clavulanic acid (99). BLIP has been shown to bind to and inhibit the TEM-1  $\beta$ -lactamase with a  $K_i$  in the range of 0.1 to 0.6 nM (100). In addition, BLIP binds to and inhibits the class A  $\beta$ -lactamases from *Staphylococcus aureus*, *Bacillus cereus*, and *Bacillus licheniformis* with  $K_i$  values of 1 to 3  $\mu$ M (99). A truncated version of BLIP, N-biotin-Gly-Ser-Gly-Cys-Ala-Ala-Gly-Asp-Tyr-Tyr-Cys-COOH was synthesized. This sequence consists of BLIP residues Ala-46 to Tyr-51 flanked on either side by cysteine residues. After synthesis the peptide was oxidized to form a disulfide

bond between the cysteines to create a cyclic peptide. This peptide binds TEM-1 with an inhibition constant of 603  $\mu\text{M}$  (101).

These examples served as a starting point for the design of peptide analogues that inhibit  $\beta$ -lactamase. I started my peptide design based on the work of Wanzi Huang *et al.*, using phage display, a 6-mer linear peptide with the sequence RRGHYY was found to inhibit class A *Bacillus anthracis* Bla1, ( $K_i = 42 \mu\text{M}$ ) and class A TEM-1  $\beta$ -lactamase, ( $K_i = 136 \mu\text{M}$ ) (89).

To sample all combinatorial possibilities for a 6-mer peptide using only the 20 L-amino acids a library of  $6^{20}$  structures would have to be constructed, such a strategy can be over whelming even with use of computer programs and undergraduate students. I decided to start my search for potential inhibitors using tetrapeptides based on the Huang 6-mer sequence; this represents a  $4^{20}$  set of compounds, still quite daunting. Huang discovered that replacing both arginines with alanines resulted in a 3-fold increased  $K_i$  for inhibiton of TEM-1  $\beta$ -lactamase, indicating that these residues contribute to inhibition. Since the active site regions of all class A  $\beta$ -lactamases are similar therefore mechanistic deductions based on one class A active site is applicable to all class A enzymes (102).

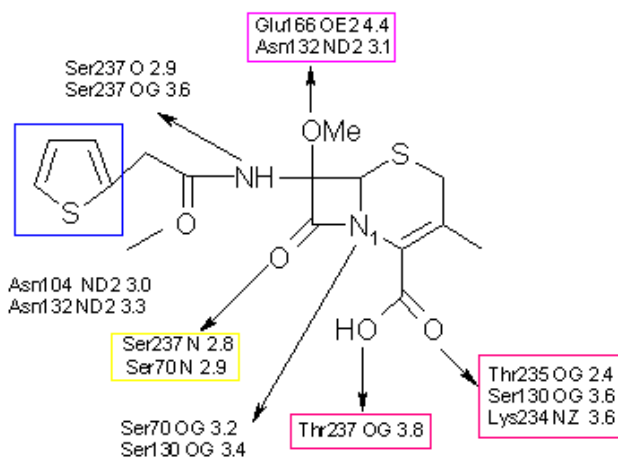
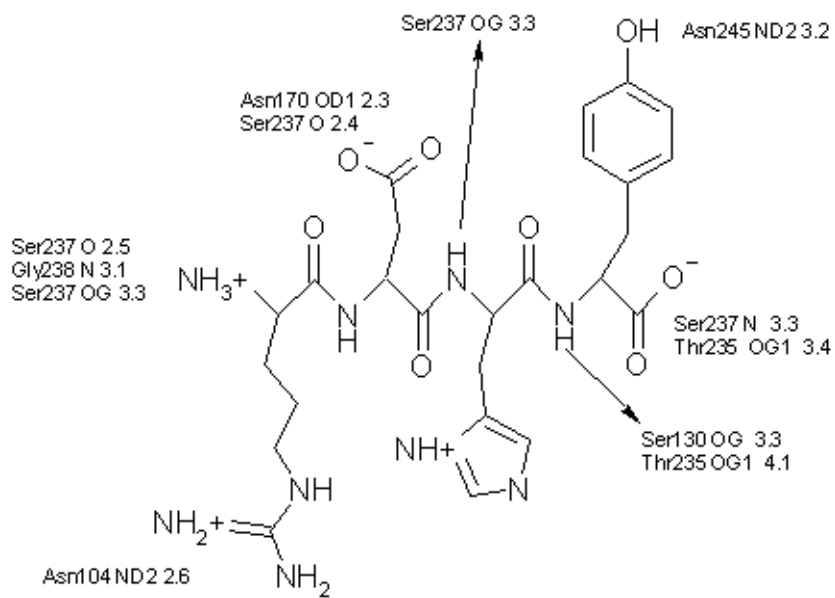
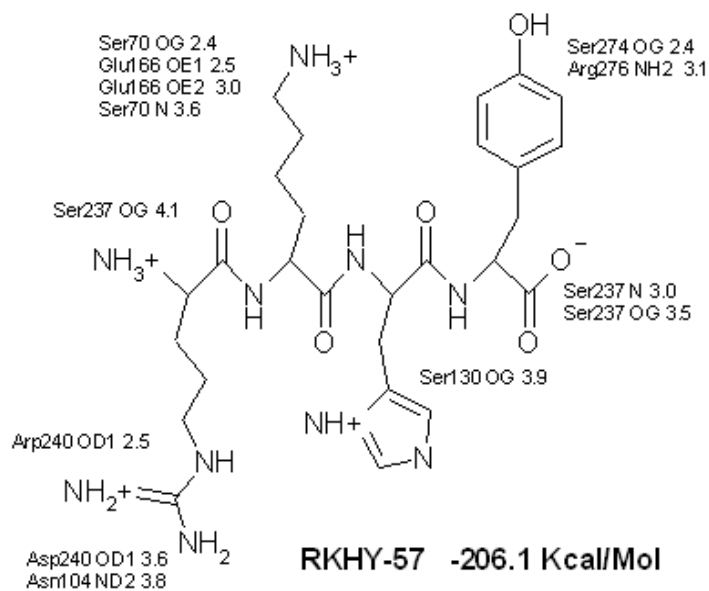


**Fig. 38. Cefoxitin's Interaction with Protein Residues in 1YM1**



**RDHY-17 -151.6 Kcal/Mol**

**Fig. 39. Interaction of RDHY in 1YM1 Active Site**



**RKHY-57 -206.1 Kcal/Mol**

**Fig. 40. Interaction of RKHY in 1YM1 Active Site**

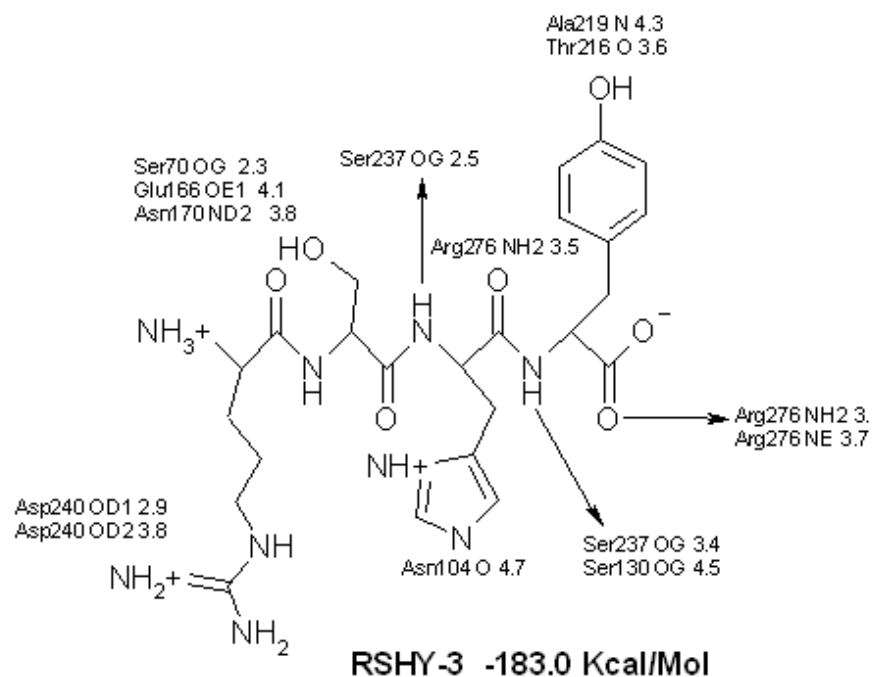


**Fig. 41. Interaction of RSHY in 1YM1 Active Site**

**Table 10. Sequence, Charge, Ki and Free Energy. Arranged by the Second Peptide in the Sequence**

Neutral non-polar	Peptide Sequence	Ki ( $\mu\text{M}$ )	Charge at physiological pH	Predicted Delta G (Kcal/mol) (Sculpt)
	<b>RGHY</b>	5.47	No charge	-185.1
	<b>RAHY</b>	71.00	No charge	546.9
	<b>RVHY</b>	Activates	No charge	-187.2

	RLHY	53.00	No charge	2499.2
	RIHY	103.23	No charge	21.3
	RMHY	47.00	No charge	771.0
	RPHY	900.00	No charge	-207.5
	RCHY	Activates	No charge	1045.0
<b>Neutral non-polar aromatics</b>				
	RFHY	16.33	No charge	530.8
	RWHY	41.70	No charge	2347.6
<b>Neutral polar</b>				
	RSHY	92.15	No charge	-183.0
	RTHY	565.20	No charge	3528.0
	RNHY	213.00	No charge	88.1
	RQHY	32.47	No charge	608.4
<b>Neutral polar aromatic</b>				
	RYHY	Activates	No charge	-137.6
<b>Acid polar</b>				
	RDHY	6.39	Neg charge	-151.6
	REHY	67.60	Neg charge	-165.6
<b>Basic Polar</b>				
	RKHY	12.70	Pos charge	-206.1
	RRHY	5.11	Pos charge	-153.9
	RHHY	Activates	Pos charge	681.6

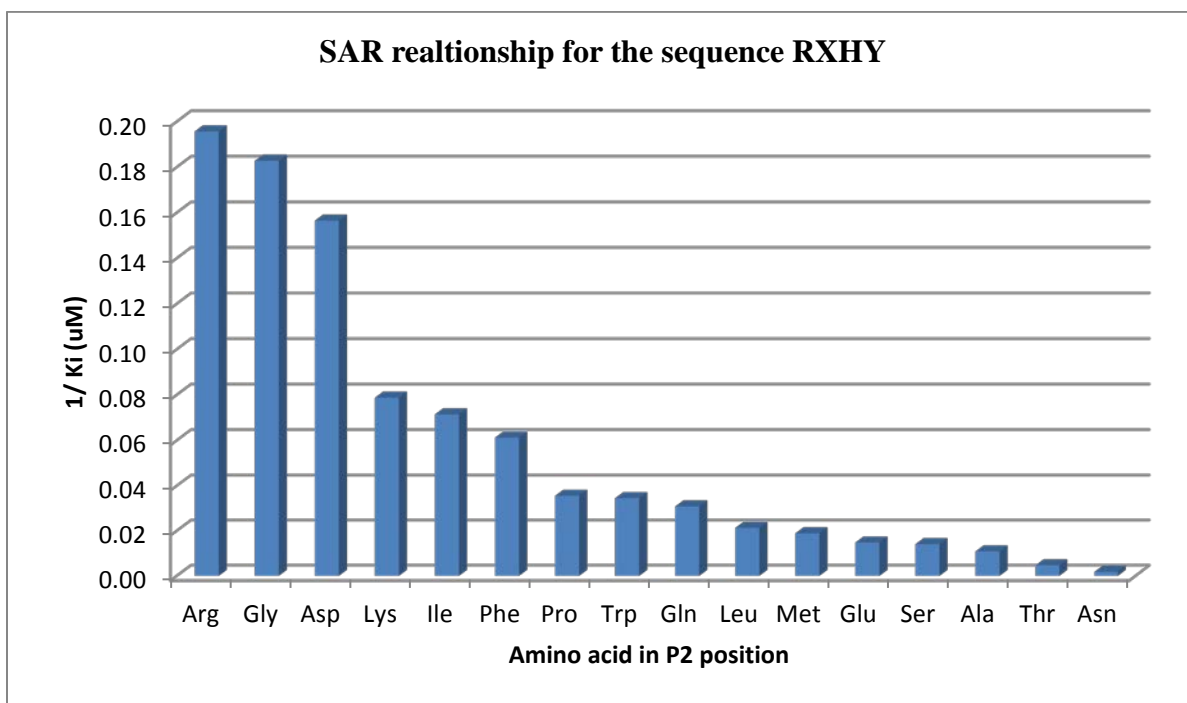


**Fig. 42. Structure Activity Relationship for RXHY Sequence**

Analysis of the structural models together with the  $K_i$ 's obtained experimentally suggests that within this library, differing in one single amino acid at P2 position, there are a few correlations that can be made. The charged acid and basic polar amino acids have small  $K_i$ 's and probably form many h-bonds within the active site contributing to binding. Glycine compared to the other neutral non-polar amino acids can adopt a complementary position because it is small and flexible.

One question raised during the molecular docking of these peptides using Sculpt relates to the conformation of the active site of the protein used as the template. In order to dock the peptide the active site remains frozen. Freezing the active site in order to dock the peptide is artificial and is reflected in the disparate  $\Delta G$ 's.

Analysis of the structural models together with the  $K_i$ 's obtained experimentally suggests that within this library, differing in one single amino acid at P<sub>2</sub> position, few correlations that can be made. The charged acid and basic polar amino acids have small  $K_i$ 's and probably form many h-bonds within the active site contributing to binding. Glycine compared to the other neutral non-polar amino acids can adopt a complementary position because it is small and flexible. On the other hand asparagine ( $K_i = 213.00 \mu\text{M}$ ) and glutamine ( $K_i = 67.60 \mu\text{M}$ ), that differ in their R side chain by one CH<sub>2</sub> interact very differently with the active site.

Some peptides showed a variation in  $K_i$  (increased  $K_i$ ) with increasing concentration of peptide, RYHY is probably aggregating through pi-pi stacking interactions between aromatic rings. RHHY, two imidazole rings so close together and charged may adopt an unusual conformation. The question of relative reactivity of peptides and  $\beta$ -lactams that contain highly specific side chains has not been directly addressed. Good peptide substrates for  $\beta$ -lactam antibiotics would have side chains resembling those of stem peptides of bacterial peptidoglycan biosynthesis. There is little data in favor of this idea and a number of indications to the contrary (103). The relationship between  $\beta$ -lactam structure and antibiotic activity is not generally predictable because of a large number of contributing factors.

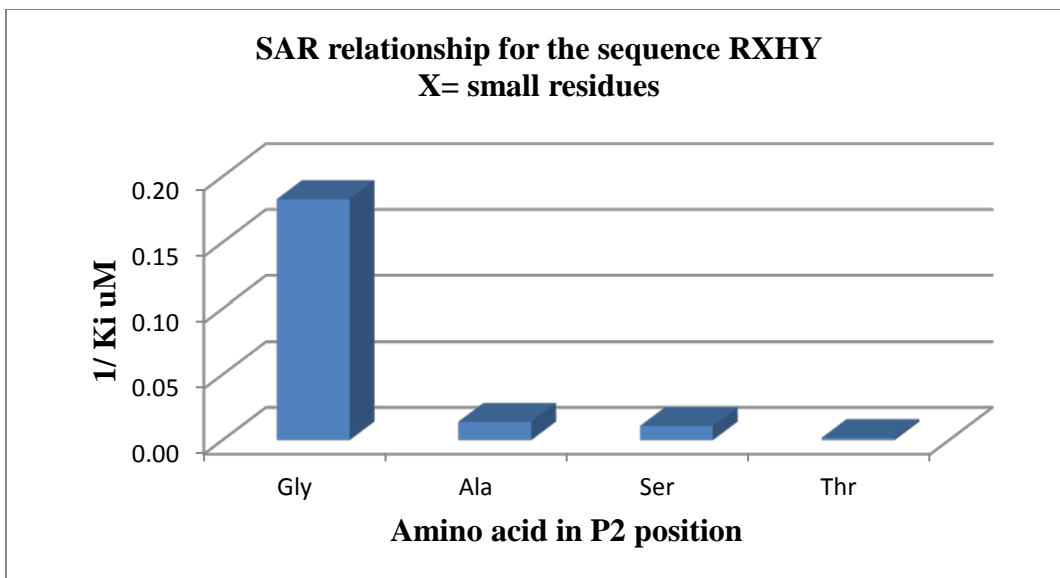


**Fig. 43. Structure Activity Relationship for Small Residues**

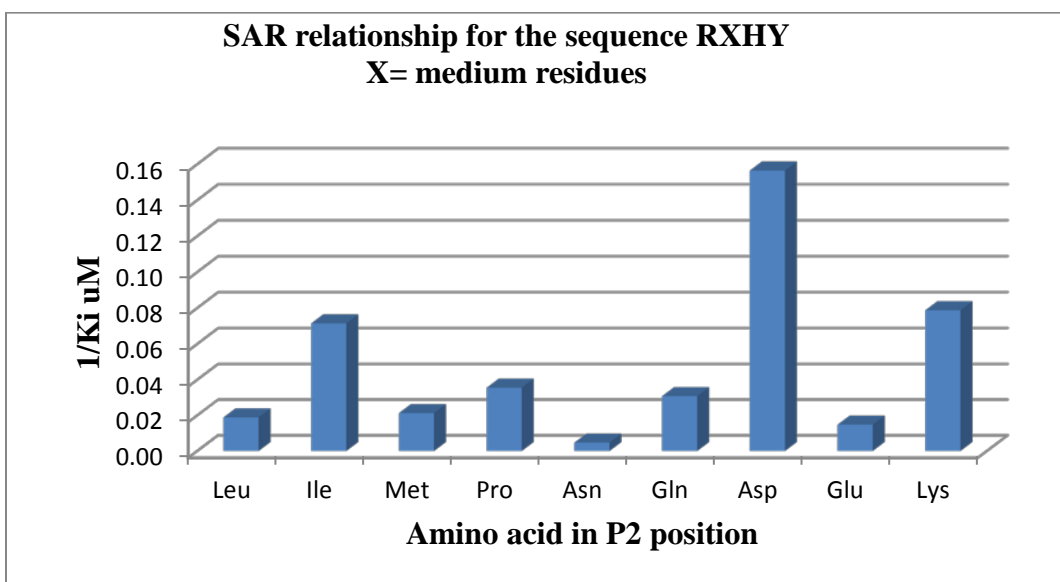


**Fig. 44. Structure Activity Relationship for Medium Residues**

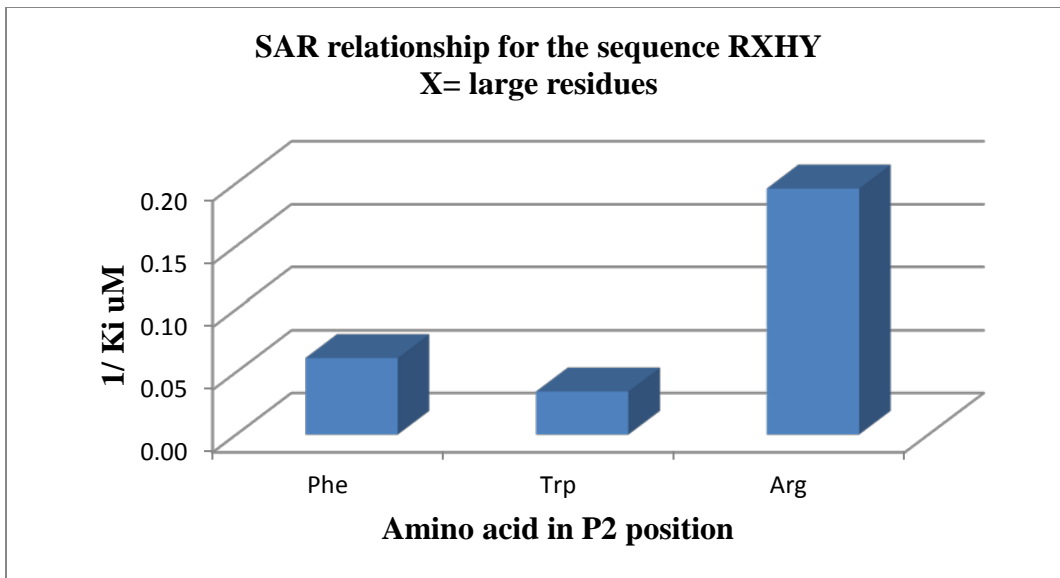


**Fig. 45. Structure Activity Relationship for Large Residues**

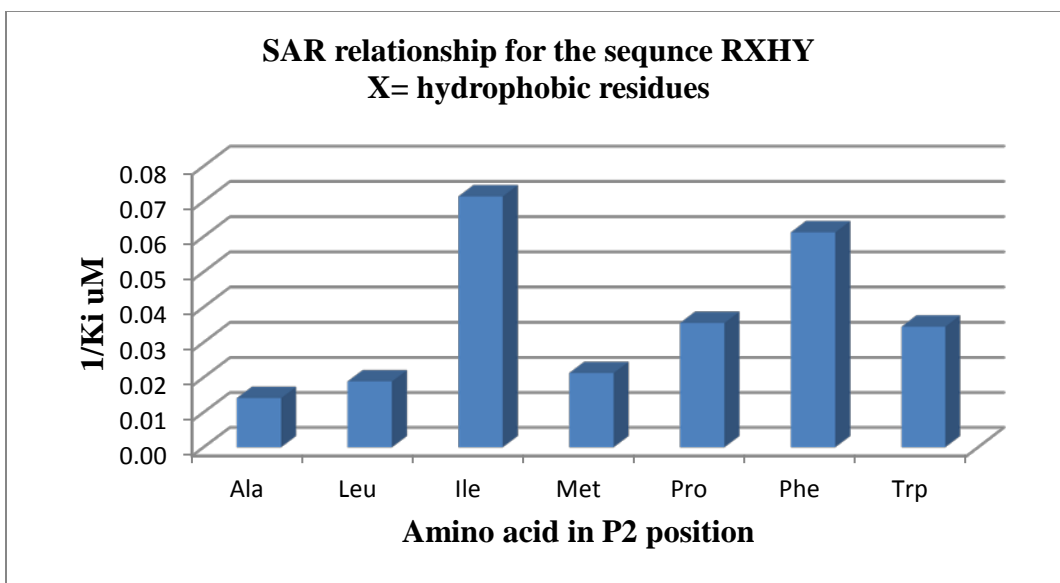


**Fig. 46. Structure Activity Relationship for Hydrophobic Residues**

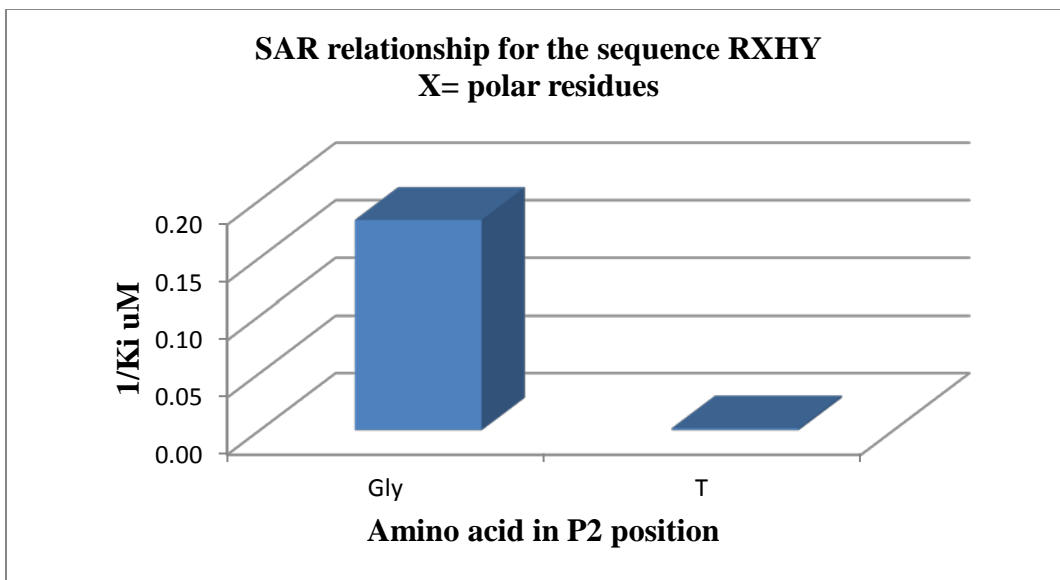


**Fig. 47. Structure Activity Relationship for Polar Residues**

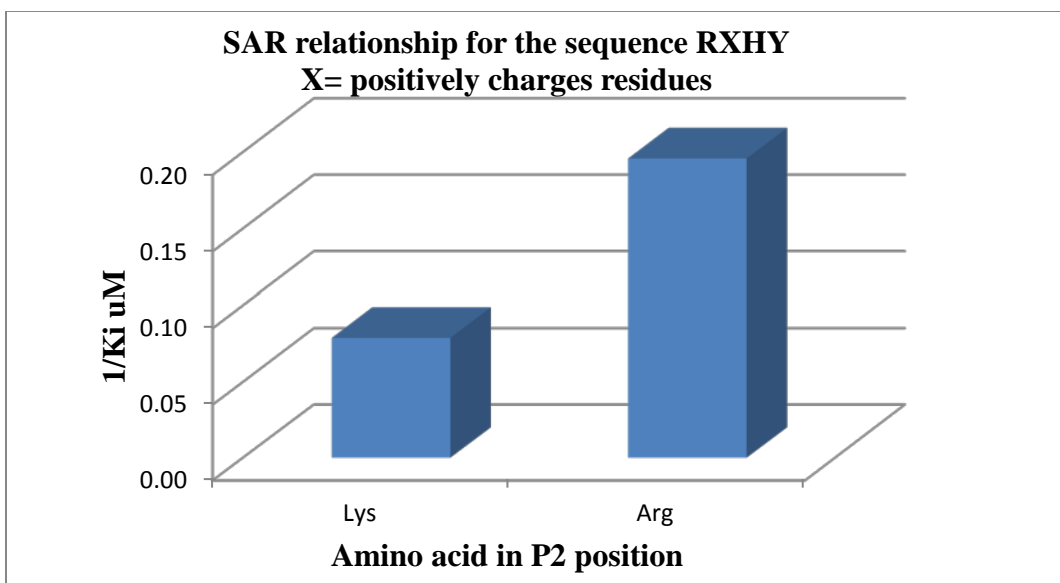


**Fig. 48. Structure Activity Relationship for Positively Charged Residues**

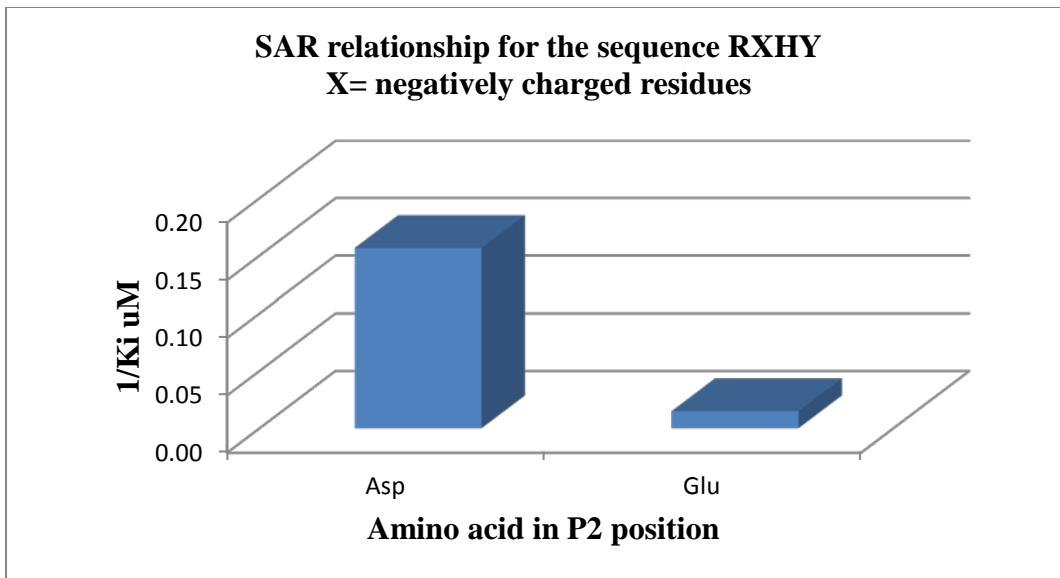


**Fig. 49. Structure Activity Relationship for negatively Charged Residues**

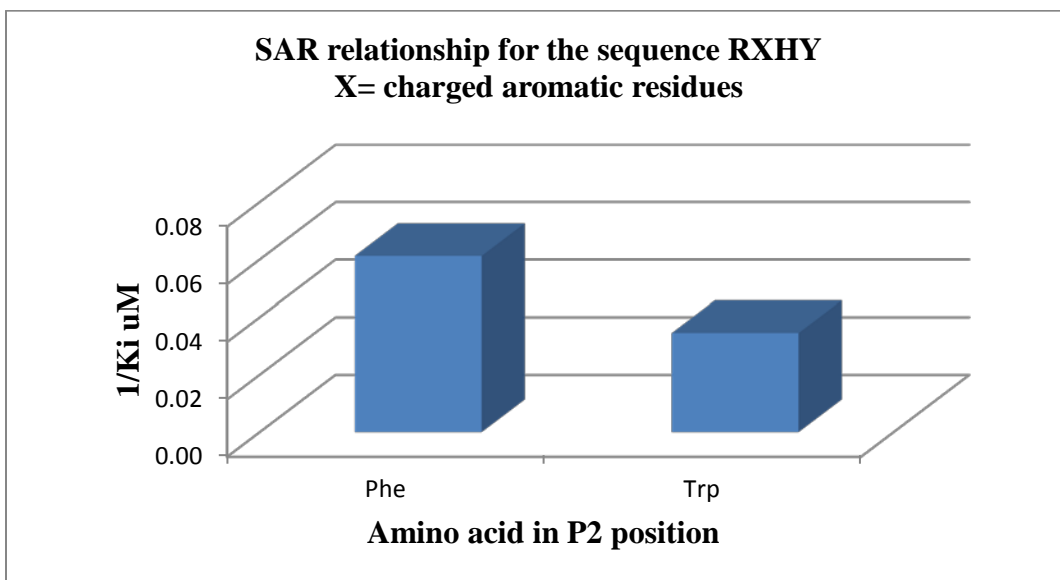


**Fig. 50. Structure Activity Relationship for charged Aromatic Residues**

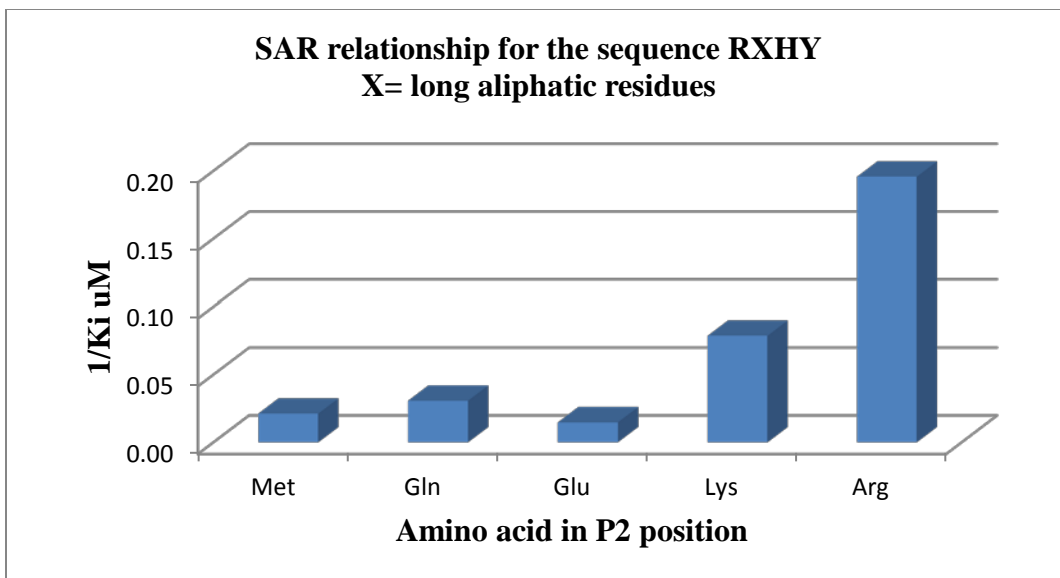


**Fig. 51. Structure Activity Relationship for Long Aliphatic Residues**

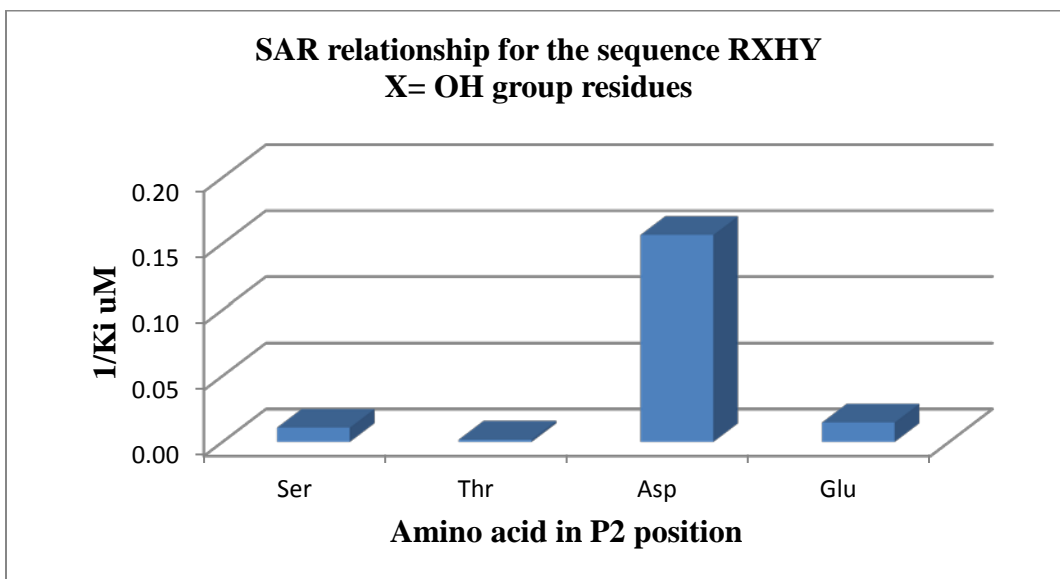


**Fig. 52. Structure Activity Relationship for OH Group Residues**

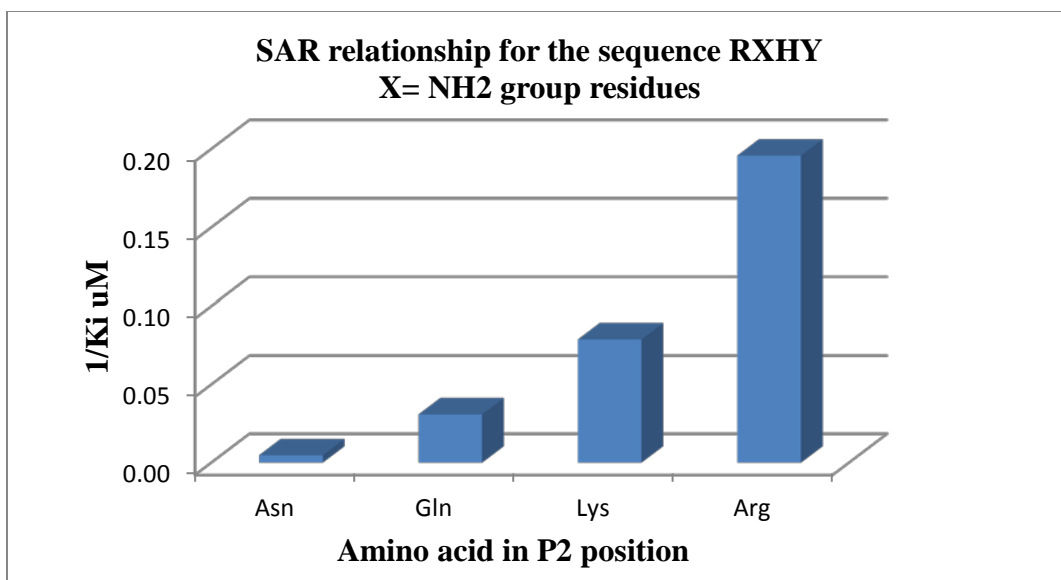


**Fig. 53. Structure Activity Relationship for NH<sub>2</sub> Residues**

## Bioinformatics Chapter 5

### Introduction

The  $\beta$ -lactamase enzymes are best understood from an evolutionary standpoint. Divergence of the major groups of bacteria occurred approximately 3.5 billion years ago (104) concurrently evolving with their bacterial cell walls and the enzymes of cell wall synthesis. (105)

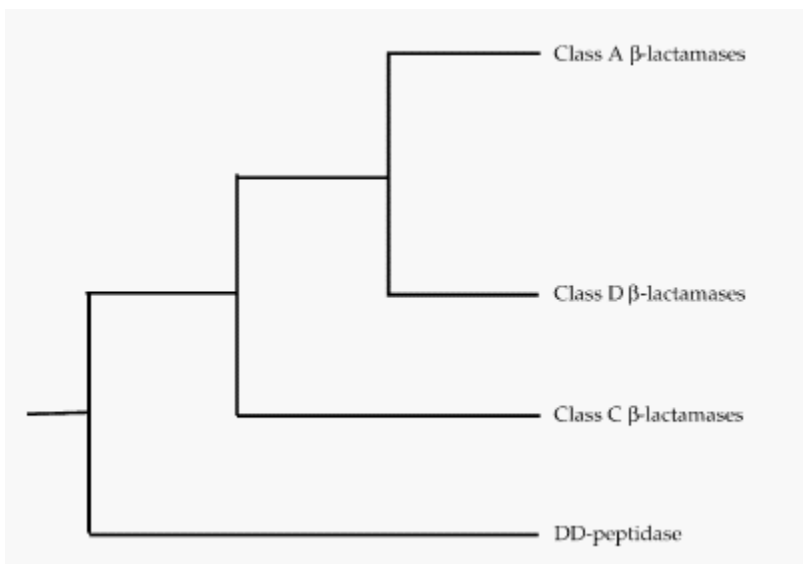


**Fig. 54. Evolutionary Relationship Between Ambler Class A  $\beta$ -Lactamases and DD-Peptidase (57)**

Recently, on the evolutionary scale,  $\beta$ -lactams evolved as chemical warfare agents among bacteria to target each other's  $\beta$ -lactamase enzymes giving individual groups an evolutionary advantage. Comparing the penicillin and cephalosporin biosynthetic genes that have been cloned, sequenced, and expressed (106) shows that bacterial and fungal  $\beta$ -lactam biosynthetic genes share very high sequence identity. Essentially the same biosynthetic pathway produces the most common  $\beta$ -lactam antibiotics, penicillins and cephalosporins, by a wide variety of microorganisms, including some filamentous fungi, many Gram-positive bacteria, and a few Gram-negative bacteria. This fact implies that these biosynthetic genes were transferred horizontally between the two groups of organisms, and indirect evidence suggests the transfer

occurred from the bacteria to the fungi, where they came to our attention via the mold *Penicillium notatum* in 1928. Finally, to combat  $\beta$ -lactamase enzymes,  $\beta$ -lactamase inhibitors (107) and inhibitory proteins were selected for and optimized in certain bacteria. (100)

Bacterial cell walls must be assembled, maintained, and remodeled of the bacteria is to stay alive. This work is done by sets of enzymes called transpeptidase/carboxypeptidase, or DD-peptidases, also called penicillin-binding proteins (PBPs). Carboxypeptidases cleave D-alanine from one peptidoglycan strand evolving energy for the transpeptidase to cross-link adjacent strands. There are 2 groups of PBPs, lowmolecular weight that exhibit carboxypeptidase activity, and high-molecular weight PBPs that exhibit transpeptidase activity. Structural evidence supports the hypothesis that  $\beta$ -lactamases most likely descended from cell wall biosynthetic PBPs. (108)

Targets of  $\beta$ -lactams antibiotics are membrane PBPs. These targets are serine protease enzymes that hydrolyze the amide bond according to an acylation/deacylation mechanism involving acyl-enzyme intermediates. Beta-lactam antibiotics are acylated in the active site of PBPs forming stable covalent non-catalytic acyl-enzymes that are not easily hydrolyzed. Beta-lactamases also catalyze the cleavage of  $\beta$ -lactams in acylation/deacylation mechanisms but differ from DD-peptidases in that acyl-enzyme intermediates are quickly hydrolyzed (Figure 55).

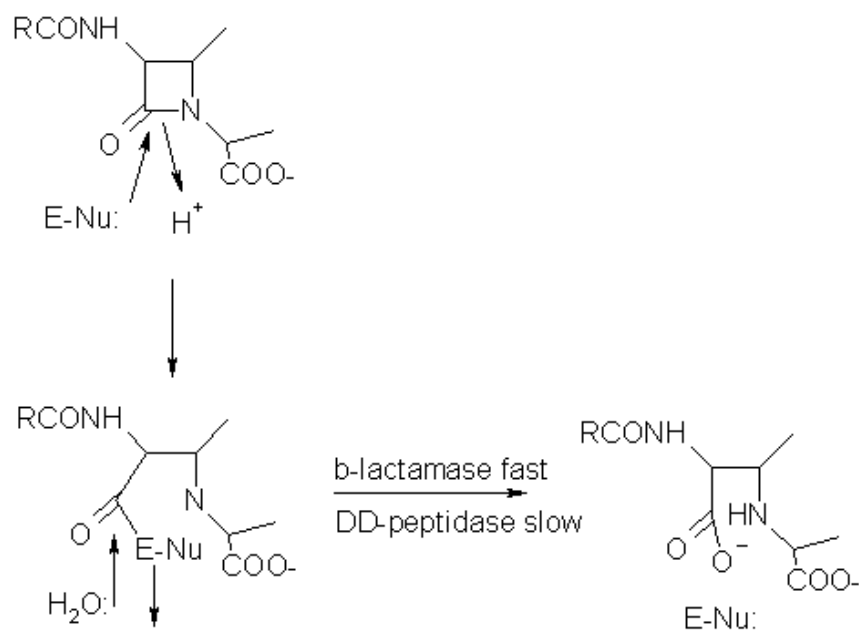


**Fig. 55. Representation of  $\beta$ -Lactamase and DD-Peptidase Reactions**

The DD-peptidase reaction begins with the binding of a donor peptidoglycan polymer to the enzyme. Following donor strand, (R) binding a nucleophilic serine attacks the carbonyl carbon of the C-terminus of the D-alanyl-D-alanine peptide in the acylation half of the reaction releasing the terminal D-alanine. The cross link is formed in the deacylation half by the acyl transfer of the D-alanine donor strand to the amino group of a neighboring acceptor strand (R'). The structural similarity of  $\beta$ -lactam antibiotics to the C-terminal D-alanyl-D-alanine of the donor strand makes PBPs the target of these antibiotics (Figure 56).

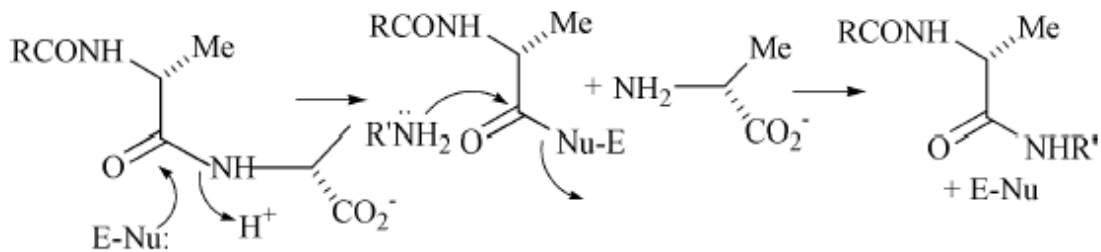


**Fig. 56. DD-Peptidase Reaction (109)**

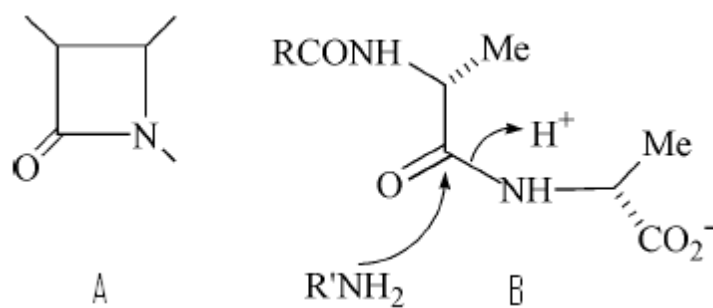


**Fig. 57.  $\beta$ -Lactam, B, D-alanyl-D-alanine Peptide (110)**

It is now clear as-Tipper and Strominger first suggested-that  $\beta$ -lactamases evolved from DD-peptidases (Fig. 6) given that fact that penicillin is irreversibly incorporated into the carboxypeptidase and transpeptidase enzymes of bacterial cell wall biosynthesis. (25)

### **Identification of Y-49 Recombinant Beta-Lactamase Protein**

Most bacterial species consist of a wide spectrum of distinct clones or clonal complexes defined as ancestral genotypes and strains including minor variations. *Mycobacterium tuberculosis*, in contrast to many other pathogenic bacterial species, displays little evidence for the transfer and recombination of genes between cells and therefore has an extremely low level of genetic

variation. The *Mycobacterium tuberculosis Complex* which includes the closely related species *M. tuberculosis*, *M. bovis*, *M. africanum*, *M. microti*, and *M. canetti* make-up a compact clonal group dominated by minimizations in diversity, (111) This reduced genetic diversity is proposed to be the result of ancient horizontal DNA exchange, followed by population bottlenecks or selective sweeps where entire chromosomes were fixed in the population and subsequently clonally amplified. (112)

The *Mycobacterium tuberculosis Complex* represents one of the most extreme examples of genetic homogeneity, with only 0.01%–0.03% synonymous nucleotide variation. (113) Given the fact that the *M. tuberculosis* genome is highly conserved it is considered a "closed pan-genome" A pan-genome is defined as the genes in all strains of that species comprising the "core genome" present in all strains.

Despite this limited genetic variation, there is a high degree of phenotypic variability among *M. tuberculosis* isolates, including differences in virulence and immunogenicity affecting clinical outcomes and epidemiology. (114)

The H37, virulent parent strain, of *Mycobacterium tuberculosis* was originally isolated in 1905 by Edward R. Balwin from the lungs of a 19 year-old patient with chronic tuberculosis. In 1935 William Steenken looking for stable avirulent derivatives revealed that the parent strain could be dissociated into avirulent and virulent colonies depending on the pH of the solid egg media. (115) He first described the colonies as R (resistant) and S (susceptible) to the environment of the culture media, but both colonies were rough in appearance. He realized his labeling was misleading and changed the designation of the virulent variety from S to Rv (rough virulent) (116) The original H37 strain was discontinued and the Rv and Ra strains are maintained at the Trudeau Institute, Inc. in Saranac Lake, New York and the American Type Culture Collection

(ATCC) in Rockville, Maryland. Both Rv and Ra are used world-wide as reference strains to study the pathogenesis and virulence of *M. tuberculosis* since the 1940s.

### Genomic Features of H37Rv and H37Ra

*M. tuberculosis* H37Ra ATCC25177 is a single circular chromosome of 4,419,977 bp, 4084 genes, with an average GC content of 65% (GenBank accession number CP000611). A total of 4034 protein-coding sequences represent 90% of the genome. Compared with the H37Rv genome (GenBank accession AL123456) reveals a highly conserved gene content and order between these two strains. The genome size of H37Ra is 8,445 bp larger than that of H37Rv (4,411,532 bp), as a result of 53 insertions and 21 deletions. Besides these insertions and deletions, 198 single nucleotide variations are identified between H37Ra and H37Rv.

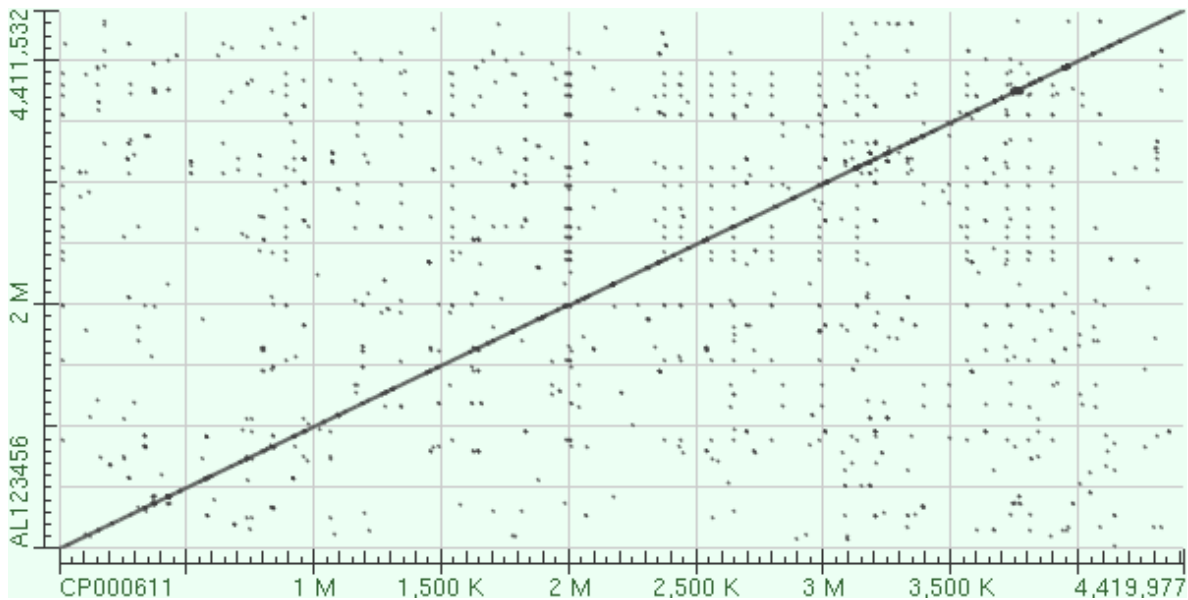


**Fig. 58. Global sequence alignment of H37Ra (CP000611) compared to H37Rv (AL123456)**

Dot plots allow for quick identification of regions of local alignment shows 99% identity between sequences.

### **Choosing a Molecular Model**

The first step was to verify the identity of our recombinant expressed protein (gift from Dr. Douglas Kernoodle, Vanderbilt University, Nashville, TN), which is a plasmid construct transformed into *E. coli* Top 10, since Dr. Kernoodle's group does not identify the protein. Dr. John Blanchard and his group at Albert Einstein College of Medicine cite the same strain as Dr. Kernoodle's group and crystallized the following two proteins 3M6B.pdb and 3IQA.pdb. (117)

Using a Vector Alignment Search Tool (VAST) search on 3IQA.pdb shows that 3IQA.pdb has the same peptide sequence as 3M6B.pdb, which does not cite *M. tuberculosis* strain H37Rv. The strain identifier is missing from the 3M6B.pdb file. The molecular modeling work was done using 3M6B.pdb protein structure. This suggests that the molecular modeling was done on the same protein expressed from Dr. Kernoodle's expression system.

A VAST search uses sets of coordinate data that are compared using a vector based method. There are three major steps that take place in the course of a VAST comparison. First, the known three-dimensional coordinate data of all the  $\alpha$ -helices and  $\beta$ -sheets that make up the core of the protein are identified. Straight line vectors are calculated based on the position of these secondary structural elements. VAST marks how one vector is connected to the next as well as marking the vector as an  $\alpha$ -helix or  $\beta$ -sheet. Only these determined vectors are used to compare with other proteins. Next the program aligns these vectors looking for same type and relative orientation. The object is to identify highly similar core substructures. A final refinement takes place using Monte Carlo methods (a class of computational algorithms that rely on repeated random sampling to compute their results) at each residue position to optimize the structural alignment.

For a more complete check, PubMed Genome was used to find the DNA sequence for strain H37Rv. Dr. Kernoodle identifies his protein as Y-49 recombinant  $\beta$ -lactamase protein produced by a chromosomal gene coming from *M. tuberculosis* strain H37Rv sequenced by the Sanger Center Cambridge, UK (118). The complete genome of H37Rv has 3999 coding genes. The list of expressed proteins in this genome was retrieved and a  $\beta$ -lactamase-like protein plus a class A  $\beta$ -lactamase was found (119). The identifiers are the following; for the  $\beta$ -lactamase protein (accession number NP\_216584.1 and locus tag Rv2068c), with this information the DNA and peptide sequence was retrieved.

#### **DNA sequence Gene ID 888742 H37Rv Strain**

```
ATGCGCAACAGAGGATTCGGTTCGTCGCGAACTGCTGGTAGCGATGGCAATGCTGGT
TTCCGTGACGGGGTGTGCACGGCATGCGAGCGGGGCCCGTCCGGCATCGACAACCT
TGCCGGCCGGAGCGGATCTGGCGGATCGCTTCGCCGAGCTGGAGCGCAGATACGAT
GCCCCGGCTTGGGGTGTATGTGCCCGCCACCGGCACCACCGCCGCGATCGAATACCG
CGCCGATGAGCGGTTTCGATTCTGCTCCACGTTCAAGGCGCCGCTCGTGGCGGGCGGT
GCTGCACCAAAACCCGCTCACGCATCTGGACAAACTGATCACCTACACCAGTGACG
ACATTCGGTCGATCTCCCCGGTGGCCCAACAACACGTTTCAGACCGGGATGACGATC
GGGCAGCTTTGCGATGCGGCGATAACGCTATAGCGACGGCACCGCCGCCAACCTGTT
GCTGGCCGATCTTGGCGGTCCCAGGGGGCGGCACCGCGGCATTTACCGGCTACCTCCG
CAGCTTGGGTGACACCGTGAGCCGGTTGGACGCCGAGGAACCGGAGTTGAACCGCG
ATCCGCCCCGGGGACGAACGGGATACCACAACACCGCACGCCATCGCCCTGGTGTG
CAGCAGCTTGTTCGCAACGCGTTGCCGCCCACAAAGCGGGCACTGCTCACCGAT
TGGATGGCGCGCAACACCACCGGAGCCAAGCGGATCCGAGCGGGCTTCCC GCCGA
TTGGAAGGTGATCGACAAGACCGGGACCGGTGACTACGGACGAGCAAACGACATCG
CGGTCGTGTGGTCACCGACCGGCGTGCCCTACGTGGTGGCCGTCATGTCCGATCGTG
CCGGCGGCGGGTATGACGCCGAGCCCCGTGAGGCGCTGCTCGCCGAGGCGGCGACG
TGCGTTGCCGGTGTGCTTGCATAG
```

#### **Amino Acid Sequence for Locus Tag Rv2068c H37Rv Strain**

```
MRNRGFRRELLVAMAMLVSVTGCARHASGARPASTTLPAGADLADRFAELERRYDA
RLGVYVPATGTTAAIEYRADERFAFCSTFKAPLVAAVLHQNPLTHLDKLITYTSDDIRIS
PVAQQHVQTMIGTIGQLCDAAIRYSDGTAANLLLADLGGPGGGTAAFTGYLRLSGLDTVS
RLDAEEPENRPPGDERDTTTPHAIALVLQQLVLGNALPPDKRALLTDWMARNTTGA
KRIRAGFPADWKVIDKTGTGDYGRANDIAVVWSPTGVVAVVMSDRAGGGYDAEPR
EALLAEAATCVAGVLA
```

The peptide sequence was submitted it to a FASTA similarity search.

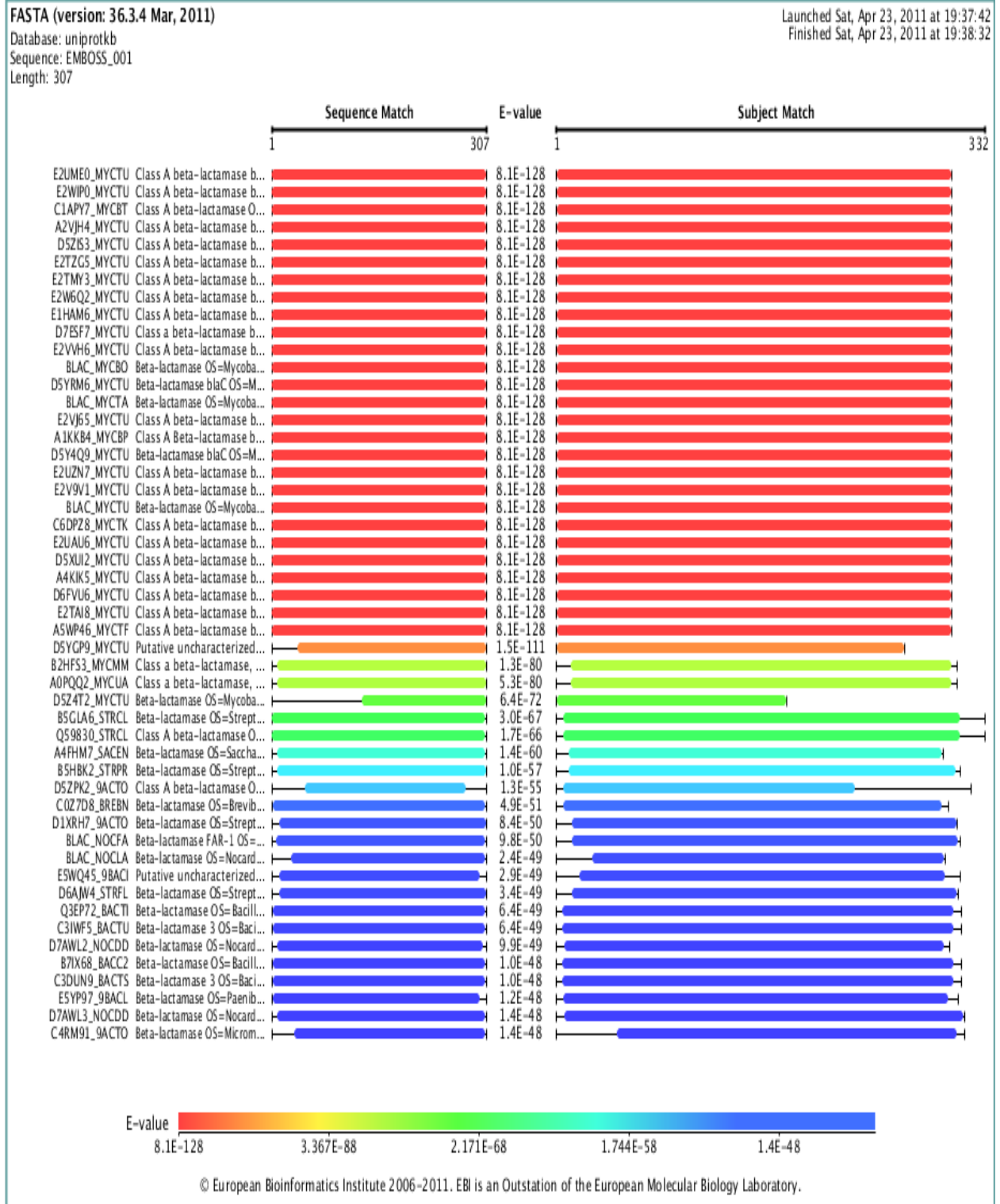


Fig. 59. Results FASTA search

The first 27 sequences are totally identical. The amino acid sequence from accession number NP\_216584.1 was compared to the sequence cited for Dr. Blanchard's 3IQA.pdb. They are not the same. Protein 3IQA.pdb has 265 amino acids and begins with DLADRF. The peptide sequence NP\_216584 has 307 amino acids and begins with MRNRGFGRRRELL. The C-terminal amino acids for both sequences are identical. Using Align Query program to confirm that the rest of the amino acids are identical it was found that the 3IQA.pdb and NP\_216584.1 sequences are identical, minus the missing first 42 amino acids highlighted in yellow. The first 42 amino acids, presumably a leader sequence that is cleaved on expression and export, are missing from 3IQA.pdb.

### **3IQA**

DLADRFAELERRYDARLGVYVPATGTTAAIEYRADERFAFCSTFKAPLVA AVLHQNPLT  
HLDKLITYTSDDIRSISPVAQQHVQTGMTIGQLCDAAIRYSDGTAANLLLADLGGPGGGT  
AAFTGYLRSLGDTVSRDLDAEPELNRDPPGDERDTTTPHAIALVLQQLVLGNALPPDKR  
ALLTDWMARNTTGAKRIRAGFPADWKVIDKTGTGDYGRANDIAVVWSPTGVPYVVAV  
MSDRAGGGYDAEPREALLAEAATCVAGVLA

### **NP\_216584.1**

**MRNRGFGRRRELLVAMAMLVSVTG CARHASGARPASTTLPAGA**DLADRFAELERRYDA  
RLGVYVPATGTTAAIEYRADERFAFCSTFKAPLVA AVLHQNPLTHLDKLITYTSDDIRSIS  
PVAQQHVQTGMTIGQLCDAAIRYSDGTAANLLLADLGGPGGGTAAFTGYLRSLGDTVSR  
DLDAEPELNRDPPGDERDTTTPHAIALVLQQLVLGNALPPDKRALLTDWMARNTTGA  
KRIRAGFPADWKVIDKTGTGDYGRANDIAVVWSPTGVPYVVAVMSDRAGGGYDAEPR  
EALLAEAATCVAGVLA

>\_ 3IQA 265 aa vs.  
>\_ NP\_216584.1 307 aa

scoring matrix: , gap penalties: -12/-2

86.3% identity; Global alignment score: 1653

```

                                     10
294897 -----DLADRFAELERRYDARLG
                                     :
_   MRNRGFGRRELLVAMAMLVSVTGCARHASGARPASTTLPAGADLADRFAELERRYDARLG
      10      20      30      40      50      60
      20      30      40      50      60      70
294897 VYVPATGTTAAIEYRADERFAFCSTFKAPLVAAVLHQNPLTHLDKLIITYTSDDIRSISPV
      :
_   VYVPATGTTAAIEYRADERFAFCSTFKAPLVAAVLHQNPLTHLDKLIITYTSDDIRSISPV
      70      80      90      100     110     120
      80      90      100     110     120     130
294897 AQQHVQTGMTIGQLCDAAIRYSDGTAANLLLADLGGPGGGTAAFTGYLRS LGD TV SRL DA
      :
_   AQQHVQTGMTIGQLCDAAIRYSDGTAANLLLADLGGPGGGTAAFTGYLRS LGD TV SRL DA
      130     140     150     160     170     180
      140     150     160     170     180     190
294897 EEPENRDPPGDERDTTTPHAIALVLQQLVLGNALPPDKRALLTDWMARNTTGAKRIRAG
      :
_   EEPENRDPPGDERDTTTPHAIALVLQQLVLGNALPPDKRALLTDWMARNTTGAKRIRAG
      190     200     210     220     230     240
```



From the one hundred hits our final working population eighteen representative sequences.

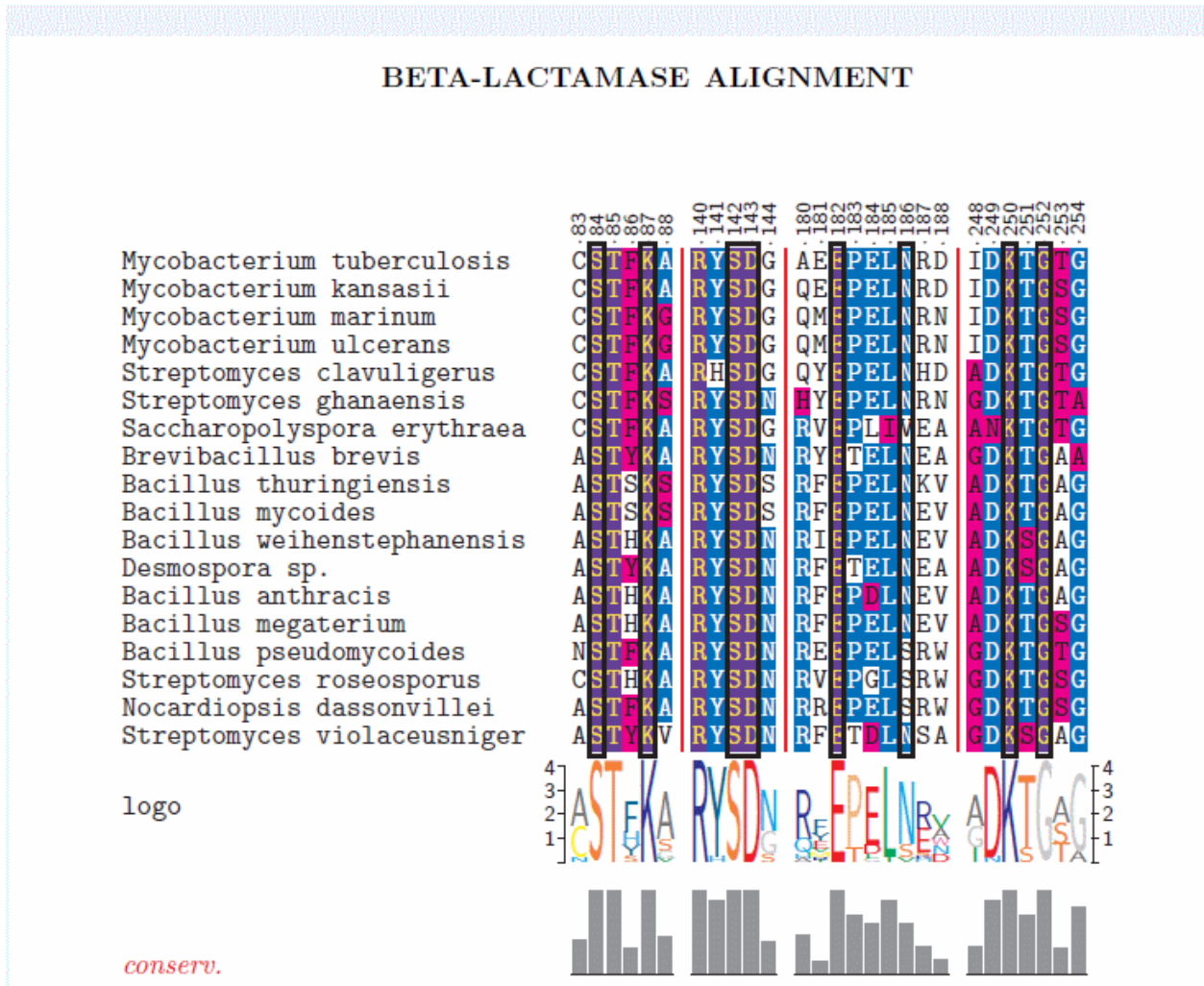


**Fig. 60. Conserved motifs for population of 18  $\beta$ -lactamases**

The first sequence on the list is our strain of interest, followed by *M. kansasii* causative agent of a pulmonary infection that resembles tuberculosis, followed by *M. marinum* the only *Mycobacterium* that is not aerobic, and *M. ulcerans* is the third most common mycobacterial pathogen in humans, after *M. tuberculosis* and *M. leprae*.

The two important genera of the Actinobacteria taxon (Gram-positive bacteria with high G + C content of DNA), *Streptomyces* and *Mycobacterium*, are known for their separate but unique impact on humans. The best known *Mycobacterium* species, tuberculosis and leprae have afflicted humans since the beginning of time and are still major threats to public health. On the other hand, *Streptomyces* species are known for producing antibiotics. More than half of presently marketed antibiotics are produced by species of the *Streptomyces* genus, (A) such as cefoxitin, chloramphenicol, neomycin, streptomycin, tetracycline, and clavulanic acid.

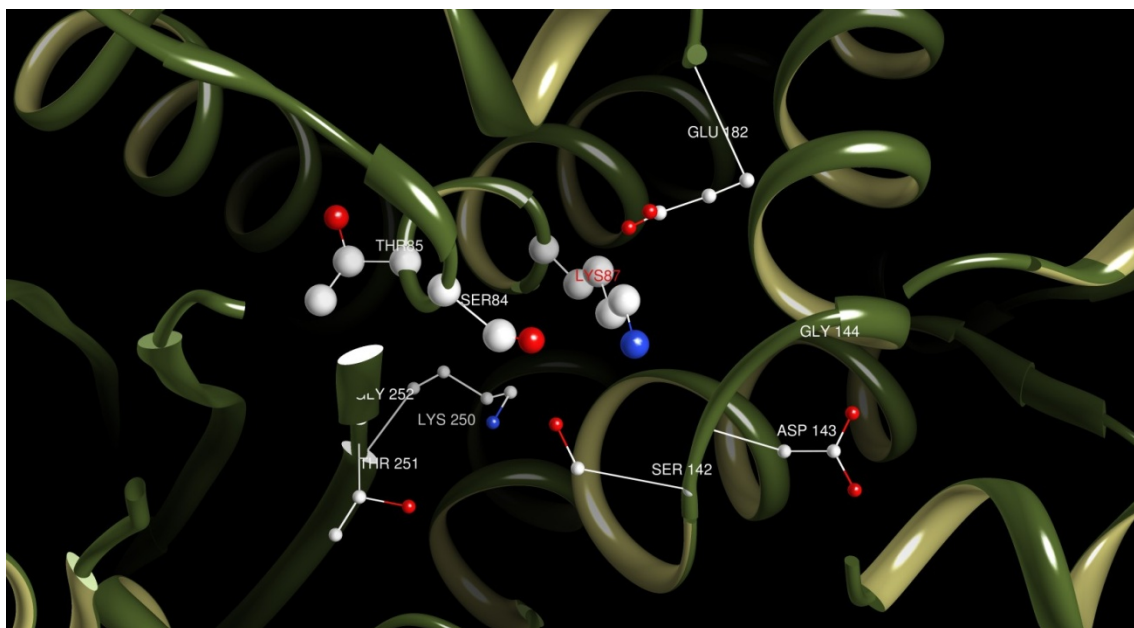
All the bacillus species chosen produce a class A  $\beta$ -lactamase with the exception of *Brevibacillus brevis*, that produces a  $\beta$ -lactamase precursor. As can be seen from the alignment there are four distinct highly conserved areas;

Element 1 is the sequence SXXK that contains the active site serine residue (Figure 61)

Element 2 is the SDN/G loop, between helices  $\alpha 4$  and  $\alpha 5$ . This S142 is involved in maintaining the functional position of the two domains and the protonation of the substrate's leaving group

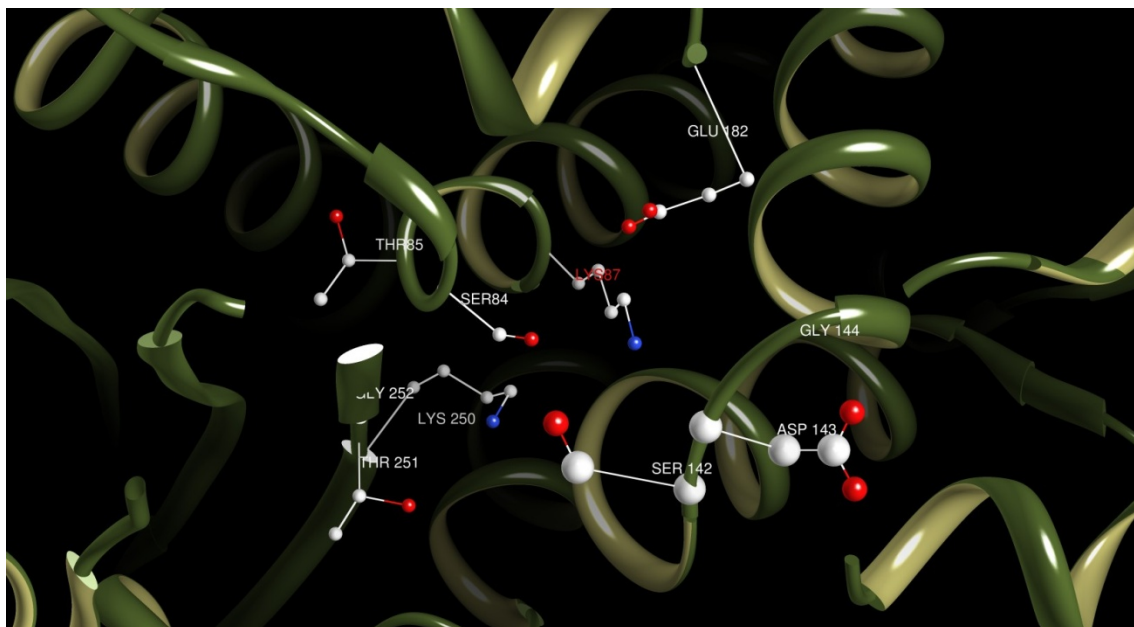
Element 3 is the acidic residue E182 that's side chain points into the substrate's binding cavity

Element 4 KTG located in the  $\beta 3$  strand facing the SDN/G loop on the other side of the active site serine.



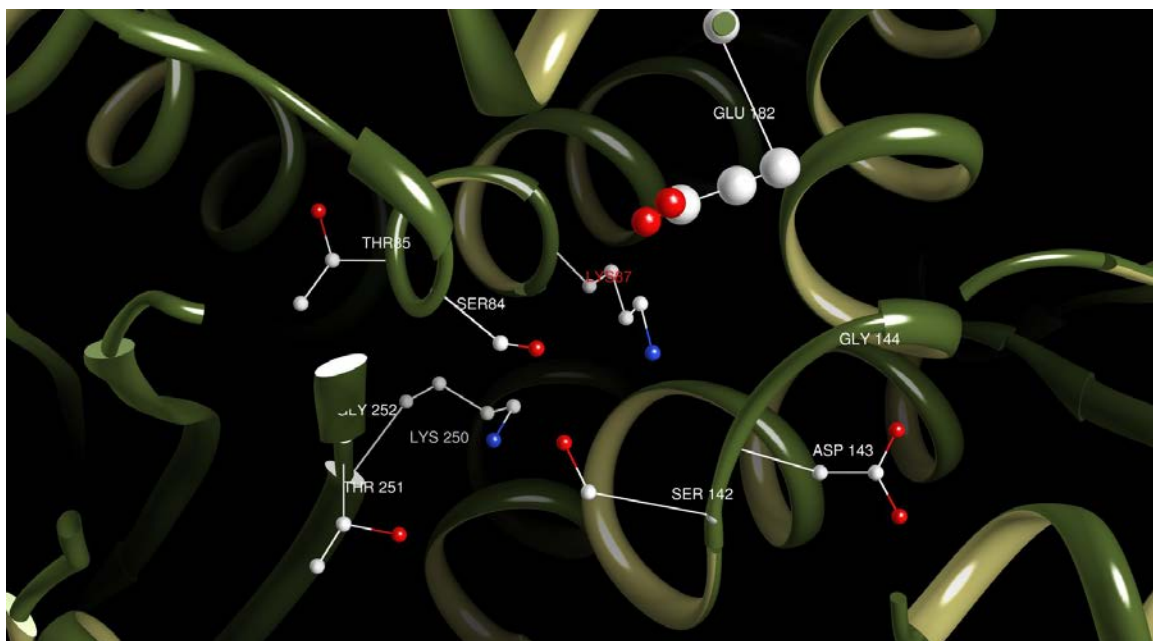
**Fig. 61. Active site Serine 84 and Lysine 87 Element 1**

Molecular graphics images were produced using the UCSF Chimera package from the Resource for Biocomputing, Visualization, and Informatics at the University of California, San Francisco



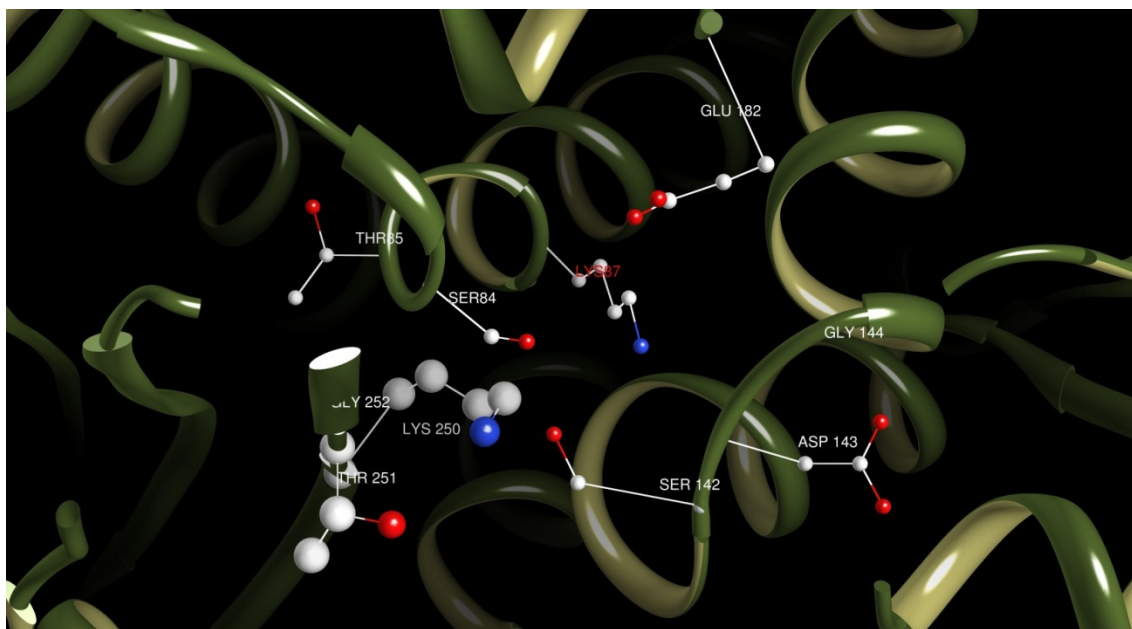
**Fig. 62. Serine 142, Aspartic Acid 142 and Glycine 144 Element 2**

Molecular graphics images were produced using the UCSF Chimera package from the Resource for Biocomputing, Visualization, and Informatics at the University of California, San Francisco



**Fig. 63. Glutamic Acid 182 Element 3**

Molecular graphics images were produced using the UCSF Chimera package from the Resource for Biocomputing, Visualization, and Informatics at the University of California, San Francisco

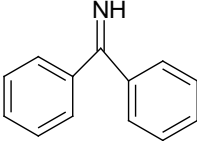
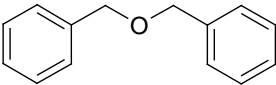
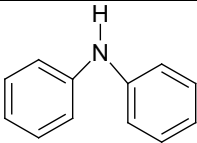
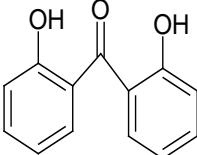
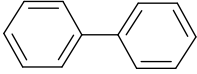
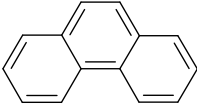
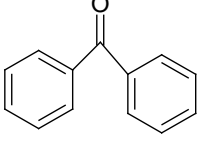
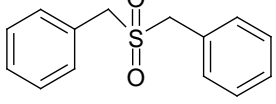


**Fig. 64. Lysine 250, Threonine 251 and Glycine 252 Element 4**

Molecular graphics images were produced using the UCSF Chimera package from the Resource for Biocomputing, Visualization, and Informatics at the University of California, San Francisco

## Screened Compounds and Inhibitors Chapter 6

Table 11. Screened Compounds

Compound	Structure	$K_i$
Benzophenone Imine (Synthesized by S. Zakia)		No Inhibition (70 $\mu\text{M}$ highest inhibitor concentration)
Dibenzylether		No Inhibition (70 $\mu\text{M}$ highest inhibitor concentration)
Diphenylamine		No Inhibition (70 $\mu\text{M}$ highest inhibitor concentration)
2,2-Dihydrobenzophenone		No effect from 20 $\mu\text{M}$ to 40 $\mu\text{M}$ only shows inhibition after 50 $\mu\text{M}$
Biphenyl		123 $\pm$ 18 $\mu\text{M}$
Phenanthrene		28 $\pm$ 2 $\mu\text{M}$
Benzophenone		25 $\pm$ 2 $\mu\text{M}$
Dibenzylsulfone		17 $\pm$ 3 $\mu\text{M}$

### Example K; Calculations for Screened Compounds

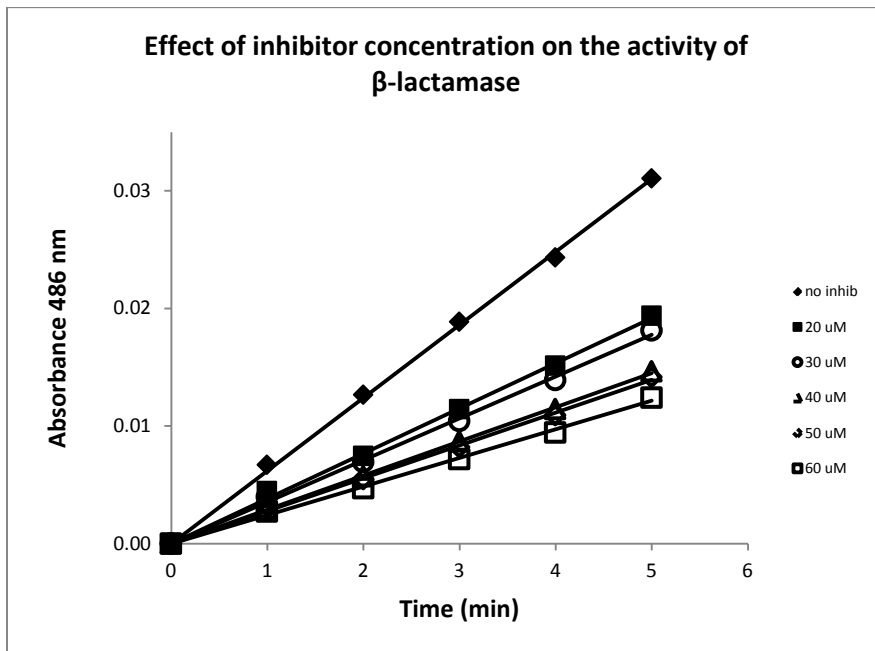


Fig. 65. Raw Data of Change in absorbance vs. Time for the Inhibitor Benzophenone

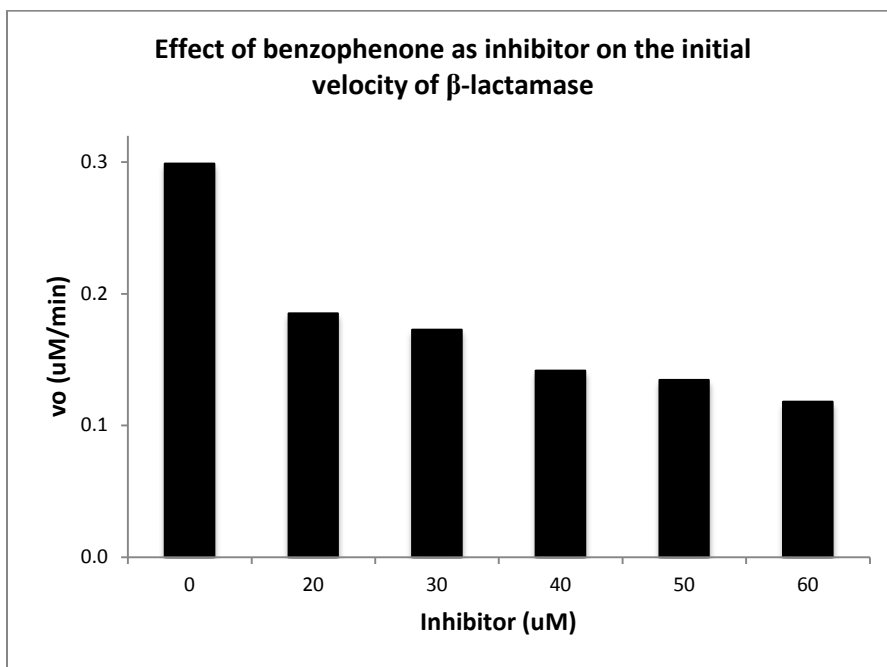
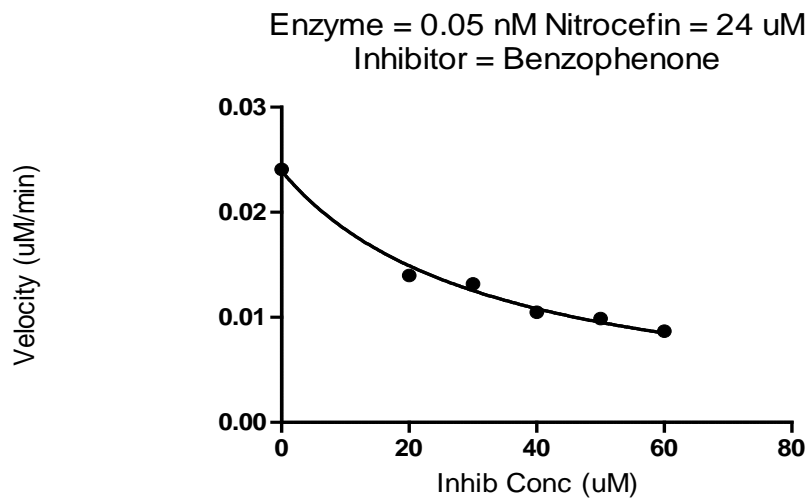


Fig. 66. Effect of Increasing Concentration of Benzophenone on the Velocity of the Reaction



**Fig. 67. Velocity vs. the concentration of Benzophenone as Inhibitor.  $K_i$  of Benzophenone =  $25 \pm 2 \mu$ M**

From GraphPad Software, San Diego California USA,

2-Aminoethanol

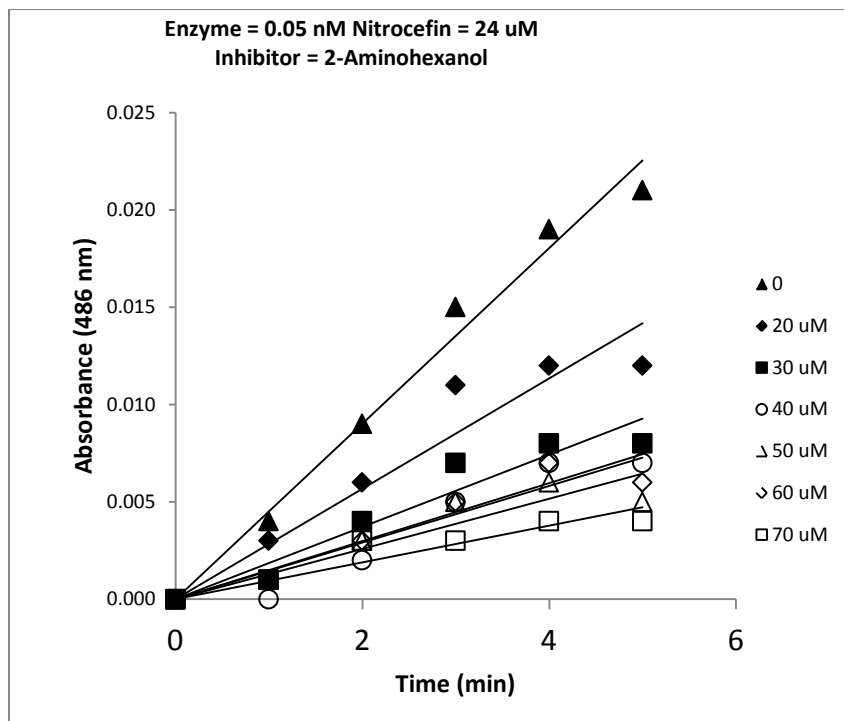


**Fig. 68. Raw Data of Change in Absorbance vs. Time for the Inhibitor 2-Aminoethanol**

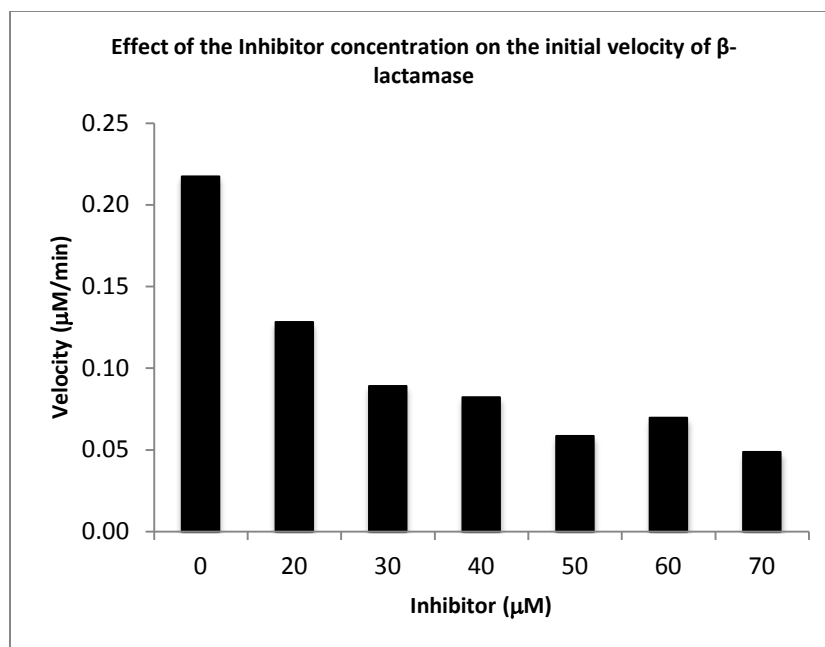


**Fig. 69. Effect of Increasing Concentration of 2-Aminohexanol on the Velocity of the Reaction**

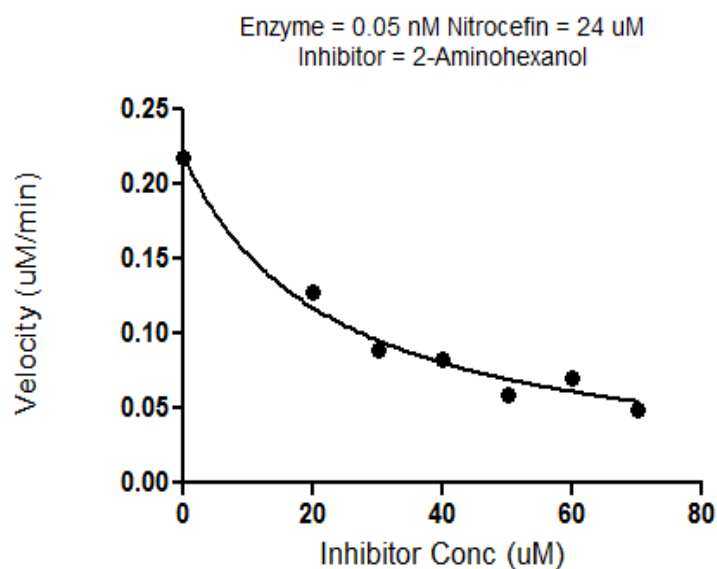


**Fig. 70. Velocity vs. the Concentration of Benzophenone as Inhibitor for the Determination of  $K_i$**   
From GraphPad Software, San Diego California USA,  $K_i$  of 2-Aminohexanol =  $19 \pm 4 \mu\text{M}$

## Docking Images

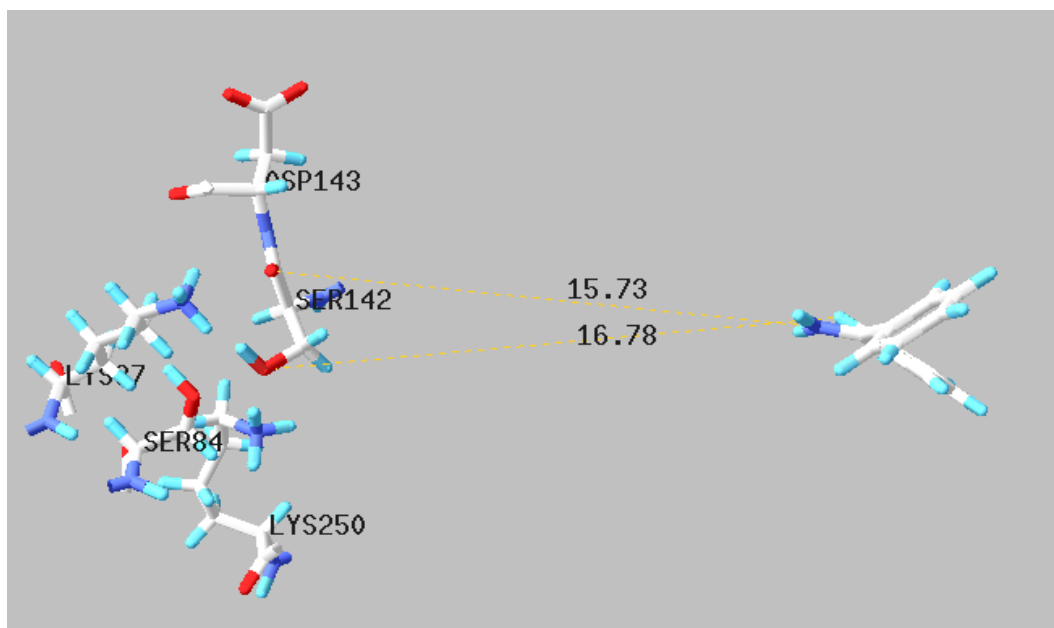


**Fig. 71. Benzophenone Imine no Inhibition**

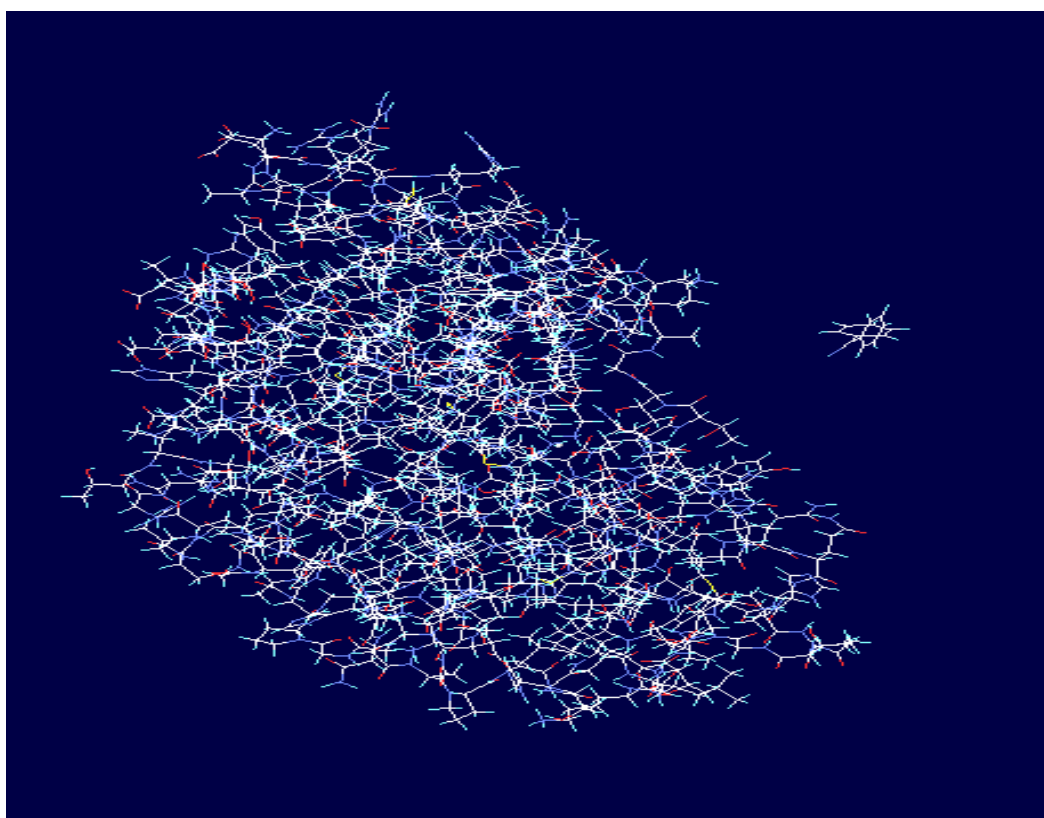


**Fig. 72. Benzophenone Imine Global Docking**

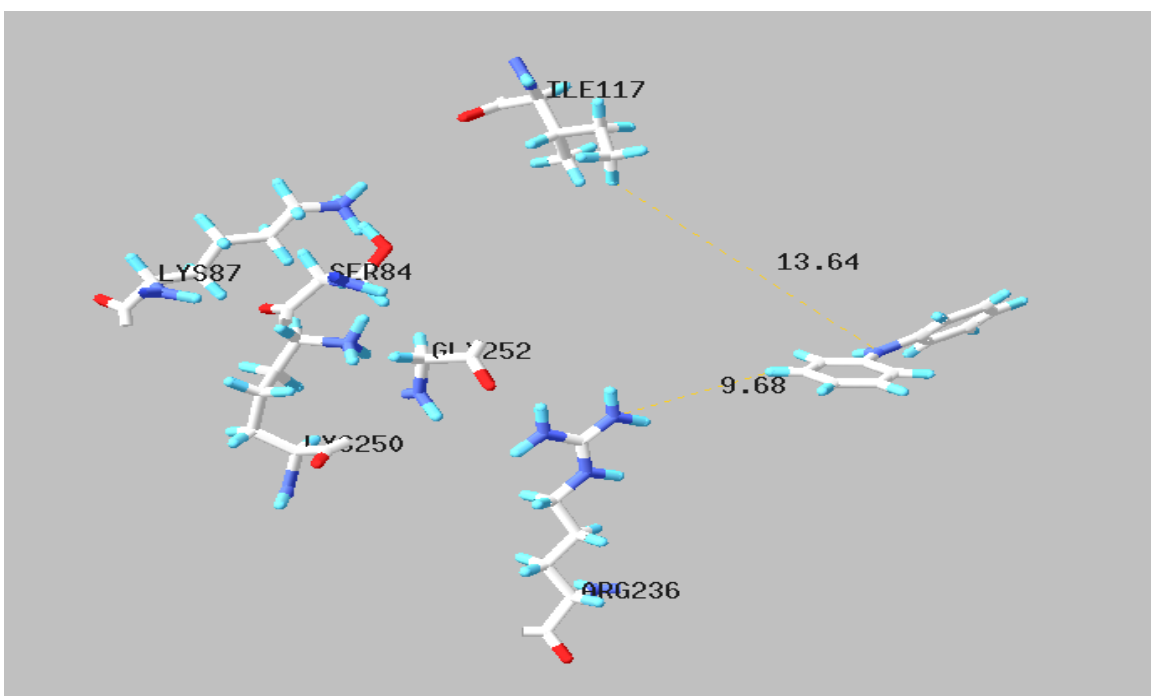


**Fig. 73. Diphenylamine no Inhibition**

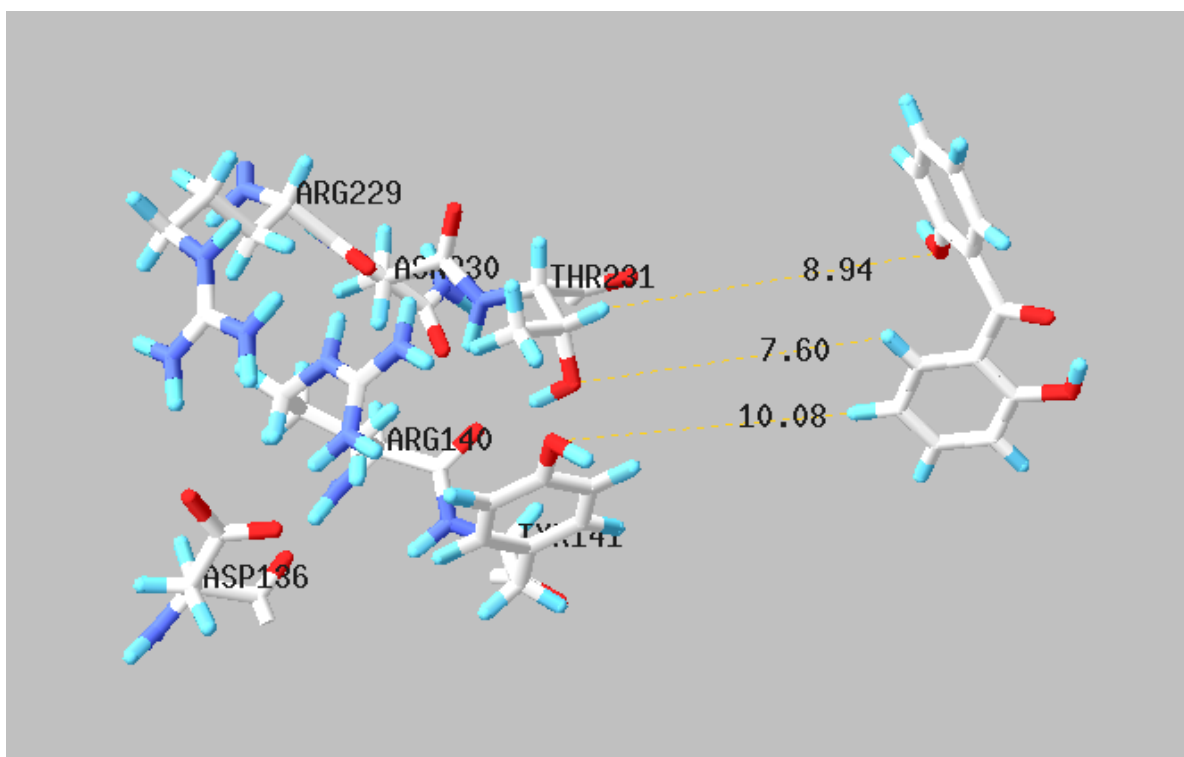


**Fig. 74. 2, 2-Dihydroxybenzophenone (Inhibits slightly after 50  $\mu$ M concentration)**

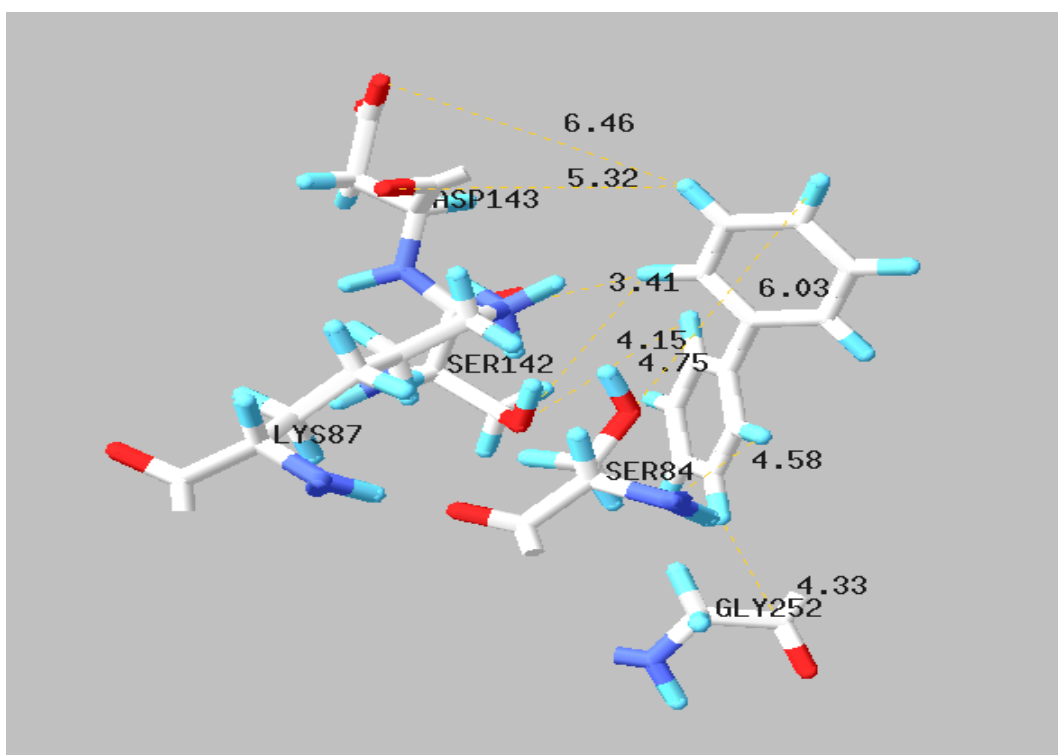


**Fig. 75. Biphenyl  $K_i = 123 \pm 18 \mu\text{M}$**

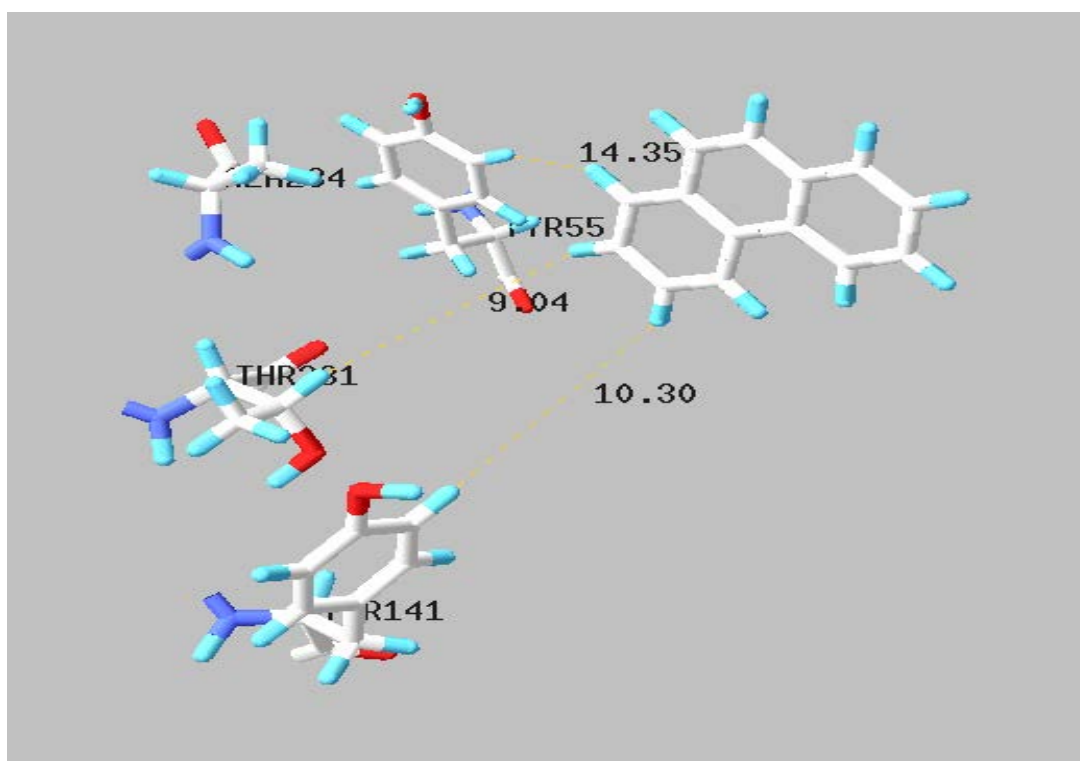


**Fig. 76. Phenanthrene  $K_i = 28 \pm 2 \mu\text{M}$**

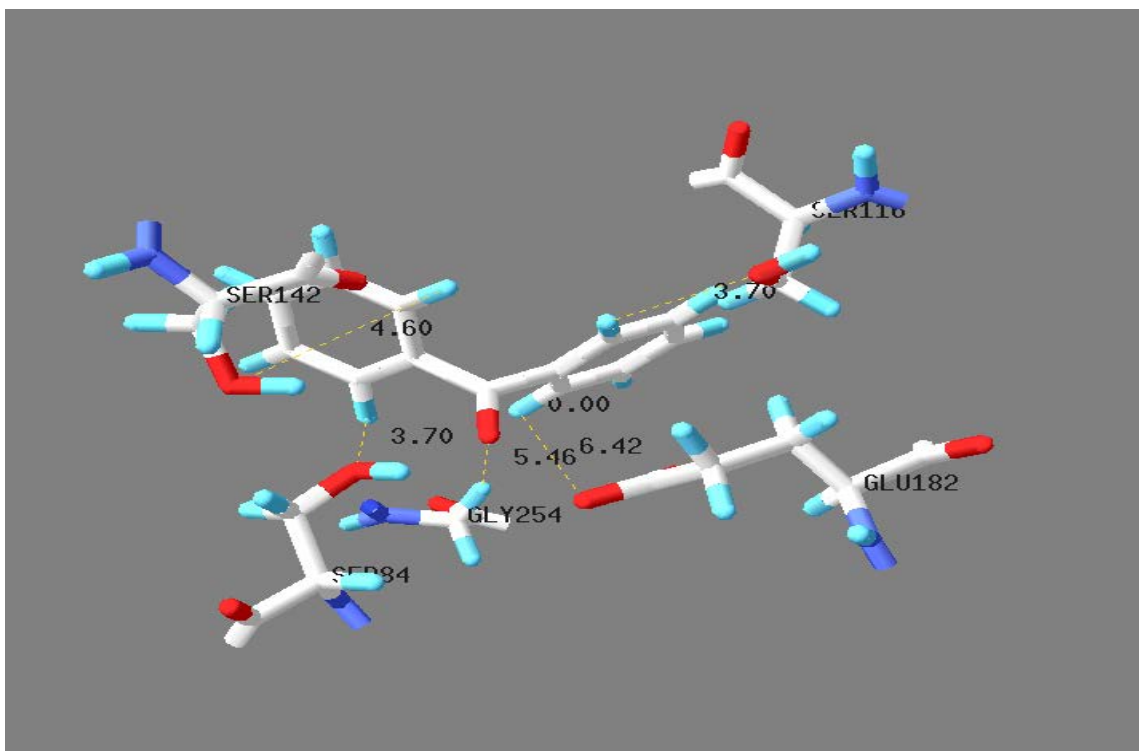


Fig. 77. Benzophenone  $K_i = 25 \mu\text{M}$

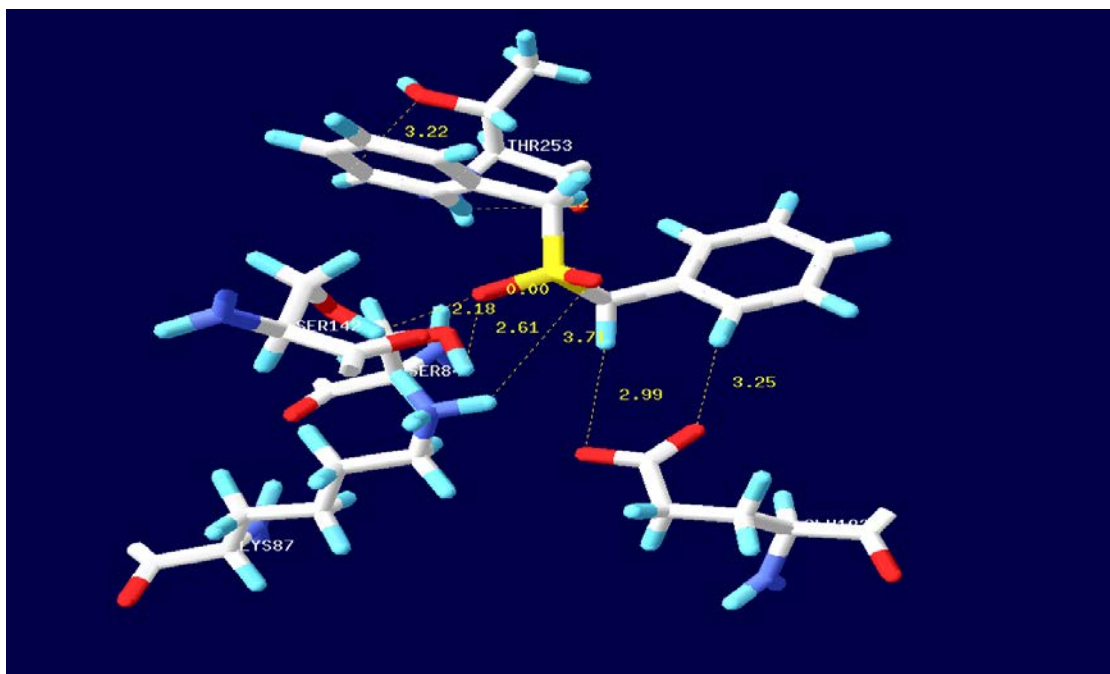
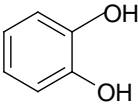
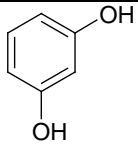
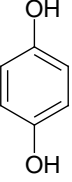
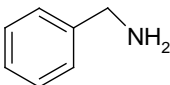
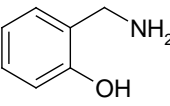
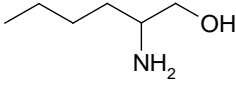
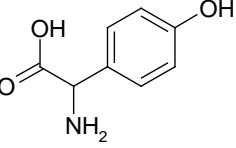
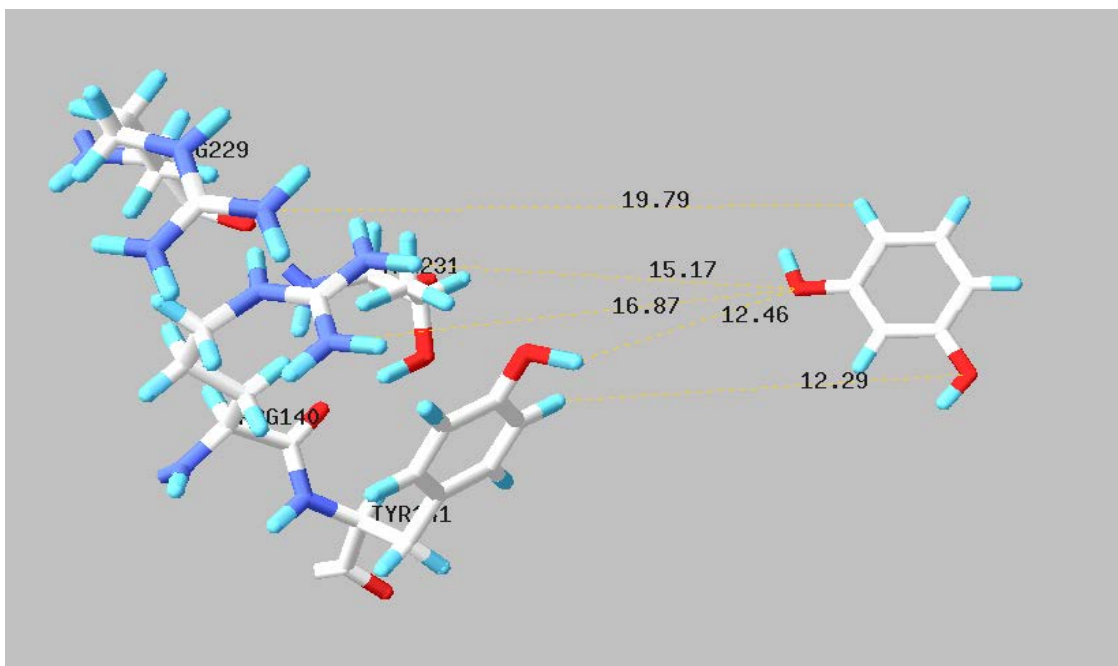


Fig. 78. Dibenzylsulfone  $K_i = 17 \pm 3 \mu\text{M}$

**Table 12. Screened Compounds**

<b>Compound</b>	<b>Structure</b>	<b>K<sub>i</sub></b>
Catechol		No Inhibition (70 μM highest inhibitor concentration)
Resorcinol		No Inhibition (70 μM highest inhibitor concentration)
Hydroquinone		64±5 μM
Benzylamine		41±3 μM
2-Hydroxy benzylamine		31±2 μM
2-Aminohexanol		19±4 μM
<i>p</i> -Hydroxyphenyl glycine		5±2 μM



**Fig. 79. Resorcinol No Effect**

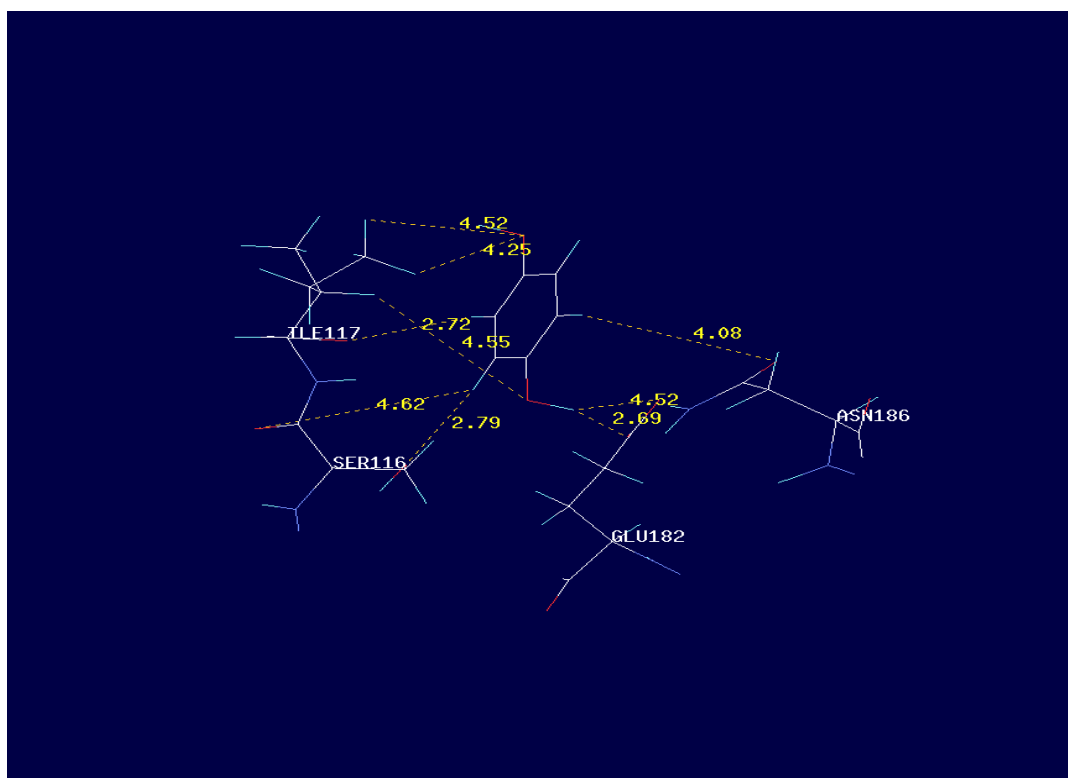


**Fig. 80. Hydroquinone  $K_i = 64 \pm 5 \mu\text{M}$**

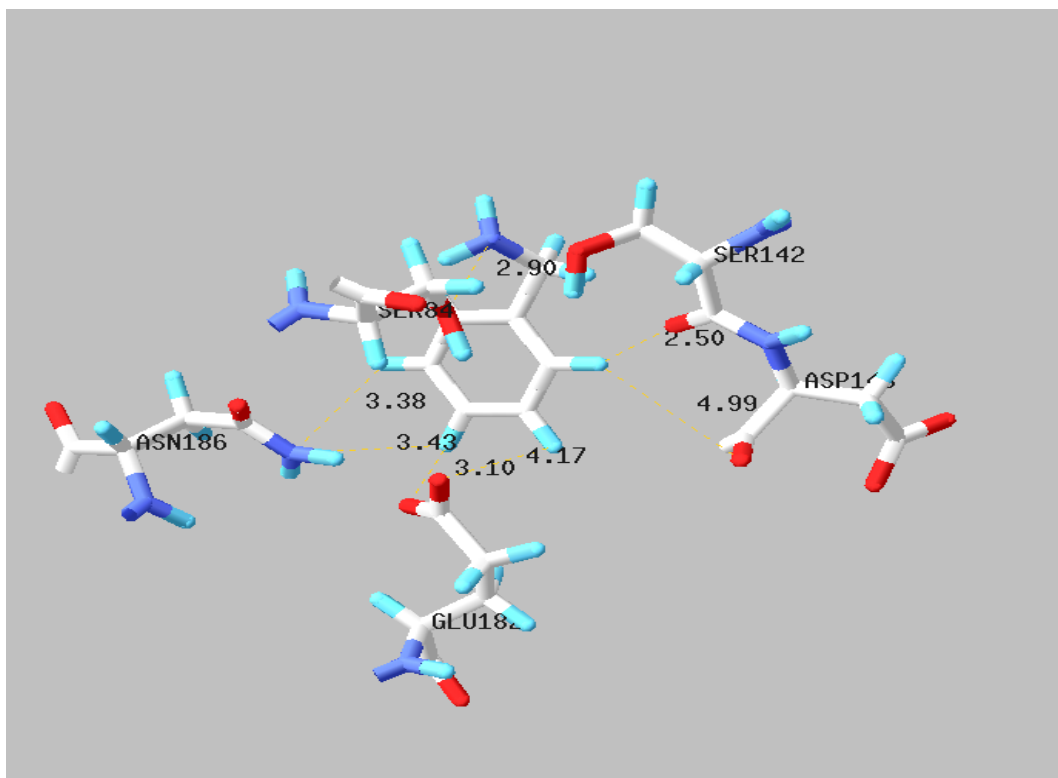


**Fig. 81. Benzylamine  $K_i = 41 \pm 3 \mu\text{M}$**

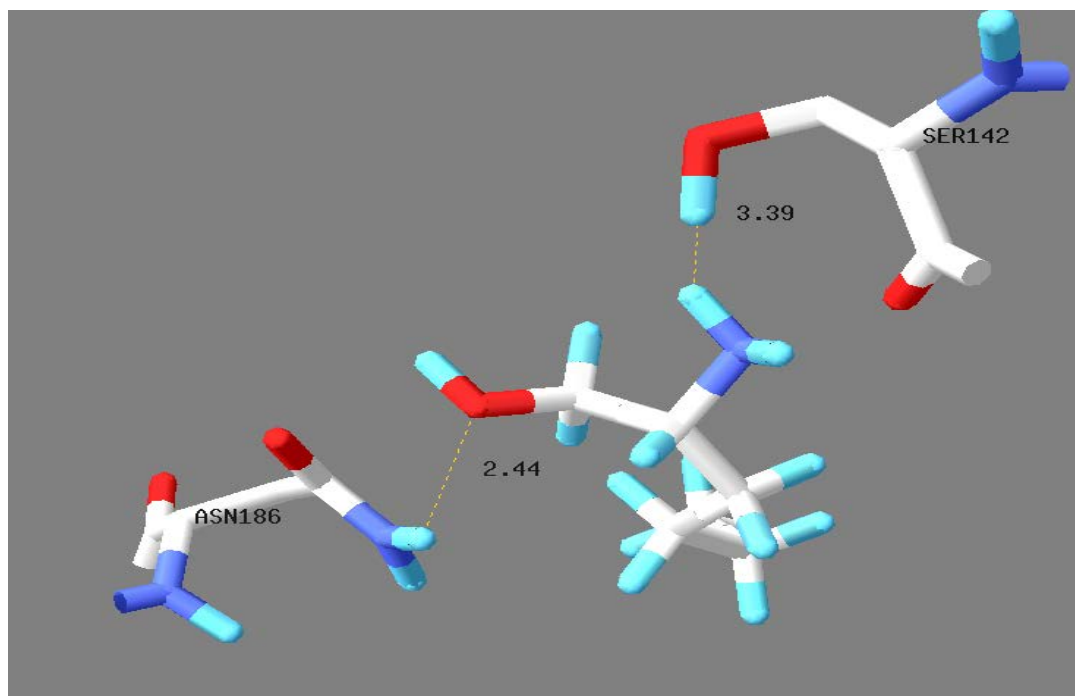


**Fig. 82. 2-Aminohexanol  $K_i = 19 \pm 4 \mu\text{M}$**

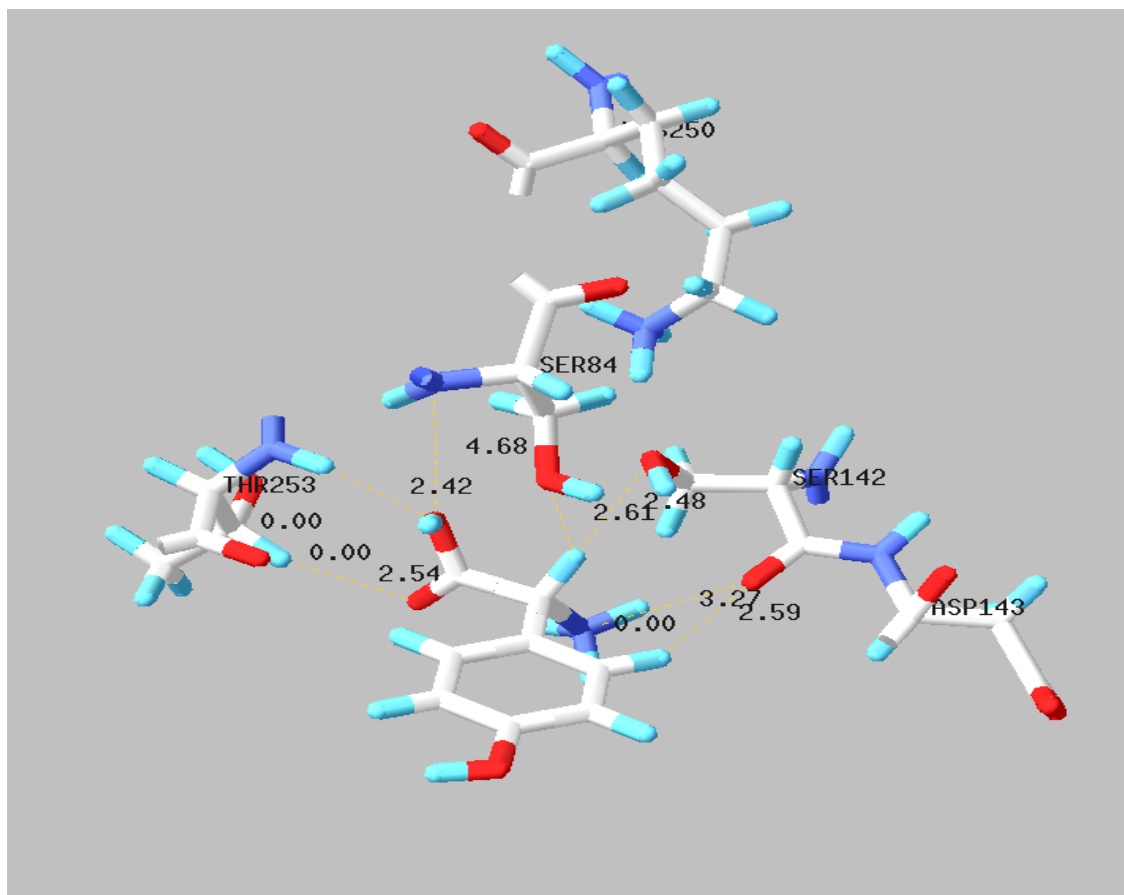
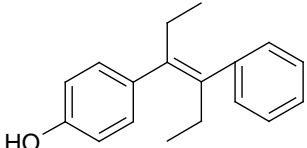
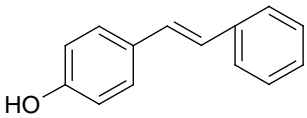
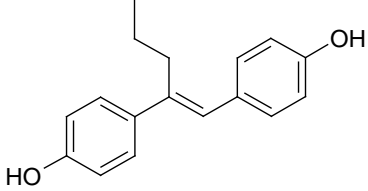
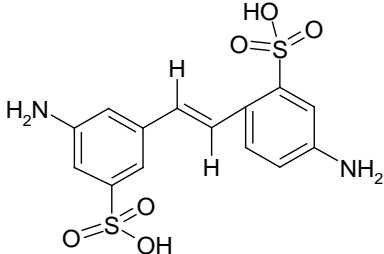
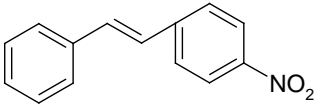
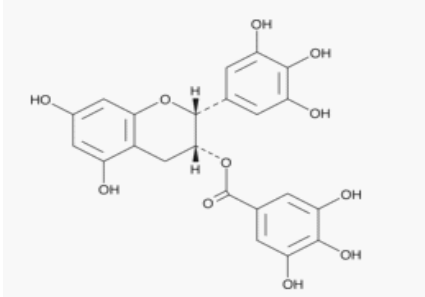
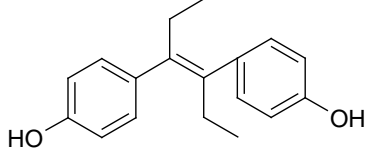
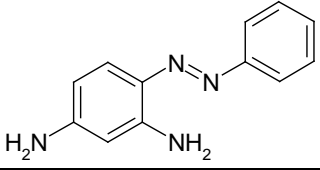
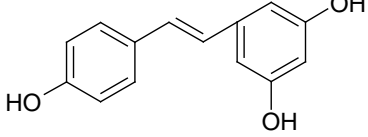
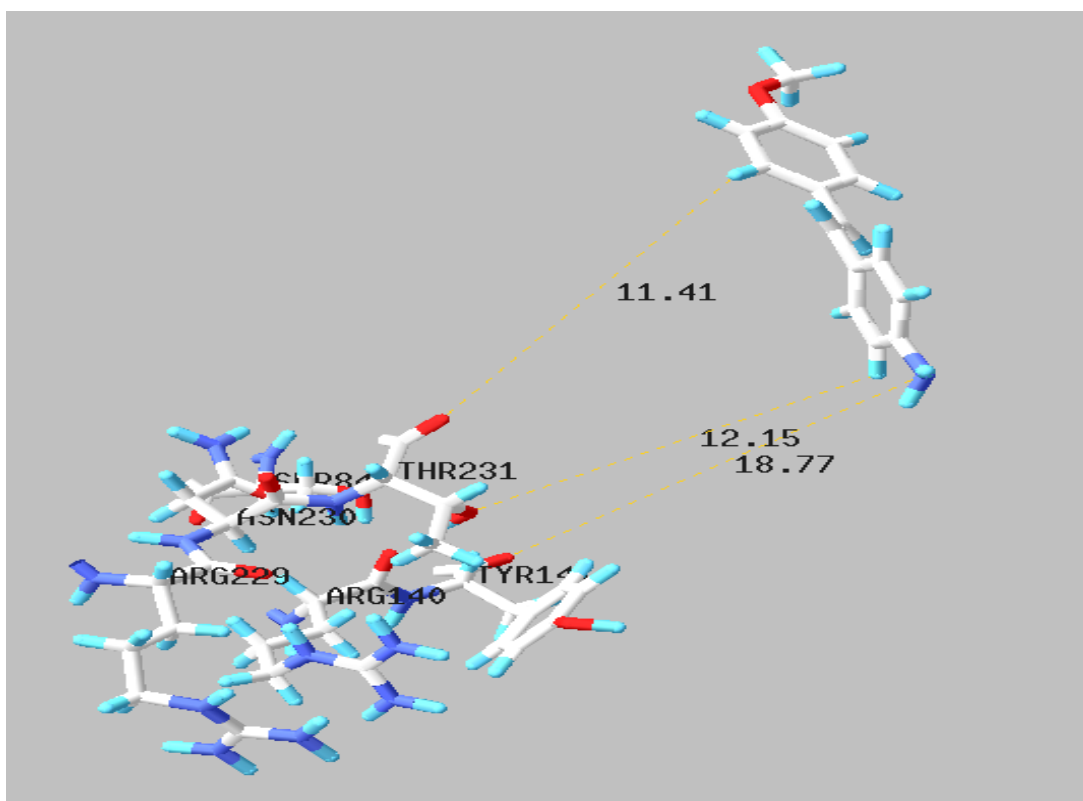


Fig. 83. *p*-Hydroxyphenylglycine  $K_i = 5 \pm 2 \mu\text{M}$

Table 13. Screened Compounds

Compound	Structure	$K_i$
4-Amino 4 methoxystilbene	<chem>Nc1ccc(C=Cc2ccc(OC)cc2)cc1</chem>	Activates
Trans-Stilbene	<chem>C=C(c1ccccc1)c2ccccc2</chem>	Inhibits from 10 $\mu\text{M}$ to 20 $\mu\text{M}$ and activates after 30 $\mu\text{M}$
4,4' Dihydroxy ethylstilbene	<chem>CC=C(O)c1ccc(O)cc1</chem>	191 $\pm$ 11 $\mu\text{M}$

4-Hydroxy diethylstilbene		182±12 μM
4-Hydroxy stilbene		141±12 μM
4,4' Dihydro n-propylstilbene		137±10 μM
4,4'-Diaminostilbene-2,2'-disulfonic Acid		58±5 μM
4-Nitrostilbene		56±8 μM
EGCG Epigallocatechin gallate		50±6 μM
Diethylstilbestrol		32±5 μM
2,4 Diaminoazobenzene		30±6 μM
Resveratrol		14±4 μM



**Fig. 84. 4-Amino 4-methoxystilbene Activates**

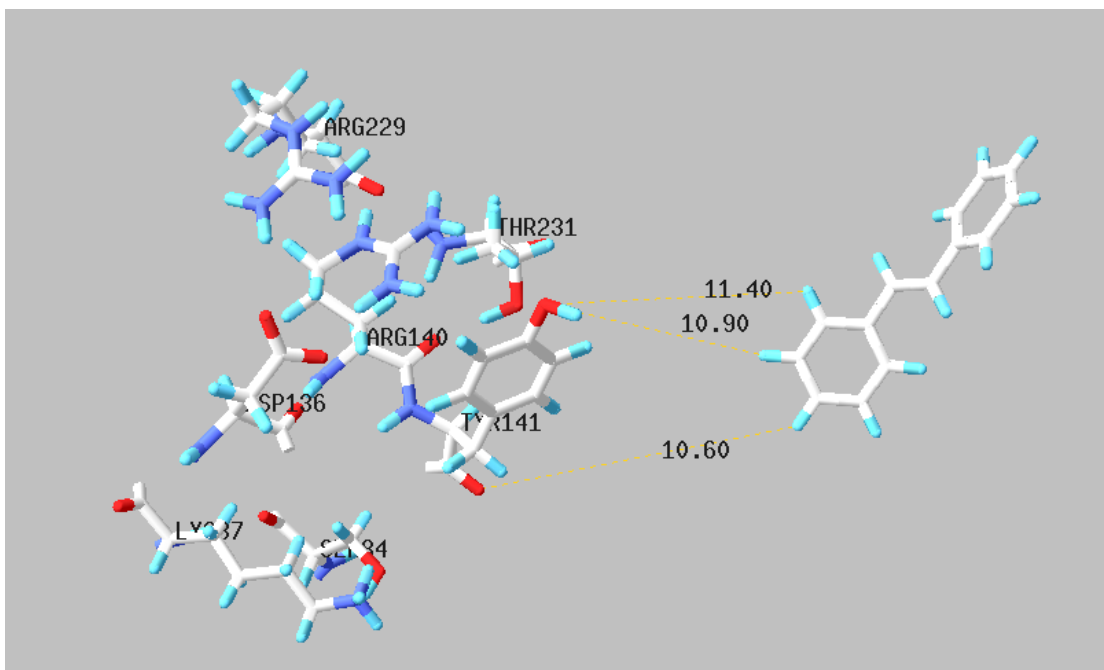


**Fig. 85. Trans stilbene**

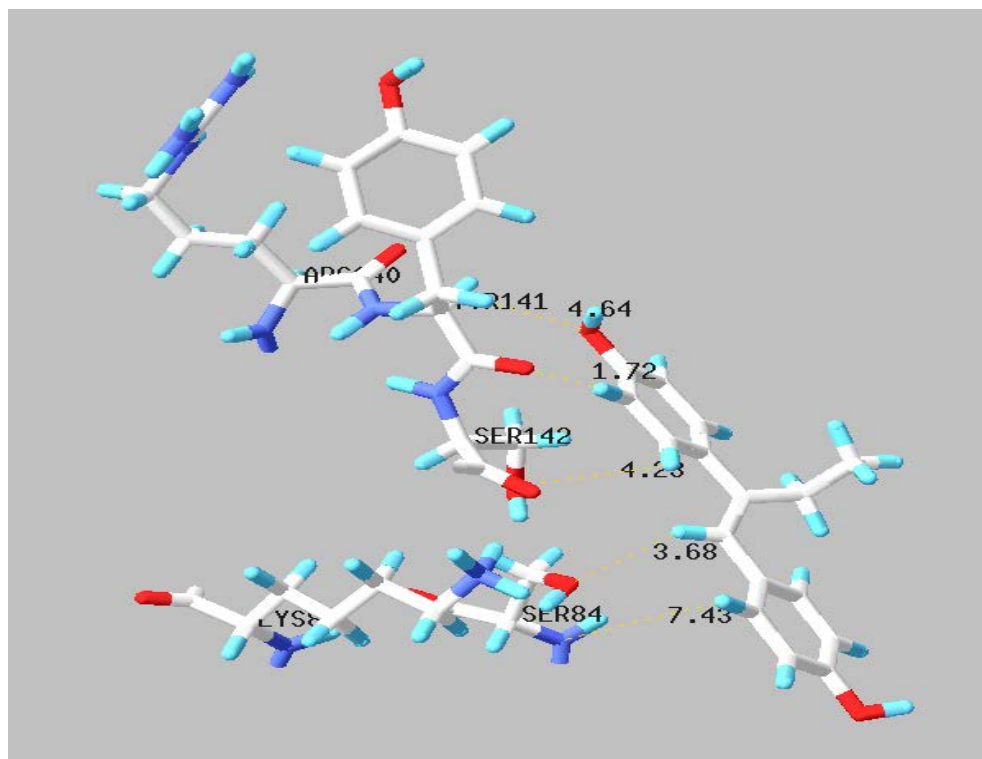


Fig. 86. 4,4-Dihydroxyethylstilbene  $K_i = 191 \pm 11 \mu\text{M}$

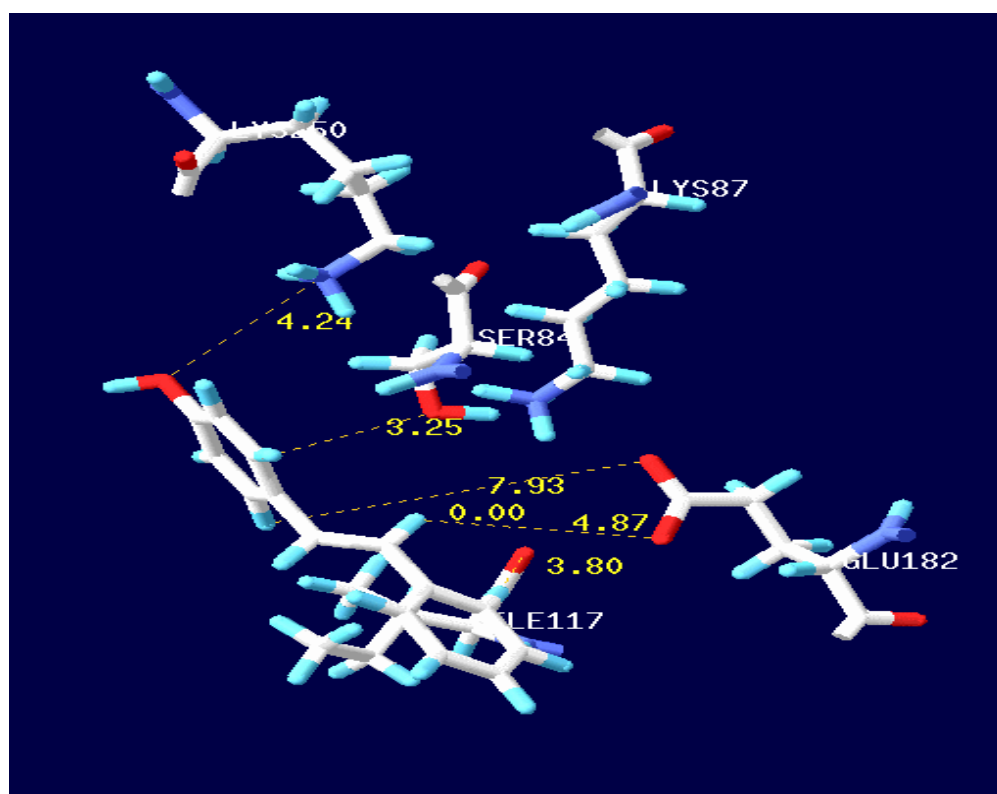
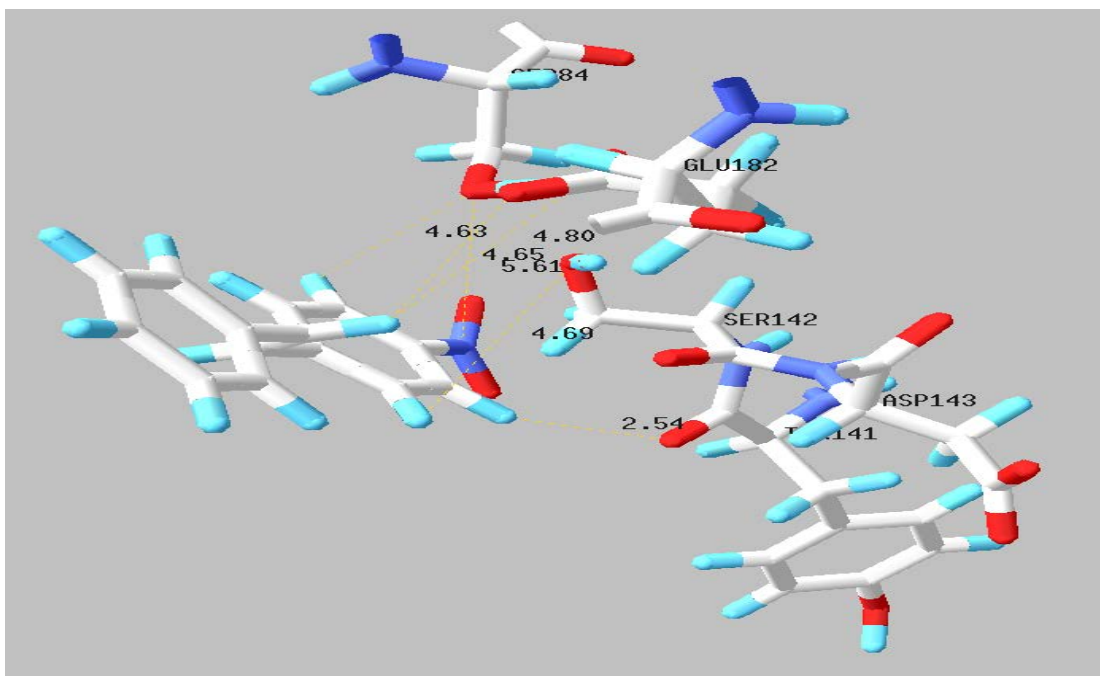
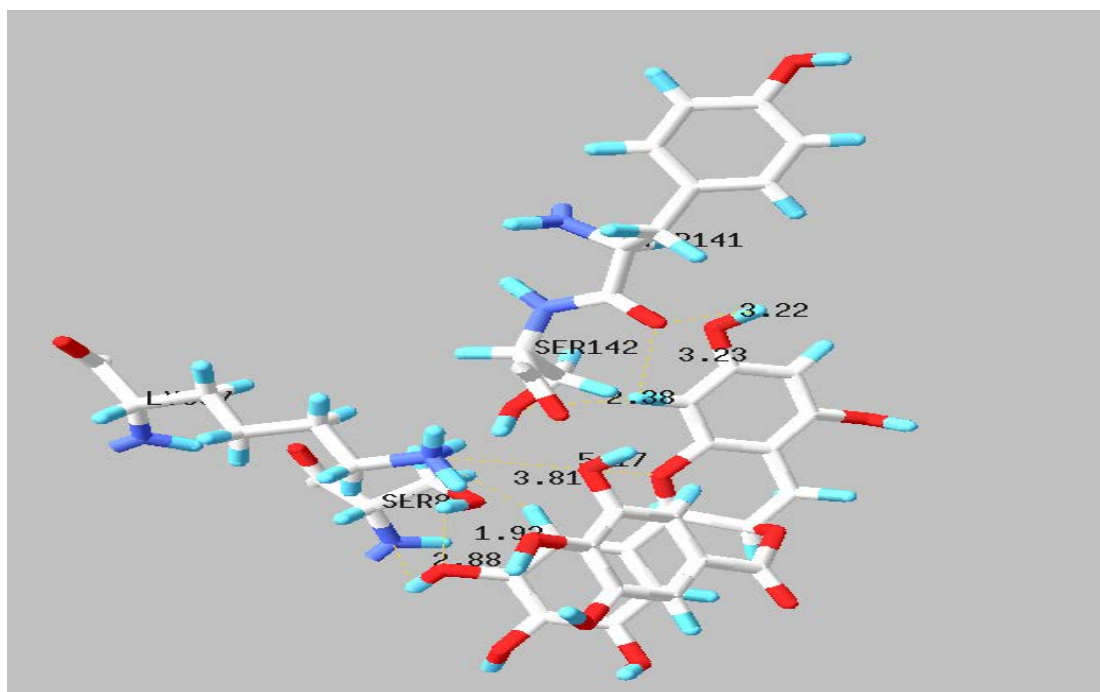


Fig. 87. 4-Hydroxystilbene  $K_i = 141 \pm 12 \mu\text{M}$



**Fig. 88.** 4-Nitrostilbene  $K_i = 56 \pm 8 \mu\text{M}$



**Fig. 89.** Epigallocatechin Gallate (EGCG)  $K_i = 50 \pm 6 \mu\text{M}$

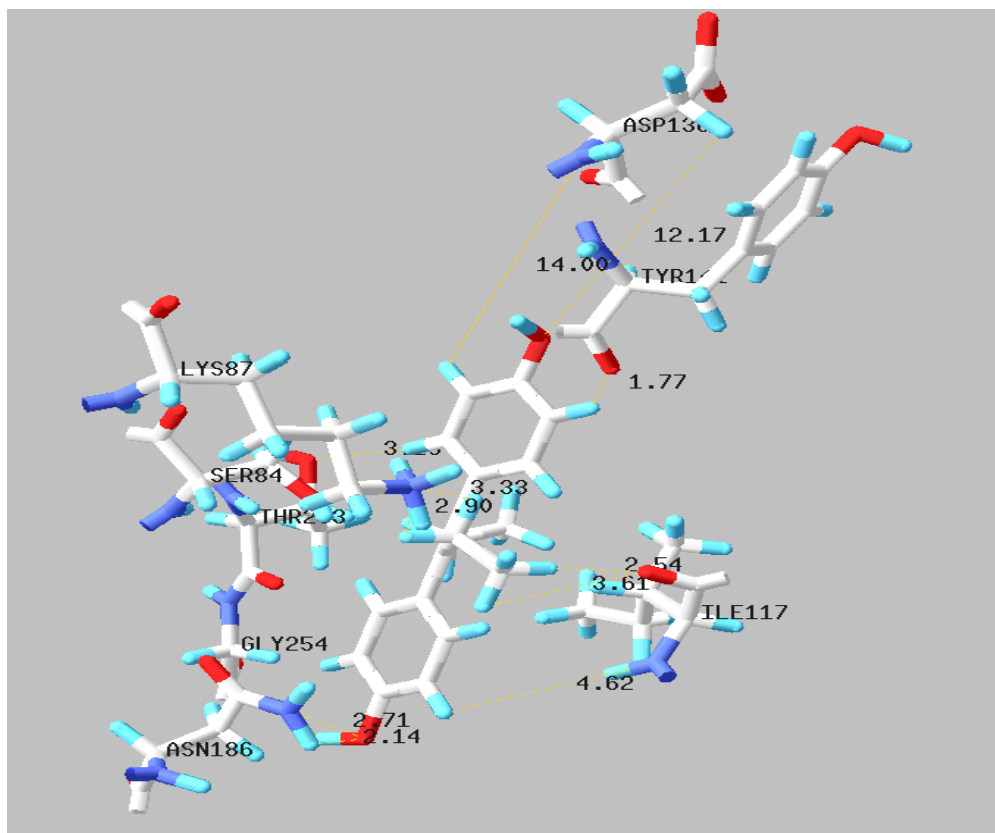


Fig. 90. Diethylstilbestrol  $K_i = 32 \pm 5 \mu\text{M}$

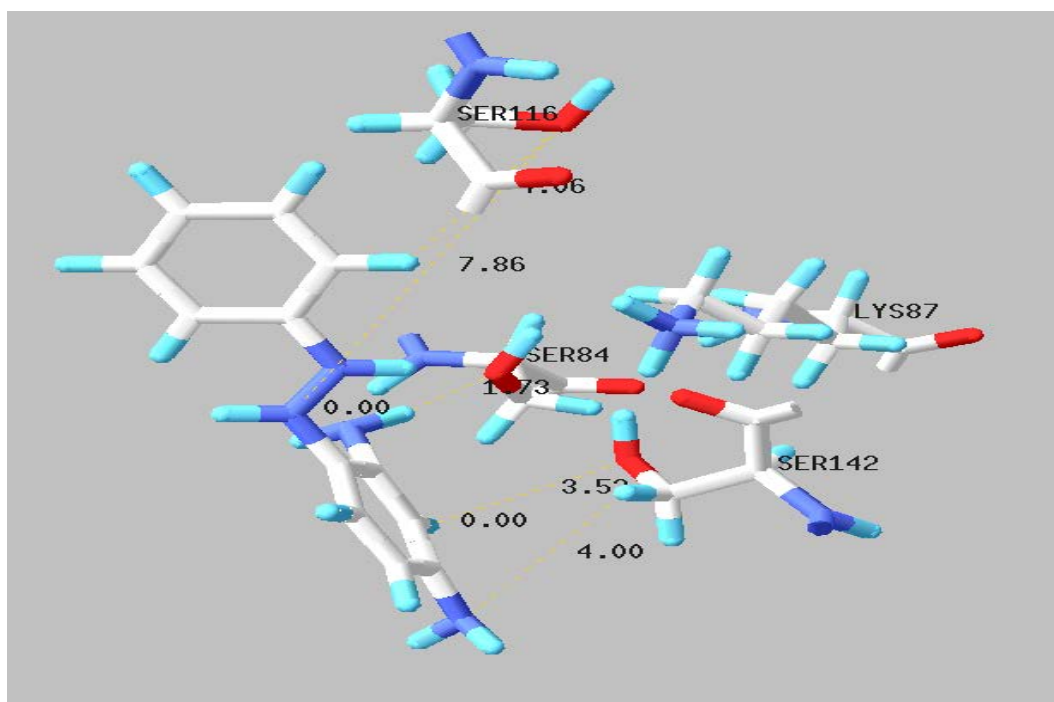
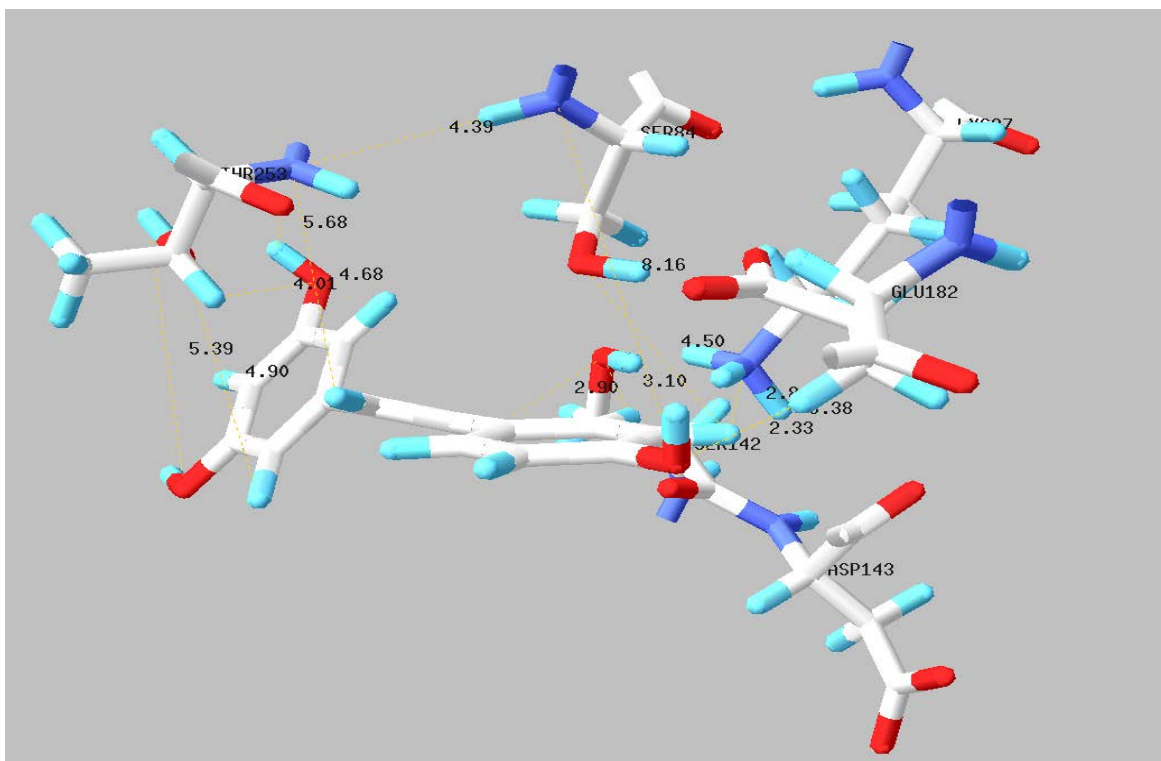


Fig. 91. 2,4-Diaminoazobenzene  $K_i = 30 \pm 6 \mu\text{M}$



**Fig. 92. Resveratrol  $K_i = 14 \pm 4 \mu\text{M}$**

### Discussion

There are several non- $\beta$ -lactam based inhibitors reported in the literature. Some of these inhibitors were found by screening natural products other were found by screening libraries of compounds and yet others were found by computational approaches involving molecular docking. When it was determined that the active site of class A  $\beta$ -lactamases were strongly positively charged (120) Pratt *et al.* introduced a series of phosphonate monoesters that putatively phosphorylated the active site serine of both A and C class  $\beta$ -lactamases (121). They found that compounds where X is an electron withdrawing group were better inhibitors than the corresponding unsubstituted analogs.

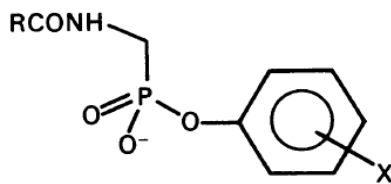


**Fig. 93. General Structure of phosphonate Monoesters (121)**

In 1994 the crystal structure of a complex formed between *p*-nitrophenyl [N-(benzyloxycarbonyl)aminomethyl] phosphonate and a class C  $\beta$ -lactamase was obtained and proved that the mechanism of these inhibitors was indeed phosphorylation of the active site serine and again demonstrated that the active site of  $\beta$ -lactamases are very good at stabilizing negatively charged transition states. The inhibitory activity of these monoesters was amplified by varying both the R group and the leaving group (122).

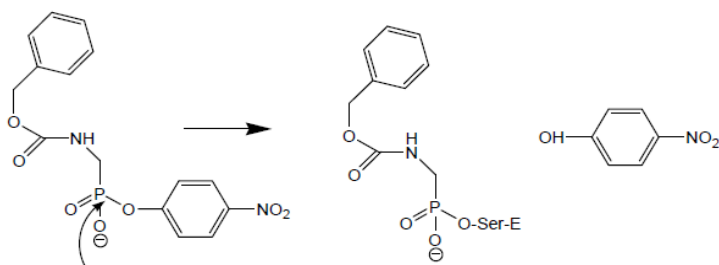


**Fig. 94. Mechanism of  $\beta$ -Lactamase Inhibition by *p*-nitrophenyl [N-(benzyloxycarbonyl)aminomethyl]phosphonate (122)**

In the normal hydrolysis mechanism of  $\beta$ -lactam substrates after the formation of the acyl-enzyme complex and the breaking of the scissile C4-N7 bond a general base abstracts a proton from water activating the water oxygen to attack the carbonyl carbon of the acyl-enzyme again forming a tetrahedral intermediate. The general acid back donates the proton to the  $\gamma$ -oxygen of serine and the serine is regenerated with the concomitant release of the inactive  $\beta$ -lactam antibiotic. Using phosphonate monoesters it was observed that leaving groups that do not

require acid catalysis conferred higher inhibitory activity. This observation was rationalized by the fact that the general acid used in the normal hydrolysis of  $\beta$ -lactam substrates is not available to the leaving group from the trigonal pyramidal transition state used by phosphonates (110).

The reaction of phosphonates with  $\beta$ -lactamases proposed that the active site not only stabilizes tetrahedral anionic transition states but can also stabilize a pentacoordinate transition state. This research led to the inspection of vanadate complexes as  $\beta$ -lactamases inhibitors (123).

Molecular modeling shows that a pentacoordinated vanadate-catechol complex readily fits into the class C  $\beta$ -lactamase active site with the proper coordination to the  $\gamma$ -oxygen of serine (124).

Typically transition state analog inhibitors with crystal structures such as phosphonates, boronates and arsonates place the inhibitors in the active site in a conformation that mimics the tetrahedral intermediate of the normal catalyzed reaction.

When boronic acids were described as forming reversible covalent bonds with serine proteases (125) by assuming tetrahedral intermediates this chemistry was applied to class A  $\beta$ -lactamases with boronic acid derivatives such as phenyl and *m*-aminophenyl compounds. Weston *et al.* used the crystallographic structure of *E. coli* AmpC  $\beta$ -lactamase in complex with *m*-aminophenylboronic acid (PDB 3BLS) as a model for designing boronic acid-based inhibitors (126) and found them to inhibit in the mM range (127). Extensive studies on boronic acids by other groups (128-131) again demonstrated that these class of compounds without the  $\beta$ -lactam motif, form adducts resembling the tetrahedral geometry of the normal hydrolysis reaction.

*O*-Aryloxycarbonyl hydroxamate an irreversible inhibitor of the class C  $\beta$ -lactamase, has a mechanism that involves cross-linking of active site residues. The inhibitor is stabilized by the side chains of Tyr150 and Lys315 instead of the typical backbone nitrogens of Ser64 and Ser318.

The inactivation leads to a cross-linking of Ser64 and Lys315 residues. Clavulanic acid and penicillin sulfones also cross-link the active site serine to the conserved Ser130 residue effectively killing the enzyme (132)

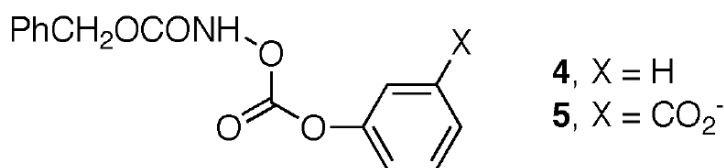


**Fig. 95. General Structure of *O*-Aryloxycarbonyl Hydroxamates (126)**

In the context of previous work done and with these non-traditional  $\beta$ -lactamase inhibitors in mind this dissertation presents three different classes of inhibitors, peptides, biphenyl compounds and a boronic acid.

### **Biphenyls, Aromatic Ketones and Stilbenes**

In 1944 Faulkner discovered the bactericidal properties of some stilbenes and diphenyl derivatives. The common feature for all compounds that he tested and displayed bactericidal properties was the presence of one or more phenolic-type hydroxyl groups attached to the ring and ethyl groups between the rings (46).

Stilbenes are small molecules with molecular weights in the range of 200 to 300 g/mol.

They are naturally-occurring plant secondary metabolites and are derived from the phenylpropanoid pathway. Stilbenes are structurally similar to estrogen and are produced in many unrelated plant species (47). When a plant is subjected to abiotic stress, which is the

negative impact of non-living factors on a living organism, such as drought, temperature, heavy metals, and salinity, the phenylpropanoid pathway is activated and stilbenes are produced and secreted. Stilbenes are the plant's protective molecules; they are able to defend the plant from bacterial attack, as well as ultraviolet exposure (133). The most widely studied stilbene is resveratrol which has been shown to slow the progress of cancer. It has been known for more than sixty years that resveratrol inhibits bacterial and fungal growth in vitro (48, 49).

In 2005 Xue and Seto designed a combinatorial library to probe the serine protease plasmin. This library was designed to position the ketone functional group of the cyclohexanone ring with the active site serine to form a possible hemiketal link. Four of their compounds had  $IC_{50}$  values between 2.7-3.6  $\mu\text{M}$  and hence were good inhibitors of plasmin (50).

The key features of small molecule interactions with the  $\beta$ -lactamase active site are:

1. Interaction of any electrophilic center with either the active-site Ser84 or Lys87 to putatively form a hydrogen bond within the active site cavity.
2. Correct orientation of the OH groups to elicit hydrogen bonding interactions with either the main chain carbonyl oxygen of Ser142 and Gly252 or the amino group of Asn186.

Benzophenone and dibenzylsulfone showed good inhibition properties.  $K_i$  for benzophenone = 25.42  $\mu\text{M}$  and  $K_i$  for dibenzylsulfone = 16.56  $\mu\text{M}$ . The interaction of the nucleophilic  $\gamma\text{O}$  of the active site Ser87 with the carbonyl carbon of benzophenone and the sulphur center of dibenzylsulfone (+2 oxidation state) mimics the same interaction with a  $\beta$ -lactam antibiotic. This was also demonstrated by the fact that benzophenone imine and diphenyl amine had no inhibitory effect over the reaction.

The imine C=N bond is non-polar giving the nucleophilic gamma oxygen of Ser87 no attack site and the lone pair electrons of nitrogen in diphenylamine are involved in  $\pi$ - $\pi$  interactions with the phenyl groups. This resonance effect makes it less susceptible to nucleophilic attack. Biphenyl's high  $K_i$  (123.3  $\mu$ M) reflects its non-polar and non-electrophilic nature.

The 2,2-dihydrobenzophenone has two awkwardly placed OH groups that prevent its approach into the active site and this effect is overcome only after increasing the inhibitor concentration to 50 $\mu$ M.

Phenanthrene displays inhibition because phenyl groups provided favorable van der Waals interactions with Tyr55 that forms one side of the active site entrance.

Generally speaking of all the molecules tested as long as it was within hydrogen bonding distance of Ser84, Lys87 Ser142, Asn186, Gly252, Glu182 or Asp142, they demonstrated inhibitory effect which demonstrates that docking for this class of compounds is highly correlated with successful experimental inhibition.

### **Boronic Acids**

The quest for novel inhibitors of class A  $\beta$ -lactamases led to the discovery of the boronic acid transition state inhibitors. The inhibition mechanism by boronic acids on serine proteases has been elucidated, and it is not surprising that it involves the formation of a tetrahedral complex with the active site serine in a manner analogous to that expected during normal substrate hydrolysis where the boronic acid esterifies the gamma hydroxyl group of the active site serine (134) . In 1971 Philipp and Bender used several substituted benzene boronic acids to inhibit chymotrypsin and subtilisin in the mM to  $\mu$ M range (135) . In the blood coagulation cascade thrombin is the final serine protease and usually chosen as a target for the development of anti-

coagulant drugs. Peptides containing alpha-aminoboronic acids with neutral side chains were found to be highly effective, slow-binding inhibitors of thrombin with association binding constants in the  $\mu$ -molar range (136). One of the most well known anti-coagulants is a boronic acid derivative Ac-(D)Phe-Pro-boroArg-OH (137). In a separate study a novel boronate was synthesized as a thrombin inhibitor by conjugating a boronic acid moiety with a hirudin-based recognition moiety (138). This was shown to have a very high affinity for the target protein.

TEM-1 was the first plasmid-mediated  $\beta$ -lactamase discovered. In 1997 a collaboration between the Department of Biochemistry of the University of Alberta Canada, the Department of Pure and Applied Sciences of the University of Tokyo, and the European Molecular Biology Laboratory of Hamburg Germany created a RTEM deacylation-defective (E166N) mutant from *E. coli* that clearly shows penicillin G covalently bound to the active site serine putting to rest the discussion that deacylation is not the reverse of acylation (69). Deacylation is accomplished by nucleophilic attack on the carbonyl carbon of the ring by a water molecule assisted by the general base, Glu166. Researchers in the University of Alberta, Canada used the same mutant with the substrate penicillin G, 45 (1R)-1-acetamido-2-(3-carboxyphenyl)ethane boronic acid, designed to mimic the interactions observed in the RTEM Penicillin G/TEM-1 complex and found it to be a potent TEM-1 inhibitor. The structure of the acylated complex was solved at 1.7 Å resolution, which suggested a novel transition state of the deacylation step in the  $\beta$ -lactamase-catalyzed reaction pathway (102).

One of the best of the reversible inhibitors of AmpC, TEM and CTX-M  $\beta$ -lactamases is a ceftazidime-like boronic acid compound (see Fig. XXX compound 6), bind with a  $K_i$  value of  $\sim 4$  nM (109, 139).

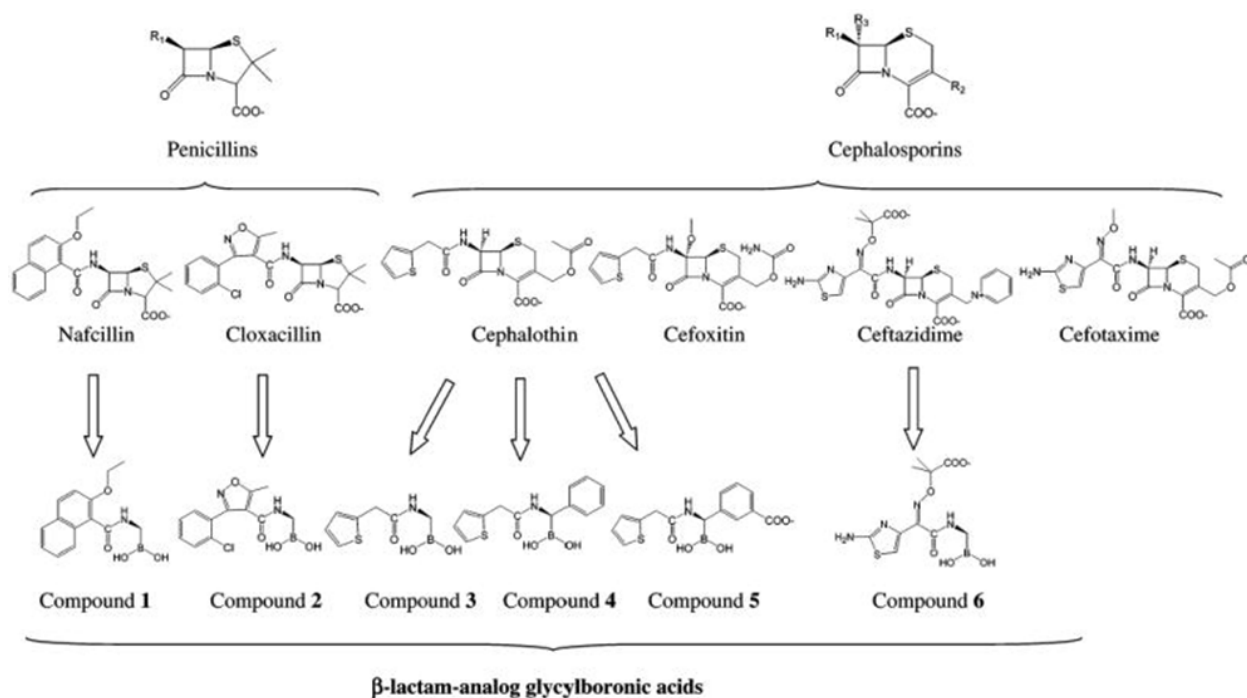


**Fig. 96. Characteristic  $\beta$ -lactam Antibiotics and Related  $\beta$ -Lactamase Inhibitors (139)**

The 2-carboxythiophene 5 boronic acid ( $K_i = 50\text{pM}$ ) appears to be the most potent small-molecule inhibitor for this class of enzyme. Its binding affinity exceeds those of other boronic inhibitors of  $\beta$ -lactamase. This compound does not have peptide groups that could interfere with membrane transport and are subject to proteolysis. In addition, it has a chemical structure that makes it a better candidate for further combinatorial development

## Boronic Acid Thiophenes

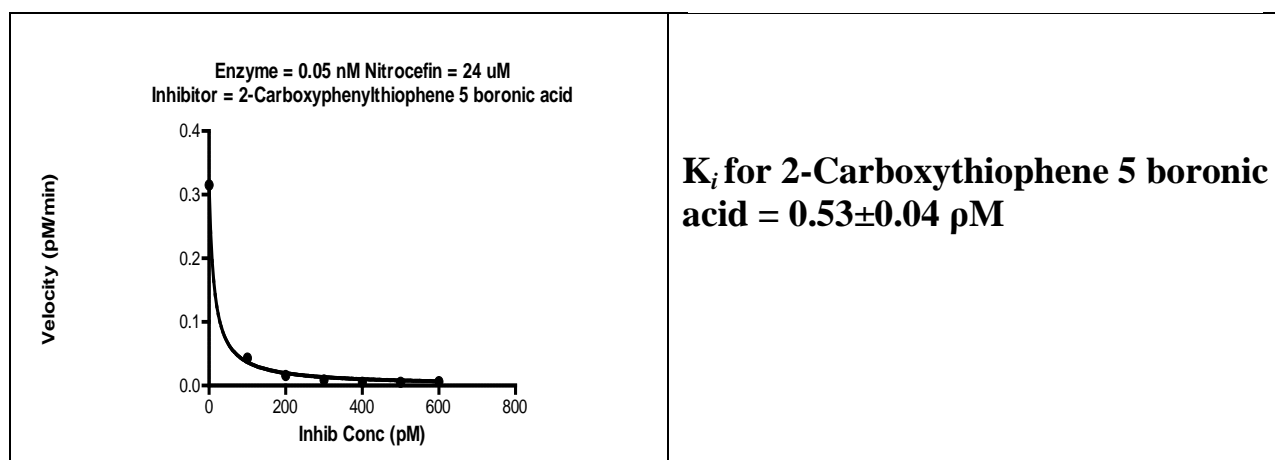
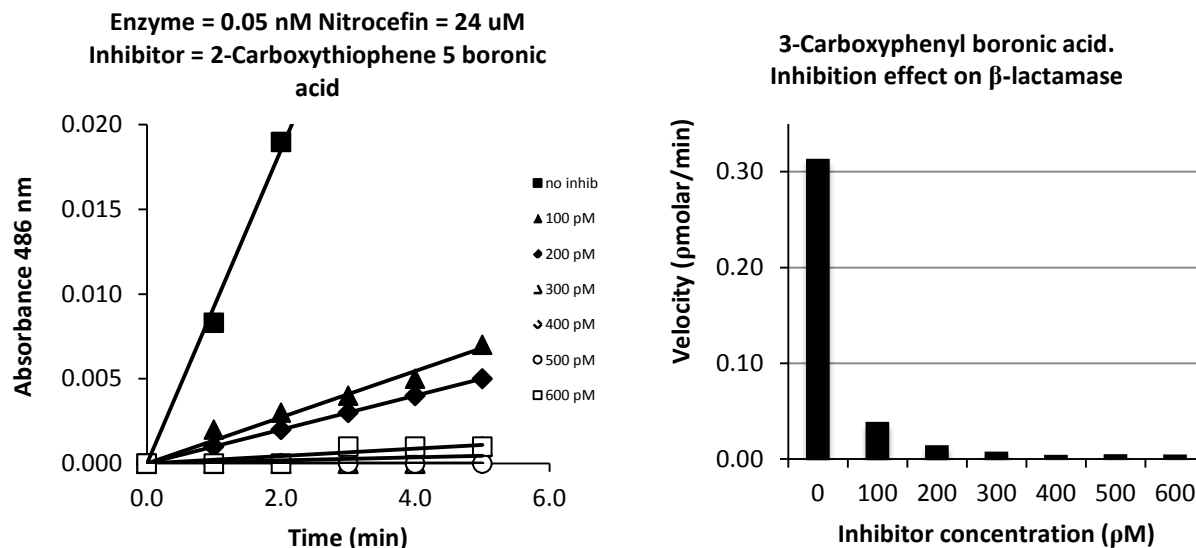


Fig. 97. 2-Carboxythiophene 5 Boronic Acid Kinetic Data

## Boronic Acid Inhibitors

Boronic acid compounds as pharmaceutical agents are directly related to their unique electronic and physicochemical properties. Boron occupies a special place in the periodic table. It is the first element in Group 13 (IIIA) of the periodic table usually referred to as the aluminum family. Boron is quite different from other members of the family. One difference is that boron is not a metal, but a metalloid. All other members of the family (aluminum, gallium, indium, and thallium) are metals. It is in the same period as carbon, but has one less electron. It has a

covalent radius similar to carbon. The fact that there are many boron-based reagents in organic synthesis reflects boron's unique reactivity. Boronic acids are usually trivalent compounds that have one alkyl substituent a carbon-boron bond, for example, and two hydroxyl groups leaving one open p-orbital. This ability to accept an electron pair makes these compounds Lewis acids, and with appropriate substitutions they have the ability to shift from neutral and trigonal planar  $sp^2$  boron to anionic tetrahedral  $sp^3$  boron giving them a carbon-like configuration.

Unlike carboxylic acids boric acids are not found in nature but are easily synthesized by acidifying borax with carbon dioxide. Their acidic nature had been known for years but the structure of the boronate ion was not discovered till 1959 by Lorand and Edwards (140). They demonstrated that the trivalent form, in equilibrium with the anionic tetrahedral species, transfers a proton to water to form hydronium ions, characterizing the acidic nature of boronic acids in water.

The first phenylboronic acid was prepared and isolated in 1860 by Frankland (141). He reacted diethylzinc with triethylborate and obtained triethylborane, the second slow oxidation yields boronic acid, and the third oxidation of boranes gives boric acids which are even more stable. Boronic acids have relatively low toxicity, are easy to handle, are chemically stable at ambient temperatures, and eventually degrade into "environmentally friendly" boric acid making them attractive compounds for researchers and industry alike.

### **Boronic Acids as Carbon Analogs**

Boronic acids have always been of interest in the area of organic chemistry; Suzuki cross coupling reactions which is the palladium-catalyzed cross coupling between organoboronic acid and halides, (142) Diels-Alder reactions, (143) carboxylic acid activation, (144) and as templates in organic synthesis (145). Medicinal chemistry has recently taken interest in boronic acids

compounds given their unique structural features and the discovery of biologically active compounds as pharmaceutical agents. Cleaving the amide bond in the  $\beta$ -lactam ring requires the conversion of the carbonyl carbon from an  $sp^2$  to a tetrahedral  $sp^3$  carbon; it stands to reason that boronic acids would make good transition state analogs for the inhibition of hydrolytic enzymes. That being the case diphenyl boronic acids have been recognized for over 20 years to be serine protease inhibitors, and in May 2003 a dipeptidyl boronic acid inhibitor came to market under the name Velcade™ (bortezomib). It is a proteasome inhibitor that is currently used for treating multiple myeloma.

Cancer therapies exploit the unique property of boron-10 in boron neutron capture therapy (BCNT) When boron-10 is irradiated with neutrons it emit particles that penetrate only a few millimeters making these compounds useful for targeted delivery of radiation therapy.

### **Boron as Serine Protease Inhibitors**

The inhibition mechanism by boronic acids on serine proteases has been elucidated, and it is not surprising that it involves the formation of a tetrahedral complex with the active site serine in a manner analogous to that expected during normal substrate hydrolysis where the boronic acid esterifies the gamma hydroxyl group of the active site serine (134) . In 1971 Philipp and Bender used several substituted benzene boronic acids to inhibit chymotrypsin and subtilisin (135) . In the blood coagulation cascade thrombin is the final serine protease and usually chosen as a target for the development of anti-coagulant drugs. Peptides containing alpha-aminoboronic acids with neutral side chains were found to be highly effective, slow-binding inhibitors of thrombin with association binding constants in the  $\mu$ -molar range (136). One of the most well known anti-coagulants is a boronic acid derivative Ac-(D)Phe-Pro-boroArg-OH (137). In a separate study a novel boronate was synthesized as a thrombin inhibitor by conjugating a boronic acid moiety

with a hirudin-based recognition moiety (138). This was shown to have a very high affinity for the target protein.

TEM-1 was the first plasmid-mediated  $\beta$ -lactamase discovered. In 1997 a collaboration between the Department of Biochemistry of the University of Alberta Canada, the Department of Pure and Applied Sciences of the University of Tokyo, and the European Molecular Biology Laboratory of Hamburg Germany created a RTEM deacylation-defective (E166N) mutant from *E. coli* that clearly shows Penicillin G covalently bound to the active site serine putting to rest the discussion that deacylation is not the reverse of acylation (69). Deacylation is accomplished by nucleophilic attack on the carbonyl carbon of the ring by a water molecule assisted by the general base, Glu166. Researchers in the University of Alberta, Canada used the same mutant with the substrate penicillin G, 45 (1R)-1-acetamido-2-(3-carboxyphenyl)ethane boronic acid, designed to mimic the interactions observed in the RTEM Penicillin G/TEM-1 complex and found it to be a potent TEM-1 inhibitor. The structure of the acylated complex was solved at 1.7 Å resolution, which suggested a novel transition state of the deacylation step in the  $\beta$ -lactamase-catalyzed reaction pathway (102).

## References

1. Heilbron JL (2003) *The Oxford Companion to the History of Modern Science* (Oxford University Press, New York).
2. Lindblad WJ (2008) Considerations for Determining if a Natural Product Is an Effective Wound-Healing Agent. *International Journal of Lower Extremity Wounds* 7(2):75-81.
3. Hanninen O, Farago M, & Monos E (1983) Ignaz Philipp Semmelweis, the Prophet of Bacteriology. *Infection Control* 4(5):367-370.
4. Semmelweis I & (1861) *Etiology, Concept and Prophylaxis of Childbed Fever* (University of Wisconsin Press); trans Carter KCt, extensive foreword September 15, 1983).
5. Nuland SB (1988) *Doctors the Biography of Medicine* (Knopf New York).
6. Fleming A (1929) On the Antibacterial Action of Cultures of a Penicillium, with Special Reference to Their Use in the Isolation of *B. influenzae*. *British Journal of Experimental Pathology* 10:226-236.
7. Waksman SA (1961) The role of antibiotics in nature. *Perspect. Biol. Med.* 4:271–286.
8. Crowfoot D, Bunn CW, Rogers-Low BW, & Turner-Jones A (1949) *X-ray crystallographic investigation of the structure of penicillin* (Princeton University Press, New Jersey).
9. Rohlfs M, Albert M, Keller NP, & Kempken F (2007) Secondary chemicals protect mould from fungivory. *Biol Lett* 3(5): 523–525.
10. Yim G, Wang HH, & FRS JD (2007) Antibiotics as signalling molecules. *Phil. Trans. R. Soc. B* 362 (362):1195-1200.
11. Li D, *et al.* (2005) Induction of fibronectin adhesins in quinoloneresistant *Staphylococcus aureus* by subinhibitory levels of ciprofloxacin or by sigma B transcription factor activity is mediated by two separate pathways. *Antimicrob. Agents Chemother* 49: 916–924.
12. Rothstein JD (2005) Beta-lactam antibiotics offer neuroprotection by increasing glutamate transporter expression *Nature* 433:73-77.
13. Hoffman LR, *et al.* (2005) Aminoglycoside antibiotics induce bacterial biofilm formation. *Nature* 436:1171–1175.
14. An D & Parsek MR (2007) The promise and peril of transcriptional profiling in biofilm communities. *Current Opinions in Microbiology* 10(3):292-296.
15. Elander RP (2003) Industrial production of beta-lactam antibiotics. *Applied Microbiology and Biotechnology* 61(5-6):385-392.
16. Bush K & Mobashery S (1998) How  $\beta$ -lactamases have driven pharmaceutical drug discovery. From mechanistic knowledge to clinical circumvention. *Adv. Exp. Med. Biol.* 456:71-98.
17. Sensakovic JW & Smith LG (1995) Beta-lactamase inhibitor combinations. *Med Clin North Am* 79-695.
18. Sanders WE & Sanders CC (1996) Piperacillin/tazobactam: a critical review of the evolving clinical literature. *Clin Infect Dis* 22-107.
19. Brennan PJ (2003) Structure, function, and biogenesis of the cell wall of *Mycobacterium tuberculosis*. *Tuberculosis* 83(1-3):91-99.
20. Barry CE & Mdluli K (1996) Drug sensitivity and environmental adaptation of mycobacterial cell wall components. *Trends in Microbiology* 4(7):275-278.

21. Lederer E, Adam A, Ciorbaru R, Petit JF, & Wietzerbin-Falszpan J (1975) Cell-walls of mycobacteria and related organisms—chemistry and immunostimulant properties. *Mol Cell Biochem* 7:87-104.
22. Todar K (2011) Mycobacterium tuberculosis and Tuberculosis in *Online Text Book of Bacteriology*.
23. Scherman MS, *et al.* (2003) Drug Targeting Mycobacterium tuberculosis Cell Wall Synthesis: Development of a Microtiter Plate-Based Screen for UDP-Galactopyranose Mutase and Identification of an Inhibitor from a Uridine-Based Library. *Antimicrobial Agents and Chemotherapy* 47(1).
24. Kumar I & Pratt RF (2005) Transpeptidation Reactions of a Specific Substrate Catalyzed by the Streptomyces R61 DD-Peptidase: The Structural Basis of Acyl Acceptor Specificity *Biochemistry* 44(30).
25. Tipper DJ & Strominger JL (1965) Mechanism of action of penicillins: a proposal based on their structural similarity to acyl-d-alanyl-d-alanine. *Proc. Natl. Acad. Sci. USA* 54:1133.
26. YOCUM RR, WAXMAN JD, RASMUSSEN JR, & STROMINGER JL (1979) Mechanism of penicillin action: Penicillin and substrate bind covalently to the same active site serine in two bacterial D-alanine Carboxypeptidases *Proc. Natl. Acad. Sci. USA* 76(6): 2730-2734.
27. Hamilton-Miller JMT (1999)  $\beta$ -Lactams: variations on a chemical theme, with some surprising biological results. *J Antimicrob. Chemother* 44:729-734.
28. Bush K, Jacoby GA, & Medeiros AA (1995) A functional classification scheme for beta-lactamases and its correlation with molecular structure. *Antimicrob. Agents Chemother* 39(6):1211-1233.
29. Saylers AA & Amabile-Cuevas CF (1997) Why are antibiotic resistance genes so resistant to elimination? *Antimicrob Agents Chemother* 41:2321-2325
30. Davies J (1994) Inactivation of antibiotics and the dissemination of resistance genes. *Science* 264:375-382.
31. Wade D, Bowman A, Wahlin B, & Drain CM (1990) All-D amino acid-containing channel-forming antibiotic peptides. *Proc. Natl. Acad. Sci. U.S.A.* 86:4761-4765.
32. Drawz SM & Bonomo RA (2010) Three Decades of  $\beta$ -Lactamase Inhibitors. *Clinical Microbiology Reviews* 23(9):160-201.
33. Brown AG (1986) Clavulanic acid, a novel beta-lactamase inhibitor—a case study in drug discovery and development. *Drug Des. Deliv* 1:1-21.
34. English AR, Retsema JA, Girard AE, Lynch JE, & Barth. WE (1978) A beta-lactamase inhibitor that extends the antibacterial spectrum of beta-lactams: initial bacteriological characterization. *Antimicrob. Agents Chemother* 14:414-419.
35. Fisher J, Belasco JG, Charnas RL, Khosla S, & Knowles JR (1980) Beta-Lactamase inactivation by mechanism-based reagents. *Philos. Trans. R. Soc. Lond. B Biol. Sci.* 289(303-319).
36. Helfand E, *et al.* (2003) Following the reactions of mechanism-based inhibitors with -lactamase by Raman crystallography. *Biochemistry* 42:13386-13392.
37. Kalp G, Totir MMA, Buynak JD, & Carey PR (2009) Different intermediate populations formed by tazobactam, sulbactam, and clavulanate reacting with SHV-1 beta-lactamases: Raman crystallographic evidence. *J. Am. Chem. Soc.* 131:2338-2347.

38. Kalp M, Totir MA, Buynak JD, & Carey PR (2009) Different intermediate populations formed by tazobactam, sulbactam, and clavulanate reacting with SHV-1  $\beta$ -lactamases: Raman crystallographic evidence. *J Am Chem Soc* 131(6):2338-2347.
39. Imada A, Kitano K, Kintaka K, Murai M, & Asai M (1981) Sulfazecin and isosulfazecin, novel  $\beta$ -lactam antibiotics of bacterial origin. *Nature* 289:590-591.
40. Sykes RB & Phillips I (1981) Symposium on aztreonam, a synthetic monobactam. *J. Antimicrob Chemother* 8 (Suppl. E):1-146.
41. Bulychev A, Bellettini JR, O'Brien M, & Crocker P (2000) N-Sulfonyl beta-lactam inhibitors for beta-lactamases *Tetrahedron* 56(31): 5729-5728
42. Heinze-Krauss I, *et al.* (1998) Structure-based design of beta-lactamase inhibitors. 1. Synthesis and evaluation of bridged monobactams. *J. Med. Chem* 41:3961-3971.
43. Hashizume T, Yamaguchi A, Hirata T, & Sawai T (1984) Kinetic studies on the inhibition of *Proteus vulgaris* beta-lactamase by imipenem. *Antimicrob. Agents Chemother* 25:149-151.
44. Moellering H, R.C. Jr E, & Sentochnik GM (1989) The carbapenems: new broad spectrum [beta]-lactam antibiotics. *J. Antimicrob. Chemother* 24 (Suppl. A)1-7.
45. S.Ness, *et al.* (200) Structure-Based Design Guides the Improved Efficacy of Deacylation Transition State Analogue Inhibitors of TEM-1  $\beta$ -Lactamase. *Biochemistry* 39:5312-5321.
46. Faulkner GH (1944) The antibacterial action of some biphenyl derivatives *Biochem J.* 38(5):370-372.
47. Bazzano LA, He J, & Ogden LG (2002) Fruit and vegetable intake and risk of cardiovascular disease in US adults: the first national health and nutrition examination survey epidemiologic follow-up study. *Am J Clin Nutr* 76:93-99.
48. Baur JA & Sinclair DA (2006) Therapeutic potential of resveratrol: the in vivo evidence. *Nat. Rev. Drug Discov* 5:493-506.
49. Morales M, Barcelo AR, & Pedreno MA (2000) Plant stilbenes: recent advances in their chemistry and biology. *Adv. Plant Physiol* 2(39-70).
50. Xue F & Seto CT (2005) Selective Inhibitors of the Serine Protease Plasmin: Probing the S3 and S3' Subsites Using a Combinatorial Library. *J. Med. Chem.* 48: 6908-6917
51. Abraham EP & Chain E (1940) An enzyme from bacteria able to destroy penicillin *Nature* 146:837.
52. Sawai T, Mitsuhashi S, & Yamagishi S (1968) Drug resistance of enteric bacteria. XIV. Comparison of  $\beta$ -lactamases in gram-negative rod bacteria resistant to  $\alpha$ -aminobenzylpenicillin. *Jpn. J. Microbiol* 12:423-434.
53. Jack GW & Richmond MH (1970) Comparative amino acid contents of purified  $\beta$ -lactamases from enteric bacteria. *FEBS. Lett.* 12:30-32.
54. Richmond MH & Sykes RB (1973) The  $\beta$ -lactamases of gram negative bacteria and their possible physiological role. *Adv. Microb. Physiol* 9:31-88.
55. Ambler RP (1980) The structure of beta-lactamases. *Philos Trans. R. Soc. Lond. B. Biol. Sci.* 289:321-331.
56. Ambler RP, *et al.* (1991) A standard numbering scheme for the class A beta-lactamases. *Biochem* 276:269-270.

57. Jarlier VM-H, Fournier GN, & Philippon A (1988) Evolution and dissemination of  $\beta$ -lactamases accelerated by generations of  $\beta$ -lactam antibiotics. *Rev. Infect. Dis* 10:867-878.
58. Paterson DL & Hujer KM (2003) Extended-spectrum b-lactamases in *Klebsiella pneumoniae* blood stream isolates from seven countries: dominance and widespread prevalence of SHV and CTX-M-type b-lactamases *Antimicrob Agents Chemother* 47:3554-3560.
59. Bradford PA (2001) Extended-spectrum b-lactamases in the 21st century : characterization, epidemiology, and detection of this important resistance threat. *Clin Microbiol Rev* 48:933-951.
60. G. A. Jacoby MD & L. S. Munoz-Price MD (2005) mechanisms of disease: The new beta-lactamase *N Engl J Med* 352:380-391.
61. Matthew M, Hedges RW, & Smith JT (1979) Types of beta-lactamase determined by plasmids in gram-negative bacteria. *J Bacteriol* 138(3):657-662.
62. J. J. Farmer r, Fanning GR, Huntley-Carter GP, Holmes B, & Hickman FW (1985) Biochemical identification of new species and biogroups of Enterobacteriaceae isolated from clinical specimens. *J Brenner J Clin Microbiol* 13(5):919-933.
63. Woodford N, Ward E, & Kaufmann ME (2005) Molecular characterisation of *Escherichia coli* isolates producing CTX-M-15 extended-spectrum b-lactamase (ESBL) in the United Kingdom in *Health Protection Agency*.
64. Hubbard TJP, Murzin AG, Brenner SE, & Chothia C (1997) Comprehensive assessment of automatic structural alignment against a manual standard, the scop classification of proteins. *Nucleic Acids Res.* 25:236-239.
65. Wagner UG, Petersen EI, Schwab H, & Kratky C (2002) EstB from *Burkholderia gladioli*: a novel esterase with a beta-lactamase fold reveals steric factors to discriminate between esterolytic and b-lactam cleaving activity. *Protein Sci.* 11:467-478.
66. Sun TM, Nukaga M, Mayama K, Braswell EH, & Knox JR (2003) Comparison of beta-lactamases of classes A and D: 1.5 Angstrom crystallographic structure of the class D OXA-1 oxacillinase. *Protein Sci.* 12:82-91.
67. Montagne A, Lamotte-Brasseur J, & Frere JM (1998) Catalytic properties of class A beta-lactamases: efficiency and diversity. *Biochem J.* 330:581-598.
68. Jelsch C, Lenfant F, Masson JM, & Samama JP (1992) Beta-lactamase TEM1 of *E. coli*. Crystal structure determination at 2.5 A resolution. *FEBS Lett.* 299(2):135-142.
69. Guillaume G, *et al.* (1997) Site-directed mutagenesis of glutamate 166 in two beta-lactamases. Kinetic and molecular modeling studies. *J. Biol. Chem* 272(9):5438-5444.
70. Livermore DM (1995) beta-Lactamases in laboratory and clinical resistance. *Clinical Microbiology Reviews* 8(4):557-584.
71. Atanasov BP, Mustafi D, & Makenen MW (2000) Protonation of the  $\beta$ -Lactam Nitrogen is the Trigger Event in the Catalytic Action of Class A  $\beta$ -Lactamases. *Proc. Natl. Acad. Sci. U.S.A.* 97:3160-3165.
72. Strynadka NC, *et al.* (1994) Structural and kinetic characterization of a beta-lactamase-inhibitor protein. *Nature* 368:657-660.
73. Lamotte-Brasseur J, Dive G, & Dideberg O (1991) Mechanism of acyl transfer by the class A serine beta-lactamase of *Streptomyces albus* G. *Biochem. J.* 279:213-221.

74. Payne DJ, Wensheng D, & Bateson JH (2000) beta-lactamase epidemiology and the utility of established and novel beta-lactamase inhibitors. *Exp. Opin. Invest. Drugs* 9(2):247-261.
75. Bush K & Mobashery S (1998) How beta-lactamases have driven pharmaceutical drug discovery. From mechanistic knowledge to clinical circumvention. *Adv. Exp. Med. Biol.* 456:71-98.
76. Payne DJ (1993) Metallo-beta-lactamases—a new therapeutic challenge. *J. Med. Microbiol.* 39:93.
77. Godfrey AJ, Bryan LE, & Rabin HR (1981) Cloning and characterization of the *Pseudomonas aeruginosa* pbpB gene encoding penicillin-binding protein 3. *Antimicrob Agents Chemother.* 19(5):705-711.
78. Aggeler R, Then RL, & Ghosh RJ (1987) Reduced expression of outer membrane proteins in beta-lactam resistant mutants of *Enterobacter Cloacae*. *Gen. Microbiol.* 133:3383-3392.
79. Domenesch-Sanchez A & Herendez-Alles. LVJ (1999) Identification and Characterization of a New Porin Gene of *Klebsiella pneumoniae*: Its Role in -Lactam Antibiotic Resistance *J. Bacteriol* 181(9):2726-2732.
80. Webber MA & .Piddock LJV (2003) The importance of efflux pumps in bacterial antibiotic resistance. *J Antimicrob Chemother* 51:9-11.
81. Michaelis L & Menten ML (1913) The kinetics of the inversion effect. *Biochemische Zeitschrift* 49:333-339.
82. Williams JW & Morrison JF (1979) The kinetics of reversible tight-binding inhibition. *Meth. Enzymol* 63:437-467.
83. Johnson ML (1992) Why, when, and how biochemists should use least squares *Anal. Biochem.* 206:215-225.
84. Ferrara P, Gohlke H, & Price DJ (2004) Assessing scoring functions for protein-ligand interactions. *J. Med. Chem* 47:3032-3034.
85. Clark M, Guarnieri F, Shkurko I, & Wiseman J (2006) Grand canonical Monte Carlo simulation of ligand-protein binding. *J. Chem. Inf. Model* 46:231-242.
86. Santos-Filho OA & Hopfinger AJ (2001) A search for sources of drug resistance by the 4D-QSAR analysis of a set of antimalarial dihydrofolate reductase inhibitors. *J Comput-Aided Mol Design* 5:1-12.
87. Hoffman B, *et al.* (1999) Quantitative structure-activity relationship modeling of dopamine D1 antagonists using comparative molecular field analysis, genetic algorithms-partial least-squares and K nearest neighbor methods. *J. Med. Chem* 42:3217-3226.
88. Supuran CT, Scozzafara A, Briganti F, & Clare BW (2000) Protease inhibitors: synthesis and QSAR study of novel classes of nonbasic thrombin inhibitors incorporating sulfonylguanidine and O-methylsulfonylisourea moieties at P1. *J. Med. Chem* 43:1793-1806.
89. Huang W, Beharry Z, Zhang Z, & Palzkill T (2003) A broad-spectrum peptide inhibitor of {beta}-lactamase identified using phage display and peptide arrays. *Protein Eng Des Sel* 16:853-860.
90. Sobolev V, Sorokine A, Prilusky J, Abola EE, & Edelman M (1999) Automated analysis of interatomic contacts in proteins. *Bioinformatics* 15:327-332.
91. Kuntz ID, Blaney JM, Oatley SJ, Langridge R, & Ferrin TE (1982) A geometric approach to macromolecule-ligand interactions. *J. Mol. Biol* 161:269-288.

92. Cunningham BC & Wells JA (1997) Minimized proteins. *Curr. Opin. Struct. Biol.* 7:457-462.
93. Yanofsky SD, Baldwin DN, Butler JH, Holden FR, & Jacobs JW (1996) High affinity type I interleukin 1 receptor antagonists discovered by screening recombinant peptide libraries. *Proc. Natl. Acad. Sci. USA* 93:7381–7386.
94. Samanen J, *et al.* (1991) Development of a small RGD peptide fibrinogen receptor antagonist with potent antiaggregatory activity in vitro. *J. Med. Chem* 34:3114–3125.
95. S.Zhengding, Vinogradova A, Koutychenko A, Tolkatchev D, & Feng. F (2004) Rational design and selection of bivalent peptide ligands of thrombin incorporating P4-P1 tetrapeptide sequences: from good substrates to potent inhibitors. *Protein Engineering, Design & Selection* 17(8):647-657.
96. Maraganore JM & Fenton J (1990) Thrombin inhibition by synthetic hirudin peptides. *Advances in Experimental Medicine and Biology* 281:177-183.
97. Raffler NA, Schneider-Mergener J, & Famulok M (2003) A novel class of small functional peptides that bind and inhibit human  $\alpha$ -thrombin isolated by mRNA display. *Chemistry & Biology* 10(4):369.
98. Doran JL, Leskiw BK, Aippersbach S, & Jensen SE (1990) Isolation and characterization of a beta-lactamase-inhibitory protein from *Streptomyces clavuligerus* and cloning and analysis of the corresponding gene. *J. Bacteriol.* 172:4909–4918.
99. Jensen SE (1986) Biosynthesis of cephalosporins. *Crit. Rev. Biotechnol* 3:277–301.
100. Strynadka NC, *et al.* (1994) Structural and kinetic characterization of a beta-lactamase-inhibitor protein. *Nature* 368:657-660.
101. RUDGERS GW, WANZHI H, & PALZKILL T (2001) Binding Properties of a Peptide Derived from beta-Lactamase Inhibitory Protein. *ANTIMICROBIAL AGENTS AND CHEMOTHERAPY*:3279–3286.
102. Strynadka NC, Hiroyuki A, & Jensen SE (1992) Molecular structure of the acyl-enzyme intermediate in  $\beta$ -lactam hydrolysis at 1.7 Å resolution. *Nature* 359:700-705.
103. Anderson JW, *et al.* (2003) On the substrate specificity of bacterial DD-peptidases: evidence from two series of peptidoglycan-mimetic peptides. *Pratt Biochem J 1994 302 851 Biochem J 2003 373 949* 373(3):949-955.
104. Ochman H, Elwy S, & Moran NA (1999) Calibrating bacterial evolution. *Proc. Natl. Acad. Sci. U.S.A.* 96:12638-12643
  
105. Holland HD (1997) Evidence for Life on Earth more than 3850 Million Years Ago. *Science* 275:38-39.
106. Aharonowitz Y, Cohen G, & Martin JF (1992) Penicillin and cephalosporin biosynthetic genes: Structure, organization, regulation, and evolution. *Annu. Rev. Biochem* 9:461-495.
107. Challis GL & Hopwood DA (2003) Synergy and contingency as driving forces for the evolution of multiple secondary metabolite production by *Streptomyces* species. *Proc. Natl. Acad. Sci. U.S.A.* 100:14555-14561.
108. Kelly JA, Dideberg O, Charlier P, & Wery JP (1986) On the origin of bacterial resistance to penicillin: comparison of a beta-lactamase and a penicillin target. *Science* 231:1429-1431.
109. Chen Y, Shoichet B, & Bonnet R (2005) Structure, function, and inhibition along the reaction coordinate of CTX-M beta-lactamases *J. Am. Chem. Soc.* 127(5423-5434).

110. Chen CC, Rahil J, Pratt RF, & Herzberg O (1993) Structure of a phosphonateinhibited beta-lactamase. An analog of the tetrahedral transition state intermediate of beta-lactam hydrolysis. *J Mol Biol* 234:165-178.
111. Smith NH, Gordon SV, Rua-domenesh R, Hadley RSC-, & Hewinson RG (2006) Bottlenecks and Broomsticks: the molecular evolution of Mycobacterium bovis. *Nature Reviews Microbiology* 4:670-681.
112. Gutierrez MC, Brisse S, Brosch R, Fabre M, & Omais B (2005) Ancient origin and gene mosaicism of the progenitor of Mycobacterium tuberculosis. *PLoS Pathog* 1(1):e5.
113. Sreevatsan S, Pan X, Stockbauer KE, Connell ND, & Kreiswirth BN (1997) Restricted structural gene polymorphism in the Mycobacterium tuberculosis complex indicates evolutionarily recent global dissemination. *Proc Natl Acad Sci U S A* 94:9869-9874.
114. Coscolla M & Gagneux S (2010) Does M. tuberculosis genomic diversity explain disease diversity? *Drug Discov Today Dis Mech* 7(1):43-59.
115. Jr. WS, Jr. WHO, & Petroff SA (1934) Biological studies of the tubercule bacillus III. Dissociation and pathenogenicity of the R and S variants of the human tubercule bacillus (H37). *J. Exp. Med* 60:515-540.
116. Jr. WHO & Jr. WS (1936) The pathenogenesis and fate of tubercule produced by dissociate variants of tubercule bacilli *J. Infec. Dis* 59:306-325.
117. Tremblay LW, Fan F, & Blanchard JS (2010) Biochemical and structural characterization of Mycobacterium tuberculosis beta-lactamase with the carbapenems ertapenem and doripenem. *Biochemistry* 49:3766-3773.
118. Wolfe LM, Mahaffey SB, Kruh NA, & Dobos KM (2010) Proteomic definition of the cell wall of Mycobacterium tuberculosis. *J. Proteome Res* 9(11):5816-5826.
119. Philipp WJ, S. Poulet, Eiglmeier K, Pascopella L, & Balasubramanian V (1996) An integrated map of the genome of the tubercle bacillus, Mycobacterium tuberculosis H37Rv, and comparison with Mycobacterium leprae. *Proc. Natl. Acad Sci USA* 93:3132-3137.
120. Herzberg O & Moulton J (1987) Bacterial Resistance to -Lactam Antibiotics:Crystal Structure of fi-Lactamase from Staphylococcus aureus PCi at 2.5 A Resolution. *Science* 236: 694–701.
121. Rahil J & PRATT RF (1991) Phosphonate monoester inhibitors of class A  $\beta$ -lactamases. *Biochem. J.* 275:793-795.
122. Lobkovsky E, *et al.* (1994) Crystallographic Structure of a Phosphonate Derivative of the Enterobactercloacae P99 Cephalosporinase: Mechanistic Interpretation of a P-Lactamase Transition-State Analog. *Biochemistry* 33:6762.
123. Moulin A, Bell JH, Pratt RF, & Ringe D (2007) Inhibition of Chymotrypsin by a Complex of Ortho-Vanadate and Benzohydroxamic Acid: Structure of the Inert Complex and its Mechanistic Interpretation. *Biochemistry* 46: 5982.
124. Adediran SA & Pratt RF (2008) Inhibition of Serine beta-Lactamases by Vanadate-Catechol Complexes *Biochemistry* 47:9467–9474.
125. Bone R, Shenvi AB, Kettner CA, & Agard DA (1987) Serine protease mechanism: structure of an inhibitory complex of alpha-lytic protease and a tightly bound peptide boronic acid. *Biochemistry* 26:7609-7614

126. Wyrembak PN, Babaoglu K, Peltó RB, Shoichet K, & Pratt RF (2007) O-Aryloxycarbonyl hydroxamates: new  $\beta$ -lactamase inhibitors that cross-link the active site. *J. Am. Chem. Soc.* 129:9548-9549
127. KIENER PA & WALEY SG (1978) Reversible Inhibitors of Penicillinases. *Biochem. J.* 169:197-204.
128. Beesley T, *et al.* (1983) The inhibition of class C  $\beta$ -lactamases by boronic acids. *Biochem. J.* 209:229-233.
129. Crompton IE, Cuthbert BK, Lowe G, & Waley SG (1988)  $\beta$ -lactamase inhibitors. The inhibition of serine  $\beta$ -lactamases by specific boronic acids. *Biochem. J.* 251:453-459
130. Philipp M, *et al.* (1986) New Boronic Acid Inhibitors of Serine Hydrolases - B. cereus  $\beta$ -Lactamase I. *Beiträge zur Wirkstoffforschung* 30:33-41.
131. Philipp M & Maripuri S (1981) Inhibition of Subtilisin by Arylboronic Acids. *FEBS Letters* 133:36-38.
132. Brown RP, Aplin RT, & Schofield CJ (1997) Mass spectrometric studies on the inhibition of TEM-2 beta-lactamase by clavulanic acid derivatives. *J antibiot (Tokyo)* 50(2):184-185.
133. González-Lamothe R, *et al.* (2009) Plant Antimicrobial Agents and Their Effects on Plant and Human Pathogens. *Int. J. Mol. Sci.* 10: 3400-3419.
134. Koehler KA & Lienhard GE (1971) 2-Phenylethaneboronic acid, a possible transition-state analog for chymotrypsin. *Biochemistry* 10:2477-2483.
135. Philipp M & Bender MI (1971) Inhibition of serine proteases by arylboronic acids. *Proc Natl Acad Sci. USA* 68:478-480.
136. Weber CP, *et al.* (1995) Kinetic and Crystallographic Studies of Thrombin with Ac-(D)Phe-Pro-boroArg-OH and Its Lysine, Amidine, Homolysine, and Ornithine Analogs. *Biochemistry* 34(11):3750-3757.
137. Lim SLM, Johnston ER, & Kettner CA (1993) The solution conformation of (D)Phe-Pro-containing peptides: implications on the activity of Ac-(D)Phe-Pro-boroArg-OH, a potent thrombin inhibitor. *J. Med. Chem* 36(13):1831-1838.
138. Wenqian Y, Xingming G, & Wang B (2003) Boronic acid compounds as potential pharmaceutical agents. *Medicinal Research Reviews* 23(3):346-368.
139. Powers RA, Caselli E, Focia PJ, Prati F, & Shoichet BK (2001) Structures of ceftazidime and its transition-state analogue in complex with AmpC beta-lactamase: implications for resistance mutations and inhibitor design. *Biochemistry* 40:9207-9214
140. Lorand JP & Edwards JO (1959) Polyol complexes and structure of the benzeneboronate ion. *J Org Chem* 24:769-774.
141. Frankland E & Duppa BF (1860) Vorläufige Notiz über Boräthyl. *Justus Liebigs Ann. Chem* 115(3):319.
142. Miyaura N & Suzuki A (1995) Palladium-catalyzed cross-coupling reactions of organoboron compounds. *Chem Rev* 95:2457-2483.
143. Ishihara K & Yamamoto H (1999) Arylboron compounds as acid catalysts in organic synthetic transformations. *Eur J Org Chem* 527-538.
144. Latta R, Springsteen G, & Wang B (2001) Development and synthesis of an arylboronic acid-based solid-phase amidation catalyst. *Synthesis*:1611-1613.

145. Currie GS, *et al.* (2000) Chirally templated boronic acid Mannich reaction in the synthesis of optically active  $\alpha$ -amino acids. *J Chem Soc Perkin Trans 1*:2982-2990.